UCSF
UC San Francisco Electronic Theses and Dissertations

Title
Inactivation of calcium channels in a mammalian central neuron

Permalink
https://escholarship.org/uc/item/3db420nx

Author
Slesinger, Paul Avery

Publication Date
1991

Peer reviewed|Thesis/dissertation

eScholarship.org Powered by the California Digital Library
University of California

INACTIVATION OF CALCIUM CHANNELS IN A MAMMALIAN CENTRAL NEURON: A NEW ROLE FOR INACTIVATION

by

PAUL AVERY SLESINGER

DISSERTATION

Submitted in partial satisfaction of the requirements for the degree of

DOCTOR OF PHILOSOPHY

in

NEUROSCIENCE

in the

GRADUATE DIVISION

of the

UNIVERSITY OF CALIFORNIA

San Francisco

I dedicate this dissertation to my wife and family

Acknowledgements

The completion of this thesis was achieved through the support, encouragement and guidance from my family and friends. First, I would like to thank my thesis advisor Jeffry Lansman for providing invaluable advice, being available for inumerable discussions, creating an atmosphere for research in the lab that allowed me to excel, and for just being a good friend. I would like to thank the members of my thesis committee, Lily Jan, Roger Nicoll, and Dick Tsien, for their helpful comments and advice. I thank my fellow classmates in the lab whom I saw day and night, Al Franco and Teryl Elam, for making the lab a relaxing and supportive atmosphere. I thank my family and especially my parents, whose support and guidance from my birth to the present enabled me to earn my PhD. Finally, my deepest gratitude goes to Margaret for being an excellent colleague, an especially close friend and, last but not least, a loving wife.

Abstract

Ca^{2+} entry through voltage-gated Ca^{2+} channels regulates the repetitive firing behavior of neurons, activates intracellular enzymes and stimulates the release of neurotransmitters. Ca^{2+} channels inactivate in a time- and voltage-dependent manner during membrane depolarization, reducing Ca^{2+} influx. In this thesis, I describe the results of experiments which examined the inactivation of Ca^{2+} channels recorded from cerebellar granule cells using the patch-clamp technique. Large depolarizations delivered from a negative holding potential elicit a whole-cell Ca^{2+} current that inactivates along a time course which has fast and slow components that are sensitive to voltage. Single-channel recordings show a single type of Ca^{2+} channel, with properties most similar to L-type Ca^{2+} channels, that accounts for the voltage-dependence and time course of whole-cell current at positive potentials and that recovers from inactivation at negative potentials by passing through open state. Recovery from inactivation is speeded by hyperpolarization or by raising the concentration of external permeant cation, suggesting that, like inactivation of Na^+ and K^+ channels, Ca^{2+} channels inactivate through a mechanism in which an inactivation "gate" swings into the open channel and blocks the passage of ions across the membrane. Inactivation of Ca^{2+} current during membrane depolarization, which was previously thought to only reduce Ca^{2+} influx, may actually enhance Ca^{2+} entry following action potentials through channels that reopen from the inactivated state.

Table of contents

List of Figures

INTRODUCTION

Ion channel inactivation

Following activation, many voltage-gated ion channels enter an inactivated state that does not conduct current, but is distinct from the resting state. The consequence of inactivation is that the macroscopic current declines with time during membrane depolarization, as channels enter the inactivated pool. Inactivation is an important property of ion channels which reduces the amount of permeant ion that crosses the membrane during membrane depolarization. Inactivation of Na^+ channels, for example, is one of the steps that determines the duration of an action potential by terminating Na^+ influx in a time- and voltage-dependent manner, ensuring rapid repolarization.

Hodgkin and Huxley (1952a,b) first described inactivation in their classic studies of axonal Na^+ currents in squid. Hodgkin and Huxley proposed that (mostly for mathematical reasons) inactivation and activation were independent processes; that is, the Na^+ conductance increases along an exponential time course, due to channels opening during membrane depolarization, but is independently decreased by the inactivation process. Because activation was assumed to be very rapid, the time constant (τ_h) for the decay of current provided a direct measure of the rate of inactivation. Hodgkin and Huxley found that the time constant changed with voltage, suggesting that inactivation was a voltage-dependent process. Subsequent studies showed that inactivation and activation of Na^+ channels are indeed separate processes, but that inactivation is voltage-insensitive (Bezanilla and Armstrong, 1977; Armstrong and Bezanilla, 1977; Cota and Armstrong, 1989; Aldrich et al., 1983). Exposing the intracellular surface of the squid axon to a proteolytic enzyme removes Na^+ current inactivation without affecting activation (Armstrong et al., 1973). By examining the difference between currents recorded before and after enzyme treatment, it was shown that the rate of inactivation was insensitive to

voltage and that the time constant for the decay of current changed with voltage because channels inactivated only after they first opened.

To illustrate this coupling of inactivation to the activation process, consider the 3 state model below (Scheme 1). Membrane depolarization drives channels from rest (C) to the open state (O). Sojourns into the inactivated state (I) terminate a burst of openings produced by open and closed state transitions and give rise to a macroscopic current that decays. Although the rate of inactivation from the open state is insensitive to voltage, the measured rate of decay depends on the time that channels take to open. At membrane potentials which cause channels to open slowly, the rate of current decay is slow because inactivation occurs only after channels open. At more positive potentials where activation is very rapid, the time constant for inactivation reaches a minimum because inactivation is limited only by the inactivation step. The time constant for the decay of current is therefore determined by the relative contributions of the activation and inactivation processes.

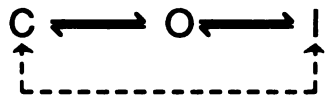

Scheme 1

Scheme 1 (solid lines) predicts that inactivated channels pass through the open state before closing at negative membrane potentials. However, large currents indicating that channels return from inactivation through the open state have not been detected, suggesting that a transition between the inactivated and closed state must exist to allow inactivated channels to return to rest without opening (dashed line: cf Bezanilla and Armstrong, 1977; Aldrich and Stevens, 1983; Armstrong and Gilly, 1979; Horn and Vandenberg, 1984).

In addition to showing that activation is separate from inactivation of Na^+ channels, the experiments with proteolytic enzymes suggested that a cytoplasmic protein, presumably connected to the channel, was responsible for inactivation. Armstrong and Bezanilla (1977) proposed a physical model for the inactivation of Na^+ current in which a "ball" attached to the end of a "chain" (inactivation gate) swings into the open channel, blocking

the flow of ions through the channel. The removal of K^+ (Hoshi et al., 1990) and Ca^{2+} current (Hescheler and Trautwein, 1988) inactivation with proteolytic enzymes suggests that the "ball and chain" model is a common mechanism for inactivation of voltage-gated ion channels.

Aldrich and his colleagues took a more direct approach to investigating the mechanism of inactivation by using molecular genetic techniques. Hoshi et al. (1990) showed that deletion of 20 amino acids in the amino terminus of shaker K^+ channels completely removes fast inactivation, which was restored by exposing the cytoplasmic surface of the channel to a peptide containing the missing 20 amino acids (Zagotta et al., 1990). These results identify a cytoplasmic fragment of the channel protein, the putative "ball", that is responsible for fast inactivation. Recent molecular experiments on Na^+ channels have also identified cytoplasmic structures of the channel involved in inactivation (Vassilev et al., 1988; Moorman et al., 1990). Although these results clearly support the ball and chain model for inactivation, other mechanism of inactivation must exist because K^+ channels undergo a slow form of inactivation that is unaltered by removing both cytoplasmic termini (VanDongen et al., 1990).

Ca^{2+} current inactivation

Unlike inactivation of Na^+ and K^+ currents, there are two distinct mechanism of Ca^{2+} channel inactivation: voltage-dependent, which is similar to that of Na^+ and K^+ currents, and current-dependent, which depends on the amount of Ca^{2+} that flows into the cell (Eckert and Chad, 1984).

The mechanism of current-dependent inactivation has been extensively studied (Eckert and Chad, 1984; Kalman and Armstrong, 1988). Intracellular Ca^{2+} increases during membrane depolarization to a level that activates two kinds of Ca^{2+}-dependent enzymes: Ca^{2+}-dependent proteases which make the channel unable to open by irreversibly cleaving a fragment of the channel, and Ca^{2+}-dependent phosphatases which remove phosphates

from the channel, speeding the rate of inactivation. Because the endogenous enzymes and nucleotides that maintain channels in a functional state are dialyzed out of the cell during whole-cell recordings, the amplitude of Ca^{2+} current decreases with time, a process called "wash-out". High-affinity Ca^{2+} buffers and enzymes which maintain channels in a phosphorylated state are therefore included in the intracellular recording solution to prevent the wash-out of Ca^{2+} current due to current-dependent inactivation.

Under recording conditions that minimize the contribution of current-dependent inactivation, many whole-cell Ca^{2+} currents still decay during membrane depolarizations, suggesting that Ca^{2+} channels can also inactivate through a voltage-dependent mechanism. The rate of Ca^{2+} current inactivation is often much slower than that of Na^{+} current and varies considerably from cell to cell (Tsien et al., 1988; Bean, 1989). One explanation for the variability in inactivation is that current-dependent inactivation may not be adequately suppressed. In fact, some forms of current-dependent inactivation occur with Ba^{2+}, which is less effective at activating Ca^{2+}-dependent enzymes than is Ca^{2+}, as the charge carrier through the channel (Kasai and Aosaki, 1988). Alternatively, the whole-cell current may be carried by different types of Ca^{2+} channels that vary in their kinetics of inactivation (Fox et al., 1987a,b).

Recordings of single-channel activity from neurons have revealed a multitude of channel types that vary in their single-channel conductance, pharmacology and rates of inactivation (for review, see Bean, 1989; Hess, 1990). Although distinct types of Ca^{2+} channels may carry different components of whole-cell current, it has been recently shown that a single type of Ca^{2+} channel accounts for both the inactivating and non-inactivating components of whole-cell Ca^{2+} current in peripheral neurons (Plummer et al., 1989; Kongsamut et al., 1989; Aosaki & Kasai, 1989). Apparently, a single type of Ca^{2+} channel opens briefly in the beginning of a voltage step or opens for the duration of the voltage step, but the mechanism underlying this switch has not been investigated in detail.

Mechanisms of Ca^{2+} channel gating

Most types of Ca^{2+} channels can enter a second conductance state during membrane depolarization (T-type: Carbone and Lux, 1987b; Fox et al., 1987b: L-type: Hess et al., 1984; Hoshi and Smith, 1987; Pietrobon and Hess, 1990: N-type: Bley et al., 1990). L-type Ca^{2+} channels, for example, enter a long-lived open state in response to dihydropyridine agonists, β-adrenergic stimulation, or strong depolarizations (Hess et al., 1984; Pietrobon and Hess, 1990; Yue et al., 1990; Hoshi and Smith, 1987). Several explanations for this shift to long-duration openings have been suggested. Hess et al.(1984) proposed a modal gating scheme in which the Ca^{2+} channel switches between different sets of states (modes), each of which produces either short or long openings. Modal gating can explain the shift to long openings produced by strong depolarizations (Pietrobon and Hess, 1990), but requires a second voltage-dependent transition between closed states, separate from the voltage-dependent activation gates. Lacerda and Brown (1989) suggested a more conventional gating model in which cooperative binding of dihydropyridines at two sites on the channel promotes long-duration openings, but their model does not consider shifts in gating caused by voltage. Both models focus on transitions between closed states of the channel.

An alternative explanation for the appearance of long openings is that the channel moves among kinetically distinct open and inactivated states during membrane depolarization and the inactivated state is the primary pathway to a second open state (see Scheme 2). Chandler and Meves (1970) first described this more conventional gating scheme to explain the incomplete inactivation of axonal Na^+ channels that occurs with strong depolarizations. By measuring the Na^+ tail current that flows through channels as they close after test pulses which varied in duration, Bezanilla and Armstrong (1977) showed that large depolarizations drive Na^+ channels into a second conductance state.

According to this model, strong depolarization push the inactivation gate out of the channel, producing a second type of opening.

$$C \rightleftharpoons O_1 \longrightarrow I \rightleftharpoons O_2 \qquad \text{Scheme 2}$$

Unlike previous models of gating in which the channel move among closed states before opening into a second conductance state, Scheme 2 predicts that changes in the stability of the inactivated state will determine the relative proportion of short- and long-duration openings. Thus, both voltage and dihydropyridine agonist may promote the transition into the long-duration open state by affecting the stability of the inactivated state.

Research Plan

The main objective of this thesis is to examine in detail the inactivation of Ca^{2+} channels using the patch-clamp technique. A number of questions remain concerning the mechanism of inactivation: Is inactivation coupled to the activation process? Is the mechanism of Ca^{2+} channel inactivation similar to the "ball and chain" model proposed for Na^+ and K^+ channels? If a single type of Ca^{2+} channel carries both inactivating and non-inactivating currents, then what determines the variability in the decay of current? Because most published studies on neuronal Ca^{2+} channels have focused on channels in peripheral neurons (Tsien et al., 1988; Bean, 1989), I will study the Ca^{2+} channels in cerebellar granule cells, a neuron in the cerebellum that relays information from brainstem nuclei to Purkinje cells (Ramón Y Cajal, 1904; Somogyi et al., 1986). Cerebellar granule cells are the most abundant neuron in the brain and are easily identified in primary cell cultures, making them suitable for patch-clamp recordings.

The specific aims are to:

1. Characterize the activation and inactivation of the whole-cell Ca^{2+} current recorded from cerebellar granule cells.

2. Identify single Ca^{2+} channels which underlie the whole-cell Ca^{2+} current.

3. Discuss models of inactivation of cerebellar Ca^{2+} channels which explain the single-channel and whole-cell data.

The next four chapters present results that have been either published or submitted for publication, and are followed by concluding remarks.

Chapter 1

INTRODUCTION

Cerebellar granule cells provide the only excitatory input to Purkinje cells and are the most abundant neurones in the central nervous system (Ramón Y Cajal, 1904; Somogyi, Halasy, Somogyi, Storm-Mathisen, & Ottersen, 1986). Patch-clamp recordings from cerebellar granule cells grown *in vitro* have shown voltage-gated Na^+ and K^+ currents (Hirano, Kubo & Wu, 1986; Hockberger, Tsen, & Connor, 1987; Cull-Candy, Marshall & Ogden, 1989) as well as receptors for excitatory amino acids and GABA (Huck and Lux, 1987; Cull-Candy, Howe, & Ogden, 1988). Although Ca^{2+} influx has been observed in granule cells with Ca^{2+} sensitive dyes (Connor, Tseng, and Hockberger, 1987), macroscopic Ca^{2+}currents have been difficult to detect with patch-clamp recordings (Hirano *et al.*, 1986; Hockberger *et al.*, 1987; Cull-Candy *et al.*, 1989). Ca^{2+} currents may have been too small to measure with the whole-cell recording technique or cytoplasmic components necessary for maintaining channels in a functional state may have been removed during whole-cell perfusion.

In this paper we describe the results of experiments which investigated Ca^{2+} channel currents in granule cells under conditions that minimized Ca^{2+} current rundown. The Ca^{2+} channel current is sensitive to dihydropyridines and inactivates with a rate that has both fast and slow voltage-dependent components. A preliminary report of these results has been published in abstract form (Slesinger and Lansman, 1989).

METHODS

Tissue Culture

Cultures of dissociated cerebellar cells were prepared following a modification of the procedure described by Hatten and Sidman (1978). Seven day-old male mice (C57BL6: Simonsen) were sacrificed by decapitation under an experimental protocol approved by the Committee for Animal Research at the University of California, San Francisco. Cerebella were dissected free from the meninges, sliced with a scalpel, incubated in 1% trypsin (Sigma) in Ca^{2+}- and Mg^{2+}-free Tyrode's for 10 minutes at room temperature, and washed with media containing 0.05% DNAse (Sigma). Cerebella were dissociated mechanically by trituration through a large and then small bore fire-polished pasteur pipette to obtain single cell suspensions, pelleted at 90g for 5 minutes and resuspended in fresh media. Trypsin was omitted in some experiments, but there were no obvious differences in the electrophysiological properties of cells isolated by mechanical or enzymatic dissociation.

Cerebellar cells were plated at a density of 0.05-0.5 x 10^6 cells/ml on glass cover slips pre-coated with 25 µg/ml poly-L-lysine (Sigma). Cultures were kept in a humidified atmosphere of 5% CO_2/95% air at 37° C in a medium containing Minimal Essential Medium (MEM) with Earle's Basal salts and 2 mM glutamine (UCSF tissue culture). MEM was supplemented with 10% horse serum (Hyclone), 25 mM KCl (Sigma) and 0.06-0.2% glucose (Sigma). Cerebellar cells could be kept in culture for up to 3 weeks, although most recordings were made within the first week of plating.

Over 80% of the cells in the cerebellum are granule cells and were identified *in vitro* by their phase-bright round or oval cell body, bipolar neurites, and size (5-10 µm) (Messer, 1977; Hockberger *et al.*, 1987; Cull-Candy *et al.*, 1988). Neurones were identified by immunostaining for neurone-specific enolase (NSE) following a modification of the procedure described by Hockeberger *et al.* (1987). Cultured cells were fixed for 30 minutes in 1.5% para-formaldehyde in Tyrodode's buffer (all incubations performed at

room temperature), permeabilized for 30 minutes in 0.5% Triton X-100 (Sigma) in 50 mM Tris (pH 7.6), incubated for 1 hour in either nonimmune or primary rabbit anti-NSE antibodies (Dako Corp.) in Tris buffer, incubated for 20 minutes in swine anti-rabbit immunoglobulins (Dako Corp.), incubated for 20 minutes in horseradish peroxidase complex and stained for 10 minutes in 3-amino-9-ethylcarbazole dissolved in N,N dimethyl formamide. Astrocytes were identified by immunostaining cultures for glial fibrillary acidic protein (GFAP) using the protocol described by Hockberger *et al.* (1987). The small, ovoid cells stained positively for NSE, but not for GFAP (cf Cull-Candy *et al.*, 1988). In addition, a higher percentage of neurones that were clustered together stained negatively for NSE whereas most isolated neurones stained positively for NSE (see Hockberger *et al.*, 1987). Whole-cell currents were recorded from only isolated neurones.

Solutions

The bathing medium contained (in mM) 2-60 $CaCl_2$ or $BaCl_2$ (Aldrich Chemicals, >99.9% purity), 10 HEPES, 10 glucose and adjusted to ~320 mOsm with tetraethylammonium-chloride (TEA-Cl, Sigma) and to pH 7.4 with TEA-OH. The intracellular solution (Cs-Asp) contained 120 aspartic acid, 1 $MgCl_2$, 10 HEPES, 15 glucose, and 20 NaCl. The pH was adjusted to 7.4 with CsOH. The osmolarity was adjusted to ~320 mOsm by adding glucose.

To minimize Ca^{2+} current rundown, 5 mM EGTA (ethyleneglycol-bis-(ß-aminoethylether)-N,N,N',N'-tetraacetic acid, Sigma) or 5 BAPTA (bis-(o-aminophenoxy)-ethane-N,N,N',N'-tetraacetic acid, Molecular Probes), 2 MgATP (magnesium-5'-adenosine triphosphate, Sigma) and 1 mM cyclic AMP (adenosine 3':5'-cyclic-monophosphate, Sigma) were included in the pipette solution (Byerly and Yazejian, 1986; Chad and Eckert, 1986; Armstrong and Eckert, 1987; Fedulova, Kostyuk & Veselovsky, 1981).

The organic Ca^{2+} channel modulators (+/-)-202-791 were prepared as 10 mM stock solutions in 100% ethanol and kept at -20° C in a light-tight container. Stock solutions were diluted with the bathing solution and used immediately before each experiment. A solution containing 0.01% ethanol had no effect on Ca^{2+} channel currents. Solutions containing Cd^{2+} and Gd^{3+} were prepared from 10 mM stock solutions of the chloride salt (Aldrich Chemical, >99.9% purity) dissolved in distilled water.

Cells were exposed to a solution containing drug by perfusing locally through a ~15 μm diameter tip pipette. The perfusion pipette was lowered into the bath and positioned 10-50 μm from the granule cell after establishment of a stable recording. To study the recovery from drug effect, the perfusion pipette was removed from the bath. A peristaltic pump was used to change the bathing solution in experiments where the effects of extracellular ions were examined. Complete solution exchange required ~4 minutes.

Electrophysiology

Glass cover slips with attached cells were placed in a recording chamber mounted on a Nikon phase-contrast microscope. Whole-cell currents were recorded following the method described by Hamill, Marty, Neher, Sakmann & Sigworth (1981). Patch pipettes were made from Boralex hematocrit glass (Rochester Scientific) and had resistances of 3-6 MΩ with Cs-Asp in the pipette and 20 $BaCl_2$/TEA in the bath. Current signals were recorded with a List EPC-7 amplifier with a 0.5 GΩ feed-back resistor, filtered with an 8-pole, lowpass Bessel filter at 2 to 20 kHz (-3 dB) and sampled at 5-100 kHz. All recordings were done at room temperature, 21-24° C.

The potential between pipette solution and bath was zeroed before making a seal. In experiments where the bathing solution was changed, liquid junction potentials were measured directly by immersing the pipette containing intracellular solution into different bathing solutions. The measured junction potentials differed by less than 5 mV. The indicated potentials are not corrected for this error.

The membrane-seal resistance ranged from 5-50 GΩ. Membrane capacitance and 10-70% of series resistance were compensated electronically after a whole-cell recording was established. Voltage command pulses were generated (0.1-0.2 Hz) and current responses simultaneously digitized and stored on a laboratory computer (PDP 11/73, Indec Systems, Sunnyvale, CA). In experiments measuring tail current relaxations, current responses produced by 2-10 identical test pulses were averaged. All current traces shown were corrected for linear leak and capacity current by subtracting an appropriately scaled leak pulse (-P/10 or -P/4) unless noted in Figure legend.

A small rising phase in the tail current was observed immediately following the prepulse in some cells. This rising phase could result from the flow of current through the uncompensated fraction of the access resistance. With a typical access resistance of 6 MΩ, there would be a maximum voltage error of ~10 mV with the largest currents we observed (~1.5 nA). 2 ms. The error was likely to be less because 10-70% of series resistance was compensated electronically and most of the currents recorded were <300 pA. None of our conclusions, however, depend critically on this error.

We found that tail currents measured in cells which had been in culture for more than 1-2 days decayed along a double exponential time course with a slow time constant of 5-40 ms. The amplitude of the slow component was typically 4-10 times smaller than the amplitude of the fast component. It is likely the slow component of tail current is an artifact of poor spatial control of the membrane potential in cells which had developed long neurites in culture (>40 μm). We restricted our analysis of tail currents to granule cells that had been in culture for 1-2 days where process outgrowth was less than <10 μm.

Data Analysis

Current records were fit with a single or double exponential using a non-linear least-squares algorithm and simplex minimization routine. Activation and inactivation

curves were obtained by normalizing the amplitude of the current to their maximum values and fitting the points to a Boltzmann relation of the form

$$\frac{I}{I_{max}} = \frac{1}{1+e^{\frac{\pm(V-V_{1/2})}{k}}} \qquad (1)$$

where $V_{1/2}$ is the half-inactivation or half-activation voltage and k, the slope factor, describes the steepness of the relation. Mean values are expressed with their standard deviation.

RESULTS

To study currents passing through Ca^{2+} channels in granule cells, outward K^+ currents were suppressed by replacing intracellular K^+ with Cs^+, inward Na^+ currents were eliminated by replacing extracellular Na^+ with TEA^+, and 20 mM Ba^{2+} was included in the bathing solution as the charge carrier through Ca^{2+} channels. We found that Ca^{2+} channel currents decreased to ~30 ± 20% (n=5) of its peak value by 15 minutes after a whole-cell recording was established. The time course of the current during the test pulse did not change appreciably as the size of the current became smaller , suggesting that the reduction in current amplitude reflected a decrease in the number of functional channels. Inclusion of 1 mM cyclic AMP in the intracellular solution, however, slowed the loss of Ca^{2+} channel current and was routinely included in subsequent recordings.

Time course of Ca^{2+} channel current

Strong depolarizations from a negative holding potential produce an inward current that activates rapidly and decays to a non-zero level by the end of a 160 ms voltage step. Figure 1A shows an example of a set of Ca^{2+} channel currents produced in response to voltage steps of increasing amplitude. A voltage step to 0 mV produced a slowly activating current which did not decay appreciably during the pulse. Voltage steps to +20 or +40 mV, however, elicited currents that decayed during the pulse. A plot of either the average peak current or the current at the end of the pulse as function of test potential from a number of experiments had a single peak near +20 mV with a half-activation voltage ($V_{1/2}$) = ~-10 mV (Fig. 1B).

A striking feature of Ca^{2+} channel currents recorded from cerebellar granule cells is that the extent of decay during positive voltage steps varied considerably from cell to cell. Fig. 1C shows a histogram of the fraction of the decaying component of current measured as the difference between the peak and steady-state current divided by the peak current. Ca^{2+} channel current decayed to 40 ± 15% (n=43) on average, although some currents

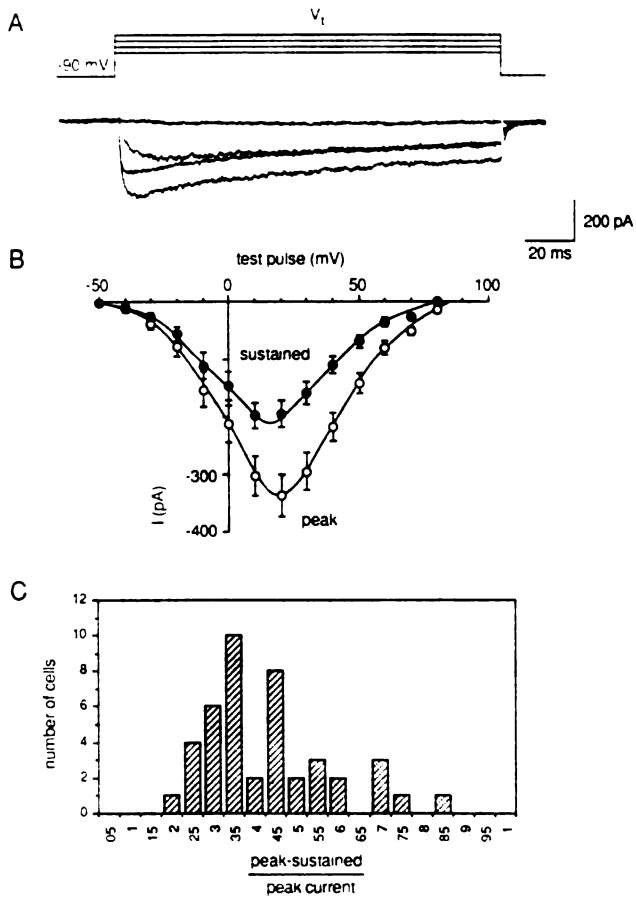

Figure 1: Time course of inward Ca^{2+} channel current recorded from cultures of cerebellar granule cells. **A**, currents elicited by voltage steps to -50, 0, +20 and +40 mV from a holding potential of -90 mV. Cell G47D. **B**, peak current and the current remaining at the end of the pulse (sustained) plotted as a function of test potential (mean ± SEM, n=17). **C**, histogram of the fraction of total current that decayed [(peak-sustained)/peak]. All recordings made with 20 mM Ba^{2+} in the bath.

decayed to ~10% of their peak value (see Fig. 3). Unlike the amplitude of decaying current, cell capacitance varied over a small range of values (4.1 ± 1.5 pF, n=43).

Activation of Ca^{2+} channel current

We examined the voltage dependence of the activation process by measuring the amplitude of tail current, which flows through channels as they close, after rapidly repolarizing the membrane potential from different test potentials. Figure 2A shows tail current relaxations measured after repolarizing the cell to a potential of -70 mV following 15 ms prepulses to potentials of increasing amplitude.

Tail currents decayed to zero current along a single exponential time course with a time constant of 0.5 ± 0.2 ms (n=5) at -70 mV. The time constant of the tail current measured at -30 mV was 0.9 ± 0.3 ms (n=5), consistent with previous results showing that more positive membrane potentials slow the decay of tail current (cf Hagiwara and Ohmori, 1982, Carbone and Lux, 1987a, but see Swandulla and Armstrong, 1988).

Making the prepulse potential more positive increased the amplitude of the tail current, but the amplitude reached a maximum for test pulses more positive than ~+30 mV. Figure 2B shows the results from a number of experiments in which the amplitude of the tail current was normalized to its maximum amplitude. The normalized amplitude of the tail current was well fit by a Boltzmann relation with half-activation ($V_{1/2}$) = +8 mV and a steepness k = 14 mV (see Figure legend for details).

Effect of the holding potential on Ca^{2+} channel current

We next examined the effect of the holding potential on Ca^{2+} channel current by measuring peak current elicited in response to a voltage step to a fixed potential after shifting the holding potential to various potentials for ~10 seconds. Fig. 3A shows two sets of currents recorded from different cells: the top set of records show a cell in which the current decayed only slightly during the pulse, while the bottom records are from a cell in

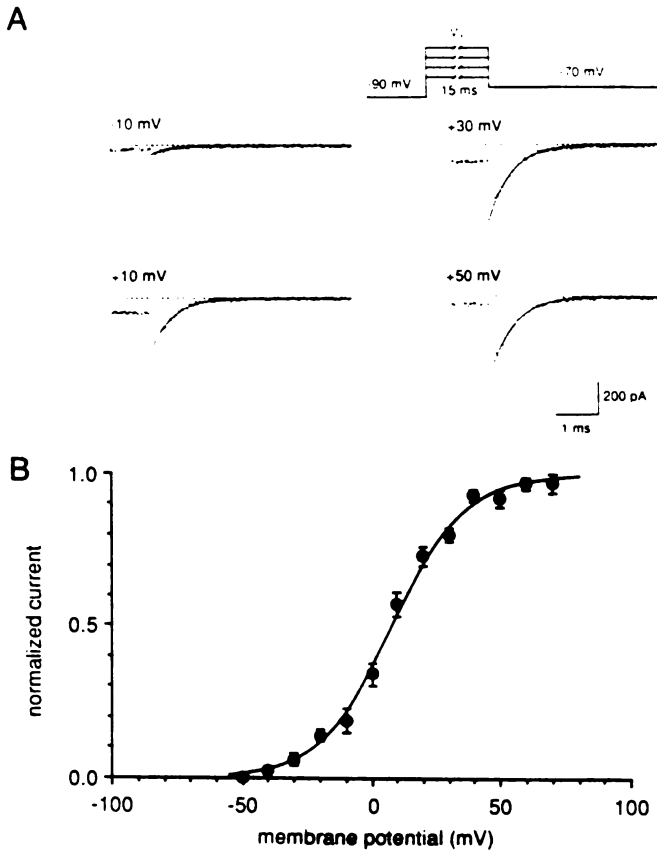

Figure 2: Activation of Ca^{2+}channel current in cerebellar granule cells. **A**, tail currents produced after repolarizing the membrane to -70 mV immediately following a 15 ms prepulse to -10, +10, +30 or +50 mV (voltage protocol at top of Figure). Smooth curve through points drawn to a single exponential having time constants of 0.48, 0.51, 0.56 and 0.57 ms with amplitudes of -65, -369, -580, and -574 pA for voltage steps to -10, +10, +30 and +50 mV, respectively. Cell H01B. **B**, amplitude of the tail current normalized to its maximal value and plotted as a function of prepulse potential (mean ± SEM, n=12). Points were fit with a Boltzmann relation of the form

$$\frac{I}{I_{max}} = \frac{1}{1+e^{\frac{-(V-V_{1/2})}{k}}}$$

where $V_{1/2}$ = 8 mV and k = 14 mV. The bathing solution contained 20 mM Ba^{2+}. Currents were sampled at 100 kHz and filtered at 20 kHz.

which the current decayed substantially. Even though the maximum decay of the current elicited from very negative holding potentials varied considerably (the holding potential is indicated next to the current trace), making the holding potential more positive than ~-60 mV abolished the decaying phase as well as reduced the amplitude of the current. The normalized amplitude of the current was plotted as a function of the holding potential and the points fit to a Boltzmann function for steady-state inactivation (see Figure legend for details). The fits were indistinguishable, suggesting that the extent of decay during the pulse does not determine the response to changes in holding potential. Figure 3B shows the average reduction in current measured from a number of cells over a range of holding potentials. The fit to a Boltzmann relation gave a half-inactivation ($V_{1/2}$) = -57 mV and a steepness k= 14 mV.

The curve describing the activation of Ca^{2+} channel current is re-plotted in Fig. 3B (small circles) and shows the voltage range in which the activation and inactivation curves overlap. At a holding potential of ~-60 mV approximately half the channels are unavailable for opening even though no channels are open at this potential. Evidently, resting Ca^{2+} channels can inactivate without first opening. This suggests that the reduction in current as the holding potential is made more positive involves voltage-dependent inactivation. The overlap between the curves shown in Fig. 3B also indicates the range of potentials where steady non-inactivating currents may flow through Ca^{2+} channels.

Effect of permeant ion on the time course of Ca^{2+} channel current

Figure 4A shows the results of experiments in which the effect of the species of inward charge carrier on the decay of current during the pulse was investigated. The bathing solution first contained 20 mM Ca^{2+} and was then exchanged with a solution containing 20 mM Ba^{2+}. The currents produced in the presence of 20 mM Ba^{2+} were larger than those recorded with 20 mM Ca^{2+} (Fig. 4A*i*, I-V). The average ratio of the peak Ba^{2+} current to peak Ca^{2+} current was 2.1 ± 0.1 (n = 3), similar to that observed for

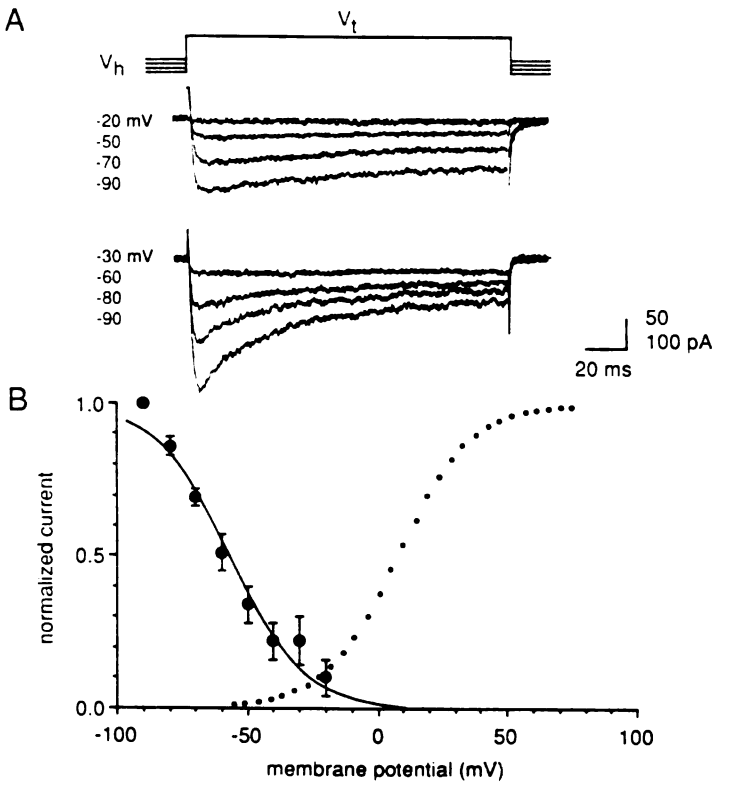

Figure 3: Effect of holding potential on amplitude and time course of Ca^{2+} channel current in granule cell with a small or large decaying current. **A**, currents elicited by voltage steps to +20 (top) or to +10 mV (bottom) after shifting the holding potential (V_h) to the potential indicated by each trace. The voltage error produced by peak current flowing through ~3 MΩ access resistance was less than 1 mV. Scale, 100 pA (top traces) and 50 pA (bottom traces). Cells G76B and G46B. **B**, average peak current normalized to maximal current produced by voltage steps plotted as a function of holding potential. Points were fit with a Boltzmann relation of the form

$$\frac{I}{I_{max}} = \frac{1}{1+e^{\frac{V-V_{1/2}}{k}}}$$

where $V_{1/2}$ = -57 mV and k = 14 mV (mean ± SEM, n=8). The inactivation curves for the two cells shown in A were also fit by a Boltzman relation where $V_{1/2}$ = -62 & -60 mV and k = 15 &12 mV, respectively. In some cells, Ca^{2+} channel current did not fully recover to its original level after the membrane was depolarized for seconds (less than 10% change), suggesting the existence of a very slow, irreversible process. The curves were not corrected for this slow process. The activation curve from Fig. 2 is shown for comparison (small circles). The pipette solution contained 5 mM EGTA. The bathing solution contained 20 mM Ba^{2+}. Currents were sampled at 5 kHz and filtered at 2 kHz.

high-threshold Ca^{2+} currents in other preparations (Hagiwara and Ohmori, 1982; Matteson and Armstrong, 1986; Swandulla and Armstrong, 1988, Fedulova *et al.*, 1981).

When the Ca^{2+} current elicited by a voltage step near the peak in the I-V was scaled by a constant to match peak Ba^{2+} current, the time courses were indistinguishable (Fig. 4A*ii*). This suggests that the species of divalent cation does not determine the time course of the decay of current. In addition, a two-fold increase in the amplitude of inward current did not alter the rate of decay. This finding was confirmed in another cell where the amplitude of the Ca^{2+} channel current was varied by elevating external Ba^{2+}. A two-fold increase in the amplitude of the current produced only a small increase in the rate of decay (Fig. 4B*ii*). Neither the species of the permeant ion nor the amplitude of the inward current influences the rate of decay during a positive voltage pulse.

The amplitude of Ca^{2+} channel current increased as the concentration of external Ba^{2+} was raised, reaching a maximum with concentrations of Ba^{2+} greater than 20 mM (cf Hagiwara and Byerly, 1981). The saturation of Ca^{2+} channel current at high concentrations of $[Ba^{2+}]_o$ is shown in Figure 4B. The peak current measured in the presence of each concentration of Ba^{2+} was normalized to current measured in the presence of 20 mM Ba^{2+} and plotted as a function of $[Ba^{2+}]_o$. Peak current reached a maximum amplitude at concentrations of external Ba^{2+} greater than 20 mM. The points were fit with an expression for binding to a single site with a dissociation constant K_d of ~3 mM. A similar K_d was obtained when the current at the end of the pulse was plotted against $[Ba^{2+}]_o$. Our estimate for the low affinity binding site is similar to the K_d found for the low-threshold Ca^{2+} channel current in dorsal root ganglion cells (Carbone and Lux, 1987a), but is somewhat smaller than that reported for the saturation of unitary Ba^{2+} currents through cardiac Ca^{2+} channels (Hess, Lansman, and Tsien, 1986).

Effect of the test potential on the rate of decay of Ca^{2+} channel current

The results show that Ca^{2+} channel current elicited by strong depolarizations from a negative holding potential decays with a rate that is independent of the amplitude of current or the species of charge carrier. The rate of decay, however, was well fit by a single

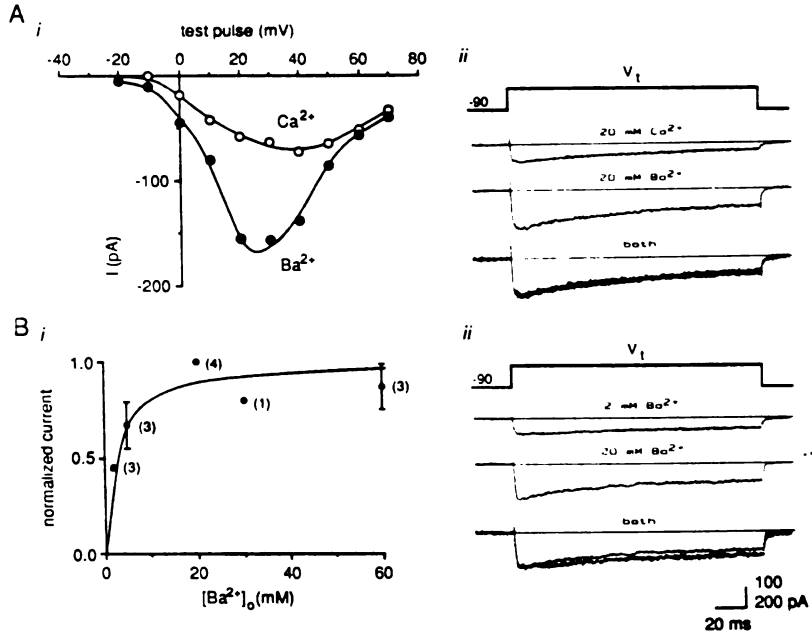

Figure 4: Effect of permeant cation species and amplitude of current on the decay of current recorded from granule cells. ***Ai***, peak current plotted as function of the test potential for a granule cell bathed first in a solution containing 20 mM Ca^{2+} (○) and then Ba^{2+} (●). ***Aii***, current elicited by a test pulse to +40 mV (top trace) while recording in Ca^{2+} is scaled by 2.0 and shown superimposed (bottom traces) on current elicited by a test pulse to +30 mV recorded with Ba^{2+} in the bath (middle trace). The pipette solution contained 5 mM BAPTA. Cell H17B. ***Bi***, peak current recorded from cells bathed in 2, 5, 20, 30 and 60 mM Ba^{2+} normalized to current in 20 mM Ba^{2+} plotted as a function of $[Ba^{2+}]_o$ (mean ± SEM; *n* indicated in figure). Points were fit by the curve

$$\frac{I}{I_{max}} = \frac{1}{1+e^{\frac{V-V_{1/2}}{k}}}$$

with a K_d of ~3 mM. The sequence of solution changes was varied in each experiment because the amplitude of the Ca^{2+} channel current decreased by roughly 6% over the 5 minute period required to change the solutions. Cells H16C, H16D, H17B and H17C. ***Bii***, current elicited by a test pulse to +20 mV (top trace) while recording in 2 mM Ba^{2+} is scaled by 2.2 and shown superimposed (bottom traces) on current elicited by a test pulse to +20 mV recorded with 20 mM Ba^{2+} in the bath (middle trace). Cell H17C. All currents were sampled at 5 kHz and filtered at 2 kHz.

exponential. The smooth curve drawn through the decaying component in Fig. 5A shows the fit to a single exponential with the indicated time constant relaxing to a sustained component. The time constants describing the decay of current were obtained from fitting individual traces like that shown in Fig. 5A and were plotted as a function of the potential during the test pulse. Fig. 5B shows the that the the rate of decay of the current was relatively independent of membrane potential at test potentials more positive than ~+10 mV. At test potentials more negative than +10 mV the amplitude of the decay was too small to obtain an accurate fit to the data.

To investigate the onset of inactivation at negative potentials a two-pulse voltage clamp protocol was used in which the amplitude and duration of a preceding test pulse was varied and the fraction of available channels assayed by a second test pulse. Figure 6 shows the results of an experiment in which the voltage dependence of the reduction of peak current was investigated. The voltage protocol and two examples of current responses are shown at the top of Fig. 6A. A prepulse to +30 mV for 300 ms reduced the peak current elicited by a test pulse to +40 mV. The effect of the prepulse potential on peak current is shown for two different prepulse durations in Fig. 6B. The current during the test pulse was normalized to that measured in the absence of a prepulse and plotted as a function of prepulse potential. The curves are U-shaped and show that positive prepulses reduced peak current, but that prepulses more positive than +30 mV were less effective at reducing peak current. Neither curve measured with the two-pulse protocol was as steep as the inactivation curve measured by changing the holding potential (crosses), suggesting that a 300 ms prepulse was too short for inactivation to reach steady-state.

Fig. 7A shows the current produced by the test pulse to +40 mV following 10, 1500 or 3000 ms prepulses to -10 mV (the voltage protocol is shown above the current records). Increasing the duration of the prepulse reduced the peak current elicited by the test pulse. The peak current during the test pulse was normalized to that obtained in the absence of a prepulse and plotted as a function of prepulse duration. Fig. 7B shows the onset of

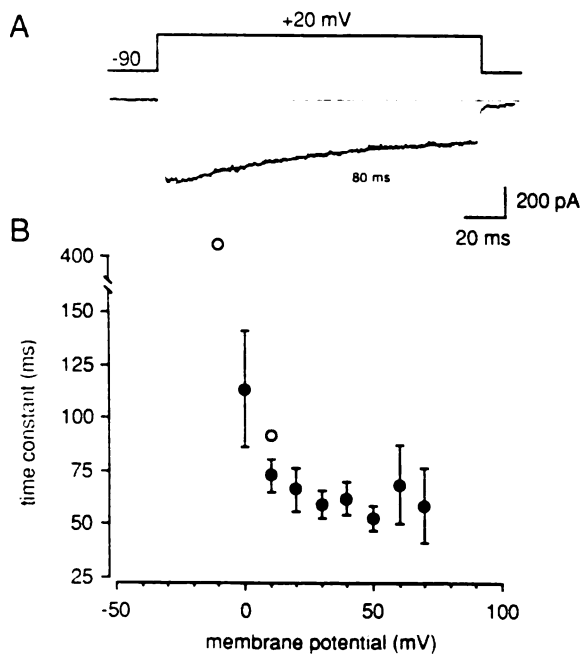

Figure 5: Time course of the decay of Ca^{2+} channel current elicited by a 160 ms voltage step to different potentials. **A**, example of current elicited by a voltage step to +20 mV. A single exponential relaxing to a sustained level (time constant indicated below trace) is superimposed on the current record. Cell G47E. **B**, time constant of the decay of current plotted as a function of test pulse (mean ± SEM, n=17). Open circles are the time constants measured for the fast component of inactivation in Fig. 7. The bathing solution contained 20 mM Ba^{2+}. Currents were sampled at 5 kHz and filtered at 2 kHz.

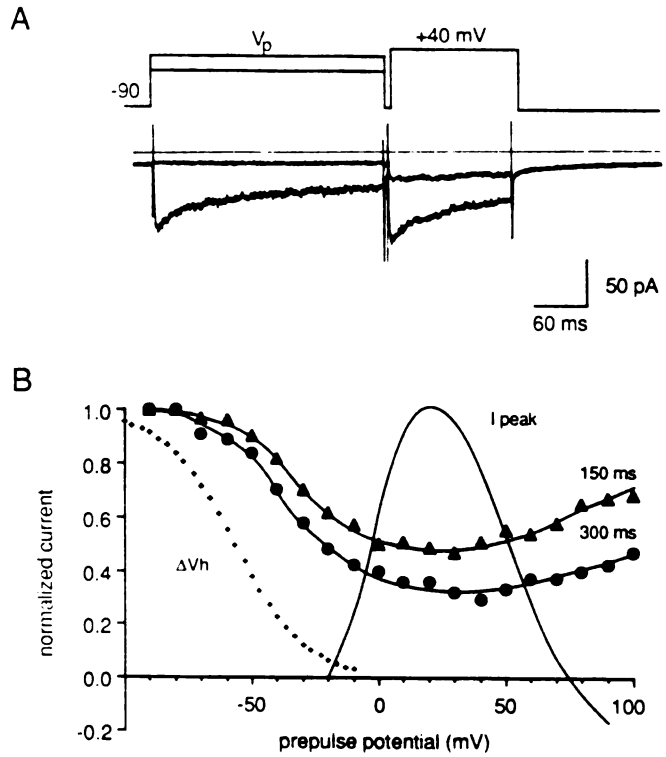

Figure 6: Effect of depolarizing prepulses on Ca^{2+} channel current elicited by a second test pulse. **A**, current records showing the effect of a 300 ms prepulse (V_p) to either -80 or +30 mV. The prepulse was followed by a 160 ms test pulse to +40 mV with a 5 ms interval between pulses. Currents are not leak subtracted and straight line indicates zero current. Holding potential was -90 mV. **B**, peak current produced by the test pulse normalized to maximal current and plotted as a function of prepulse potential for 150 or 300 ms prepulse (solid symbols). Normalized peak current elicted during the prepulse is also plotted as a function of prepulse potential (inverted). The change in normalized current after shifting to more positive holding potentials is shown for comparison (crosses: from Fig. 3). The bathing solution contained 20 mM Ba^{2+}. The pipette solution contained 5 mM EGTA. Currents were sampled at 5 kHz and filtered at 2 kHz. Cell H42B.

inactivation at -30, -10, and +10 mV. The time course of the onset of inactivation was well fit by a sum of two exponentials with fast and slow components (see Figure legend). Both fast and slow time constants decreased as the prepulse potential was made more positive.

The fast time constant for the reduction of peak current measured in the two-pulse experiment shown in Fig. 7 is compared with the time constant obtained from fitting a single exponential to the decay of current during the pulse (open circles in Fig.5B are from the fast component measured in the two-pulse experiment). The points fall along the same curve, suggesting that the fast process measured with the two-pulse experiment is the same as that responsible for the decay of current during the pulse. Consistent with the existence of fast and slow components to inactivation, the decay of current elicited by an 800 ms voltage pulse followed a double exponential time course with fast and slow time constants similar to those measured in the two-pulse experiments (data not shown).

Effect of membrane potential on the recovery from inactivation

Figure 8 shows the results of an experiment in which the time course of the recovery of Ca^{2+} channel current from inactivation after a prepulse to +30 mV for 300 ms which reduces peak current to ~40% (Fig. 6B) was investigated. Fig. 8A shows the currents produced by a test pulse to +30 mV delivered either 100, 400 or 1000 ms following a prepulse to +30 mV (the voltage protocol is shown at the at top). The amplitude as well as the decay of current elicited by the second test pulse recovered as the interval between the prepulse and the test pulse was lengthened. When the test pulse was delivered 1000 ms after the prepulse, Ca^{2+} channel current recovered to ~75% of its original peak value. The time course of recovery at two different membrane potentials is shown in Fig. 8B, where the normalized current is plotted as a function of the interpulse interval. The rate of recovery from inactivation was more rapid at more negative membrane potentials. The points were well fit by a double exponential with fast and slow components. Both rates of

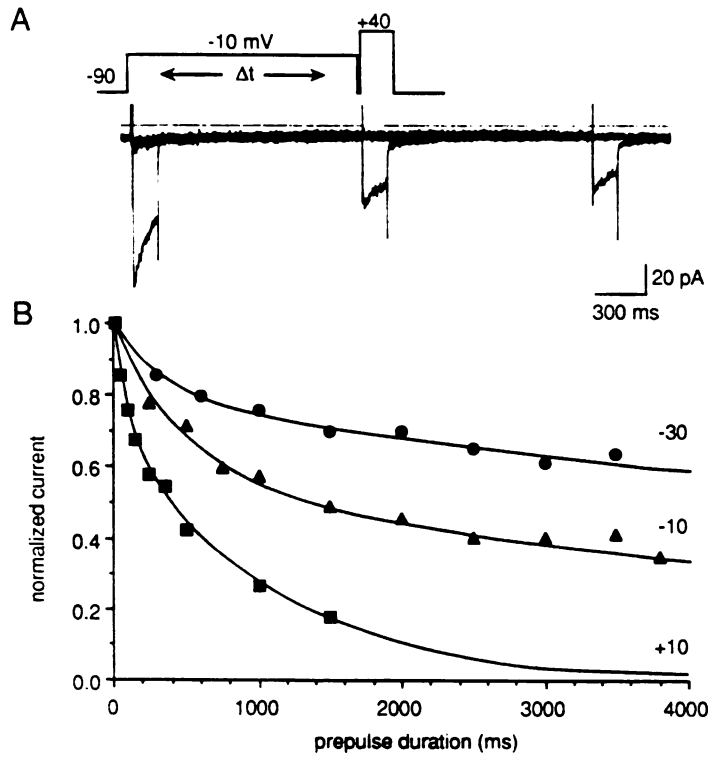

Figure 7: Effect of increasing prepulse duration on Ca^{2+} channel current elicited by a second test pulse. A, current records produced in response to a 10, 1500 or 3000 ms prepulse to -10 mV followed by a 160 ms test pulse to +40 mV (2 ms interpulse interval). The time to the onset of inward current represents the length of prepulse. Currents are not leak subtracted and straight line indicates zero current. Holding potential was -90 mV. B, peak current normalized to maximal current is plotted as a function of prepulse duration for three different prepulse potentials. The data points were fit with a sum of two exponentials having fast time constants of 340, 470 and 90 ms with amplitudes of 0.21, 0.43 and 0.32 and slow time constants of 13.4, 7.6 and 1.1 seconds with amplitudes of 0.79, 0.57 and 0.72 for -30, -10 and +10 mV, respectively. The bathing solution contained 20 mM Ba^{2+}. The pipette solution contained 5 mM BAPTA. Currents were sampled and filtered at 2 kHz. Cell G99C.

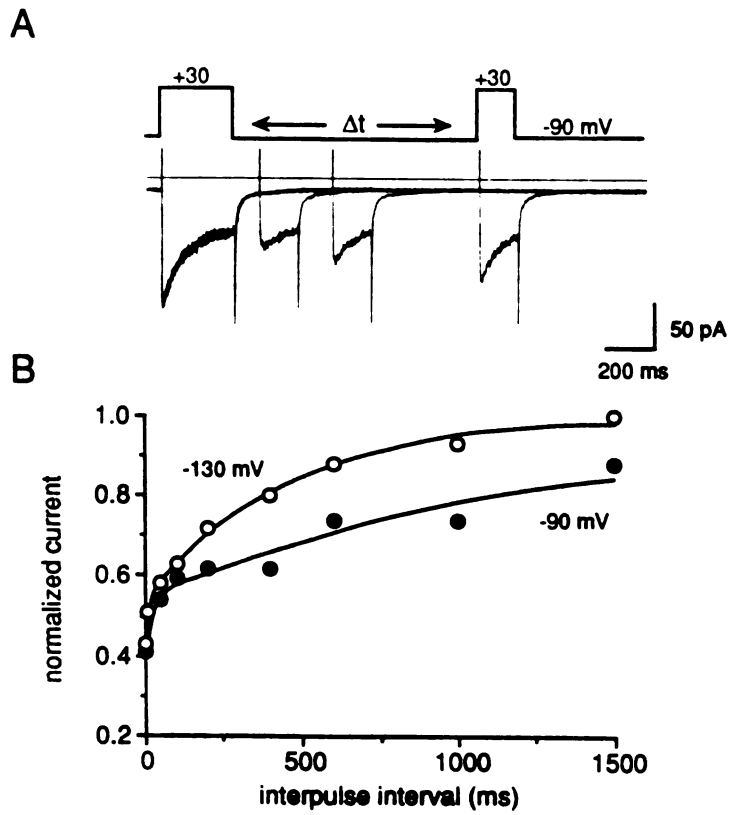

Figure 8: Effect of pulse interval duration on the recovery from inactivation produced by a prepulse. **A**, current records showing the effect of a 300 ms prepulse to +30 mV followed by a 160 ms test pulse to +30 mV. The two voltage steps were separated by either 100, 400 or 1000 ms at -90 mV. Currents are not leak subtracted and straight line indicates zero current. Holding potential was -90 mV. **B**, peak current produced by the test pulse normalized to peak current during the prepulse plotted as a function of interpulse interval at two membrane potentials. Smooth curve shows the fit of a sum of two exponentials subtracted from unity. Time constants were 20 ms (amplitude=.15) and 1358 ms (amplitude=.46) at -90 mV and 8 ms (amplitude=.14) and 458 ms (amplitude=.46) at -130 mV. The bathing solution contained 20 mM Ba^{2+}. Currents were sampled at 2 kHz and filtered at 1 kHz. Cell H90C.

recovery were faster at -130 mV than at -90 mV, suggesting the recovery process is voltage-dependent.

Modification of Ca^{2+} channel current by dihydropyridines

Ca^{2+} channel currents in neurones have been distinguished by their response to dihydropyridines, but the actions of dihydropyridines are complicated by voltage and state dependent binding and mixed antagonist/agonist actions (Docherty and Brown, 1986; Brown, Kunze & Yatani, 1986; Kamp, Sanguinetti & Miller, 1989; Kostyuk, Shuba and Savchenko, 1988). We selected the dihydropyridine agonist +(S)-202-791 because of its relatively pure agonist actions (Hof, Rüegg, Hof, and Vogel, 1985) to examine the effect of dihydropyridines on the Ca^{2+} channel current in granule cells.

Figure 9 shows an example of the effect of 1 μM +(S)-202-791 on Ca^{2+} channel current elicited by voltage steps to different potentials. Fig. 9A*i* shows that agonist increased the amplitude of the Ca^{2+} channel current produced in response to voltage steps to +10 or +30 mV, but not to +50 mV. Agonist increased peak current by 166 ± 35% (n=8) of control. Plotting peak current as a function of test potential shows the increase in current produced by agonist over a wide range of test potentials (Fig. 9B). The I-V curve is shifted by ~10 mV to more negative potentials in the presence of agonist (cf Docherty and Brown, 1986; Markwardt and Nilius, 1988).

The increase in current with agonist was very small at test potentials more positive than +50 mV. This result was unexpected because the amplitude of the tail current appeared to increase following test pulses to +50 mV in the presence of agonist (Fig. 9A*i*, bottom traces). We examined the effect of agonist on tail current relaxations produced following short prepulses. Figure 9A*ii* shows the effect of +(S)-202-791 on tail current relaxations measured following a 25 ms prepulse to +20 mV. A fit to the decaying phase of the tail current showed that the rate of deactivation was slowed in the presence of agonist (cf Hess, Lansman & Tsien, 1984). The time constant for deactivation measured after repolarizing

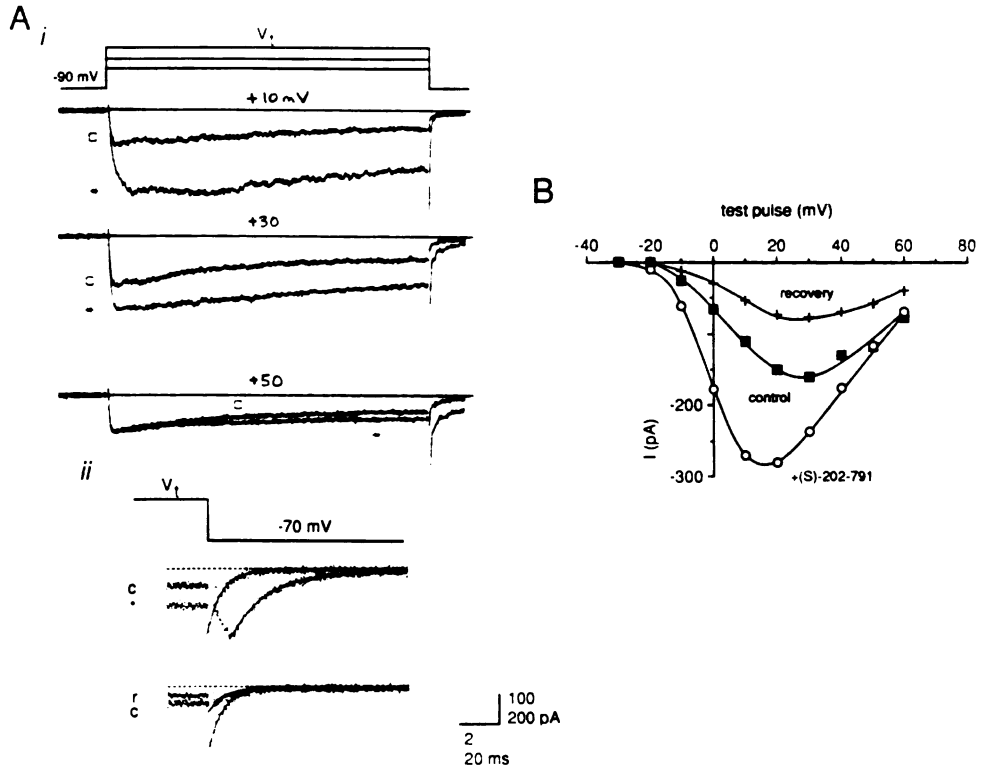

Figure 9: Response of Ca^{2+} channel currents to the dihydropyridine agonist +(S)-202-791. **A*i***, current elicited in response to 160 ms voltage steps to +10, +30, and +50 mV before (**c**) and during exposure to +(S)-202-791 (✱). Scale, 100 pA and 20 ms. **A*ii***, tail currents measured at -70 mV following a 25 ms prepulse to +20 mV (voltage protocol at top): control (**c**), during exposure to agonist (✱) and several minutes after the perfusion pipette had been removed from the bath (**r**). Smooth curve through points drawn to a double exponential with fast time constant of 0.35 ms and amplitude -438 pA before exposure to drug (**c**), 0.85 ms (amplitude not determined) during exposure to agonist (✱) and 0.33 ms with amplitude -158 pA following removal of perfusion pipette (**r**). The slow time constant had a negligible amplitude (<40 pA). Scale, 200 pA and 2 ms. **B**, peak current measured before (■), during exposure to +(S)-202-791 (**O**) and after removing the perfusion pipette containing agonist from the bath (+) plotted as function of test pulse voltage. The patch pipette contained 5 mM EGTA. Currents were sampled at 5 (**A*i***) or 100 (**A*ii***) kHz and filtered at 2 (**A*i***)) or 20 kHz (**A*ii***). Cell H11B.

the membrane to -70 mV increased from ~0.35 ms (control) to ~0.85 ms in the presence of 1 μM +(S)-202-791 (see Figure legend).

The rising phase in the tail current measured in the presence of agonist could have resulted from an artifact arising from current flow through uncompensated series resistance. However, the rising phase was observed even though the increase in the amplitude of the current during the pulse was small. Single-channel recordings reveal that in the presence of dihydropyridine agonist a fraction of the Ca^{2+} channels open after a delay folowing the repolarization (unpublished results) and could produce a rising phase in the macroscopic tail current.

The enhancement of Ca^{2+} channel current by +(S)-202-791 was reversible. After removing the perfusion pipette containing the agonist from the bath, the I-V relation (Fig. 9B) and the rate of deactivation (Fig. 9A*ii*, bottom tail currents) returned to control levels, although peak currents were smaller than before exposure to agonist. Reapplying agonist once again increased the current and slowed deactivation in a manner similar to the initial exposure, suggesting the response to agonist was reversible and that the initial recovery to a level below control was not due to an irreversible rundown of the current.

In other experiments (not shown), 10 μM of the dihydropyridine antagonist -(R)-202-791 reduced peak and sustained currents to 63%±14% and 42%±19% of control (n=11).

Inorganic Ca^{2+} channel blockers

Different components of Ca^{2+} channel current can be selectively blocked with multivalent cations (cf Narahashi, Tsunoo, and Yoshii, 1987). Gadolinium ions (Gd^{3+}) have been reported to block a decaying, but not sustained component of Ca^{2+} channel current in NG108-15 cells (Docherty, 1988). In granule cells, 20 μM Gd^{3+} blocked 94% ± 6% of peak and 86% ± 5% of sustained current elicited by a test pulse to ~+20 mV (not shown: n=3). Therefore, Gd^{3+} does not selectively block a decaying component of Ca^{2+} channel current in granule cells (cf Lansman, 1990). Cadmium blocks Ca^{2+} channel

current in cardiac myocytes (Lansman, Hess & Tsien, 1986; Tsien, Hess, McCleskey & Rosenberg, 1987) as well as in neurones (Narahashi *et al.*, 1987; Hirning, Fox, McCleskey, Olivera, Thayer, Miller & Tsien, 1988). In granule cells, 20 μM Cd^{2+} blocked 84% ± 8% of peak and 87% ± 11% of sustained current elicited by a voltage step to +10 mV (not shown: n=3).

DISCUSSION

Ca^{2+} channel currents of ~300 pA can be recorded from cerebellar granule cells for more than 15 minutes when rundown of Ca^{2+} current is minimized. The requirement for cyclic AMP in the pipette solution to prevent current rundown may explain why Ca^{2+} channel currents were not observed in previous patch-clamp recordings from granule cells (Hockberger *et al.*, 1987; Cull-Candy *et al.*, 1989). In addition, granule cells isolated from rat cerebellum may be more sensitive to rundown than those from mouse cerebellum.

The extent of the decay of current observed during a maintained depolarization from a negative holding potential varied from cell to cell. It did not appear to be associated with obvious morphological features, such as long neurites or growth cones, cell size, or time in culture. The variability in size of the decaying current may indicate that granule cells are a more heterogeneous population of cells than generally thought. Alternatively, the membrane properties of granule cells may vary in tissue culture. For example, granule cells from the 7 day old mice used for these experiments are in the process of migrating from the external to internal granular cell layer and may be in several different stages of differentiation *in vitro* (Altman, 1972; Burgoyne and Cambray-Deakin, 1988).

Mechanism of inactivation

Macroscopic Ca^{2+} channel current inactivates with a rate that has fast and slow components. Several mechanism can explain the time course of current: (1) There are two distinct types of Ca^{2+} channels which have different rates of inactivation. Recordings of single-channel activity from granule cells, however, show only one type of Ca^{2+} channel (Slesinger and Lansman, 1990). (2) A single type of Ca^{2+} channel interconverts between two closed states and, depending on the closed state prior to opening, will either inactivate rapidly or slowly. This mechanism is formally similar to (1) when the rate of interconversion between closed states is very slow. (3) The third model is similar to that proposed by Armstrong and Gilly (1979) for axonal Na^{+} channels in which the channel has

two inactivated states that can be reached from either the closed state preceding the open state or directly from the open state. This model is consistent with the two rates of onset and recovery from inactivation observed in this study. Furthermore, the data suggest that closed channel inactivation is strongly voltage-dependent (Fig. 3B), while inactivation from the open state does not depend on voltage (Fig. 5B). The voltage dependence of the onset and recovery from inactivation would then reflect primarily that of the closed-inactivated transition.

The contribution of current-dependent inactivation to the decay of current during the pulse should have been minimal under the conditions of these experiments because: *(i)* Ca^{2+} channel currents recorded in cells bathed with Ca^{2+} or Ba^{2+} decayed with similar rates (Fig. 4A*ii*), *(ii)* a 2-fold increase in amplitude of current produced by elevating the concentration of external Ba^{2+} did not alter the decay appreciably (Fig. 4B*ii*), and *(iii)* inward current decayed even though the recording electrode contained high concentrations of BAPTA (cf Chad and Eckert, 1986). The observation of a U-shaped inactivation curve at very positive potentials suggests there may be some contribution from current-dependent inactivation at positive potentials. An alternative explanation for the U-shape inactivation curve, however, is that positive prepulses can potentiate Ca^{2+} channel current giving the appearance of a reduction of inactivation by positive prepulses (cf Hoshi, Rothlein & Smith, 1984; Jones and Marks, 1989). Consistent with this interpretation, positive prepulses increase unitary Ca^{2+} channel activity in recordings from cell-attached patches on granule cells (Slesinger and Lansman, 1990).

Comparison to other Ca^{2+} currents in neurones

Low-threshold or T-type currents that activate at negative membrane potentials and inactivate completely are found in many types of mammalian neurones (Nowycky, Fox & Tsien, 1985b; Fox, Nowycky & Tsien, 1987a; Carbone and Lux, 1987a; Swandulla and Armstrong, 1988, Yaari, Hamon & Lux, 1987). Although we never observed T-type

currents in recordings from granule cells, we cannot exclude the possibility that a small fraction of macroscopic current T-type current went undetected.

High-threshold Ca^{2+} currents which activate in response to large depolarizations are common in neurones, but vary in the extent and rate of inactivation as well as their pharmacological sensitivity (Fedulova, Kostyuk & Veselovsky, 1985; Nowycky *et al.*,1985b; Fox *et al.*, 1987a; Carbone and Lux, 1987a; Kostyuk *et al.*, 1988; Yaari *et al.*, 1987; Wanke, Ferroni, Malgaroli, Ambrosini, Pozzan & Meldolesi, 1987; Hirning *et al.*, 1988). High-threshold currents have been subdivided into N-type and L-type current. N-type current decays substantially during a maintained depolarization from a negative holding potential and is selectively inactivated at positive holding potentials. L-type current decays very little during a maintained depolarization and is sensitive to dihydropyridines (Nowycky *et al.*, 1985b; Fox *et al.*, 1987a). The activation and inactivation curves as well as sensitivity to dihydropyridines of Ca^{2+} channel current recorded from granule cells are similar to the L-type current in dorsal root ganglion. On the other hand, the decaying component of current in granule cells resembles N-type current: both decay with similar rates and are abolished with more positive holding potentials. Ca^{2+} channel current in granule cells is therefore not easily classified as exclusively L-type or N-type current because it has properties of both.

Function of Ca^{2+} channels in cerebellar granule cells

The Ca^{2+} channel currents described in this paper may mediate the Ca^{2+} influx required for release of neurotransmitter. Consistent with our results showing that dihydropyridines modulate Ca^{2+} channel current, dihydropyridines have also been shown to alter $^{45}Ca^{2+}$ uptake into granule cells and affect the amount of transmitter released (Kingsbury and Balázs, 1987; Zhu and Chuang, 1987; Carboni and Wojcik, 1988). Because the number of Ca^{2+} channels available for opening can vary between 80 to 30% over a 20 mV range of holding potentials more positive than -80 mV (Fig. 3B), small

changes in the cell's resting potential (-70 mV, unpublished result) will have a large effect on the number of Ca^{2+} channels available for opening by brief depolarizations.

Chapter 2

INTRODUCTION

In neurones of the peripheral nervous system, the inward Ca^{2+} current evoked by a strong depolarization from a negative holding potential decays to a non-zero level, while a voltage step to the same potential from a more depolarized holding potential produces a non-decaying current (Nowycky, Fox & Tsien, 1985b; Fox, Nowycky & Tsien, 1987a). If a depolarized holding potential simply reduced the number of channels available for opening, then the decay of current during the pulse should have the same time course as the current elicited from a negative holding potential. This finding prompted the idea that the decaying current is distinct from the non-decaying current; that is, the decaying current is carried by Ca^{2+} channels that are available for opening only from negative holding potentials and that inactivate during the positive voltage step carry the decaying component of current (Fox, Nowycky & Tsien, 1987b). There is now considerable experimental evidence showing that the decaying component is a general characteristic of neuronal Ca^{2+} currents (reviewed by Bean, 1989).

The suggestion that specific types of Ca^{2+} channels have different roles in neuronal function has stimulated interest in identifying different types of Ca^{2+} channels (Miller, 1987; Tsien, Lipscombe, Madison, Bley and Fox, 1988). We have focused attention on the Ca^{2+} channels in cerebellar granule cells, the most abundant neurone in the central nervous system (Ramón Y Cajal, 1904; Somogyi, Halasy, Somogyi, Storm-Mathisen, & Ottersen, 1986). Like the Ca^{2+} current in peripheral neurones, the Ca^{2+} current in cerebellar granule cells decays only when the test pulse is delivered from a negative holding potential (Slesinger and Lansman, 1991a). In this paper we describe experiments designed to understand at the single-channel level the mechanism which produces decaying and non-decaying Ca^{2+} currents. Our results show that a 22 pS dihydropyridine-sensitive channel,

with properties similar to L-type channels (Fox *et al.*, 1987b), produces inactivating and non-inactivating single-channel currents which can account for the time and voltage dependence of the whole-cell Ca^{2+} current. We discuss a mechanism in which a test pulse delivered from a holding potential where a fraction of the channels are unavailable for opening produces a non-decaying current because some channels open after a delay as they return from an inactivated state. Preliminary reports of these results have been published in abstract form (Slesinger and Lansman, 1990; Lansman and Slesinger, 1991).

METHODS

Tissue Culture

Cultures of dissociated cerebellar cells were prepared as described previously in Chapter 1.

Solutions

Currents through Ca^{2+} channels were recorded with an electrode filling solution containing (in mM) 90 $BaCl_2$ (Aldrich Chemicals, >99.9% purity), 10 HEPES, and 10 glucose (pH 7.4). TEA-Cl (27 mM) was added to the Ba^{2+} solution to suppress outward K^+ channels that appeared in the single-channel recordings at positive test potentials. Currents carried by monovalent cations were recorded with 150 LiCl (Aldrich Chemicals, >99.9% purity), 10 HEPES, 10 glucose and 5 EDTA (pH 7.4) in the patch electrode. All solutions were adjusted to ~330 mOsm by adding glucose.

The bathing solution (K-MS) contained 150 KOH, 5 $MgCl_2$, 60 glucose, 1 EGTA, 10 HEPES, and was titrated with methanesulfonic acid to pH 7.4. An isotonic K^+ bathing solution was used to zero the cell membrane potential so that the patch potential would be the same as the voltage command applied to the patch clamp amplifier. In some experiments, the current-voltage relation measured after excising the patch from the cell surface had shifted along the voltage axis. This magnitude of the shift indicated a maximum voltage error of ~10 mV.

The organic Ca^{2+} channel modulators (+/-)-202-791 were prepared as 10 mM stock solutions in 100% ethanol and kept at -20° C in a light-tight container. Stock solutions were diluted with the bathing solution and were used immediately before each experiment. Exposing cells to the bathing solution containing 0.01% ethanol had no effect on Ca^{2+} channel activity. Cells were exposed to drugs by positioning a second perfusion pipette, with a tip diameter of ~15 μm, ~10-50 μm from the cell under study.

Electrophysiology

Glass cover slips with attached cells were placed in a recording chamber mounted on a Nikon phase-contrast microscope. Single-channel activity was recorded from cell-attached patches with the method described by Hamill, Marty, Neher, Sakmann & Sigworth (1981). Patch electrodes were made from Boralex hematocrit glass (Rochester Scientific) and had resistances of 2-5 MΩ with 90 mM $BaCl_2$ in the electrode and K-MS in the bath. Current signals were recorded with a List EPC-7 amplifier with a 50 GΩ feed-back resistor. Currents were filtered with a 8-pole, lowpass Bessel filter at 1-2 kHz (-3 dB) and sampled at 5 kHz. All recordings were made at room temperature (20-24° C).

The junction potential between the electrode filling solution and the bathing solution was zeroed before forming a seal between the patch electrode and the cell surface. The junction potential was rechecked at the end of each experiment and was less than 3 mV. The membrane-seal resistance ranged from 2-20 GΩ. Voltage command pulses were generated and current responses simultaneously digitized and stored on a laboratory computer (PDP 11/73, Indec Systems, Sunnyvale, CA). Test pulses were delivered at 0.2-0.4 Hz. All current traces shown were corrected for linear leak and capacity current by subtracting either an average of sweeps with no channel activity, an appropriately scaled hyperpolarizing pulse 1/4th the amplitude of the test pulse (-P/4), or a template obtained by fitting the capacity transients with a sum of two exponentials as judged by eye.

Data Analysis

The mean current was obtained by averaging individual leak-subtracted current records. The mean open channel probability (P_o) was calculated on a sweep by sweep basis by dividing the integrated current record by the time integral of the single-channel current. When the number of channels is not known, the ratio of the current integrals is P_o multiplied by the number of channels, N, where $NP_o = I/i$. Open and closed time durations were measured from idealized current records by a half-threshold detection method

(Colquhoun and Sigworth, 1983). Histograms of open and closed time durations were fit with multiple exponentials by use of a maximum-likelihood fitting routine. The fits were corrected for missed events by setting a cutoff at 0.4 ms which was subtracted from the maximum-likelihood estimate of the time constants (see Colquhoun and Sigworth, 1983).

The variance of the single-channel current fluctuations and the mean current were used to estimate the amplitude of the single-channel current at positive test potentials (cf. Fenwick, Marty & Neher, 1982; Cull-Candy *et al.*, 1988). The power spectrum of current fluctuations was measured by averaging power spectra of the current during the last 102 ms of a voltage step and subtracting the average spectrum for the background noise when no channels were open. The total current variance (σ^2) was calculated by fitting the spectral density plot with the sum of 1 or 2 Lorentzian components (Eq. 1),

$$\sigma^2 = \pi \sum_{i=1}^{n} f_{ci} S_i(0) \qquad (1)$$

where f_{ci} and $S_i(0)$ are the corner frequency and zero-frequency asymptote of the i^{th} Lorentzian, respectively. Because the probability of opening is much less than 1 (see figure 7C), the single-channel current (i) is obtained as the ratio of the variance (σ^2) to the mean current, I (Eq. 2) (Sigworth, 1980).

$$i = \frac{\sigma^2}{I} \quad (P_o << 1) \qquad (2)$$

RESULTS

Figure 1 illustrates the overall pattern of single-channel activity recorded from a cell-attached patch on the cell body of a granule cell with 90 mM Ba^{2+} in the patch electrode. Fig. 1A shows the Ca^{2+} channel activity evoked by test pulses to -20, -10 or 0 mV. Each panel of records shows the response to consecutive 160 ms voltage steps applied every 4 seconds. Depolarizing the patch from -100 mV to -20 mV produced few single-channel openings, many of which were not fully resolved. By contrast, a voltage step to -10 or 0 mV elicited channel activity during the pulse which consisted of mostly brief openings.

Test pulses more positive than ~0 mV produced more channel activity at the beginning than at the end of the voltage step. The average of many individual current responses to a test pulse to a fixed potential provides a direct measure of the probability of channel opening as a function of time. Fig. 1B shows that the mean current decays to ~65% of its peak in response to a test pulse to 0 mV. The time course of the decay was well fit by a single exponential with a time constant of ~40 ms (smooth curve). We have shown previously that the whole-cell Ca^{2+} current evoked by a voltage step to +10 mV decays to ~40% of its maximum amplitude with a time constant of 50-75 ms (Slesinger and Lansman, 1991a). Although the whole-cell Ca^{2+} current was recorded with 20 mM Ba^{2+} as the charge carrier, the rate of decay of current was found to be virtually insensitive to the amplitude of the inward current or species of divalent charge carrier (Slesinger and Lansman, 1991a). Thus, the probability of opening of single Ca^{2+} channels follows a time course that is similar to that of the whole-cell Ca^{2+} current recorded from intact cells.

We compared the increase in single-channel activity with depolarization with the voltage dependence of the activation of whole-cell Ca^{2+} current as shown in Figure 1C. Individual current responses evoked by a series of test pulses to a fixed potential were averaged to obtain the mean current at various potentials (Fig. 1B). Because the amplitude

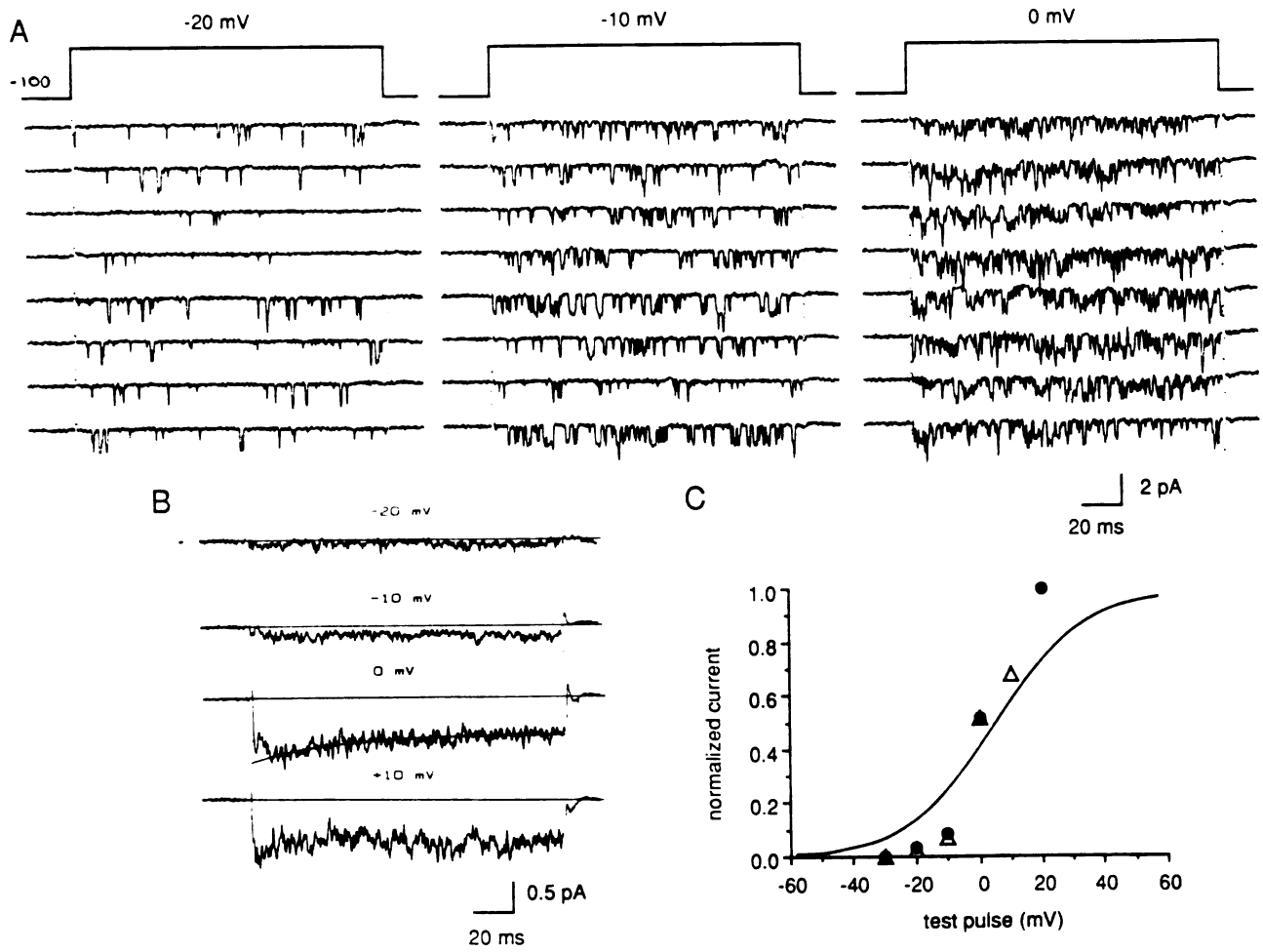

Fig. 1: Voltage dependence of Ca^{2+} channel gating recorded from a cell-attached patch on the soma of a granule cell. **A**, unitary currents recorded in response to consecutive 160 ms voltage steps to -20, -10 and 0 mV applied to the patch of membrane in the presence of 90 mM Ba^{2+}. Holding potential was -100 mV. **B**, ensemble averages of individual unitary current records produced by depolarizing the patch to -20, -10, 0 and +10 mV (average of 38, 32, 36, 14 sweeps, respectively). The mean current at 0 mV was fit by a single exponential with a time constant of 42 ms relaxing to -0.63 pA (smooth curve) using a least-squares. **C**, normalized open probability plotted as a function of test potential. Open probability was calculated by dividing peak mean current by the amplitude of unitary current calculated from Fig. 3B (open circles) and then dividing by the open probability at 0 mV to account for the number of channels per patch. The open probability at +20 mV was arbitrarily scaled to 1 for comparison with the Boltzmann relation for activation of macroscopic current (smooth curve where $V_{1/2}$ = +8 mV and k= 14 mV). Each symbol is from a different experiment. Currents sampled at 5 kHz and filtered at 1 kHz.

of single-channel current decreases with depolarization, the mean current obtained at each test potential was divided by the corresponding single-channel current to give the mean open probability ($NP_O=I/i$). In these experiments, the number of channels in the patch varied from cell to cell, so the open probability was normalized to that at 0 mV, which eliminates the number of channels in the expression for the open probability (Fox *et al.*, 1987b). Fig. 1C shows that the normalized open probability increases as the test potential is made more positive. The smooth curve shows the Boltzmann relation for activation of whole-cell Ca^{2+} current measured previously from the amplitude of the whole-cell Ca^{2+} tail current (Slesinger and Lansman, 1991a). The potential for half-activation of whole-cell Ca^{2+} current agrees well with the potential at which the single-channel open probability reaches half its maximum value. Although the steepness of the relation is different, the general agreement is good, considering that two different methods were used to measure the voltage dependence of the activation process.

We found previously that the decaying component of whole-cell Ca^{2+} current elicited by a test pulse is reduced after shifting the holding potential to more positive potentials (Slesinger and Lansman, 1991a). We investigated whether the effect of holding potential could be observed at the single-channel level. Fig. 2A illustrates the Ca^{2+} channel activity evoked by a test pulse to 0 mV from a holding potential of -30 mV (records from the same experiment as that shown in Fig. 1). There were almost no overlapping channel openings during the test pulse to 0 mV when the holding potential was -30 mV, suggesting the number of channels available for opening is reduced when compared with the activity evoked when the holding potential was -100 mV (compare Figs. 1A & 2A). Moreover, individual sweeps showed three distinct patterns of channel activity: channels that opened throughout the duration of the test pulse, channels that opened only at the onset of the voltage step (8th record), and channels that opened after a delay from the onset of the voltage step (5th record). When all sweeps were averaged they produced a non-decaying mean current (Fig. 2B, -30 mV).

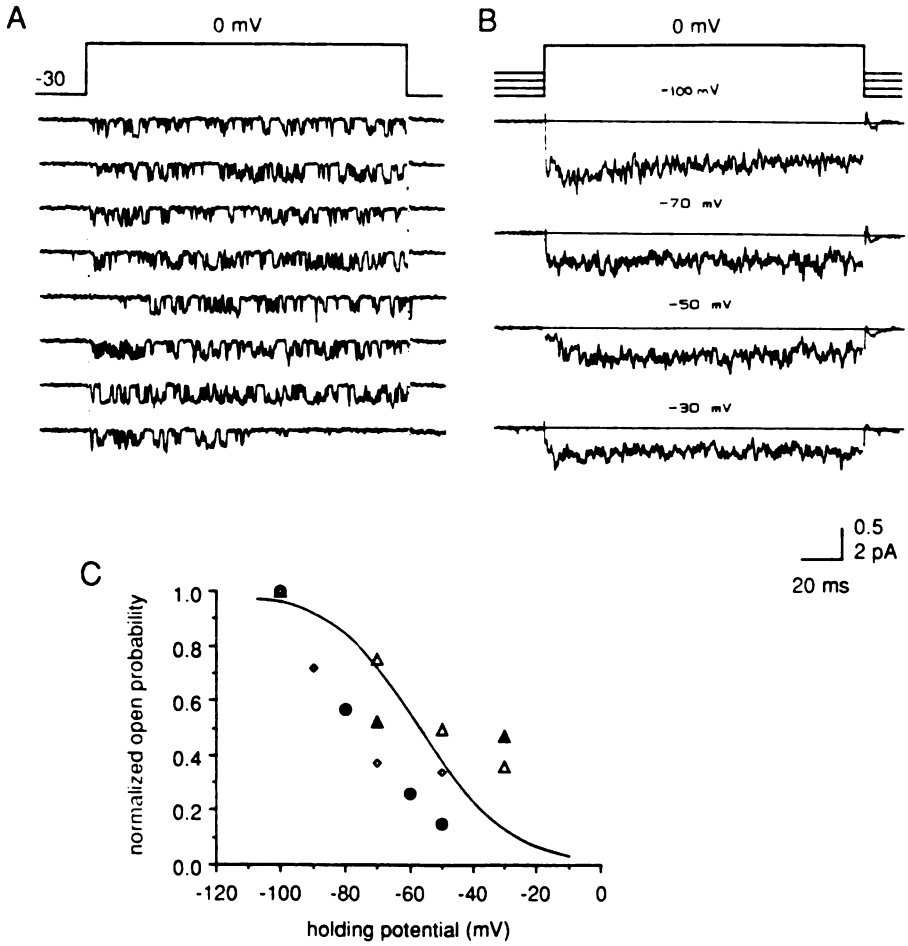

Fig. 2: Effect of holding potential on Ca^{2+} channel activity. A, unitary current records obtained in response to consecutive depolarizations to 0 mV from a holding potential of -30 mV. B, mean currents obtained from the same patch at holding potentials of -100, -70, -50 and -30 mV (average of 36, 22, 20 & 20 sweeps, respectively). C, peak mean current normalized to peak mean current recorded at a holding potential of -100 mV and plotted as a function of holding potential (each symbol is from a different experiment). Smooth curve drawn to a Boltzmann relation for inactivation of peak macroscopic current with half-inactivation $V_{1/2}$ = -57 mV and steepness k= 14 mV. Scale, 2 pA (A) and 0.5 pA (B). Currents sampled at 5 kHz and filtered at 1 kHz.

Fig. 2B shows the effect of a range of holding potentials on the mean current. Shifting the holding potential to more positive potentials progressively reduced the probability of channel opening. More positive holding potentials also reduced the decay of the mean current, consistent with the behavior of the whole-cell Ca^{2+} current (Slesinger and Lansman, 1991a). Fig. 2C compares the dependence of channel open probability on the holding potential with that of the whole-cell Ca^{2+} current. The amplitude of the mean current was normalized to mean current obtained when the holding potential was -100 mV and plotted as a function of holding potential (individual symbols). The smooth curve is drawn to the Boltzmann relation describing inactivation of whole-cell Ca^{2+} current measured in response to a fixed test potential from different holding potentials (Slesinger and Lansman, 1991a). The decrease in the open probability of single Ca^{2+} channels produced as the holding potential is shifted in the positive direction falls within same range of holding potentials that inactivate the whole-cell Ca^{2+} currents.

Estimate of single-channel conductance

The amplitude of the single-channel current was measured directly in the presence of dihydropyridine agonist, which prolongs the duration of the single-channel openings (Hess, Lansman & Tsien, 1984). The amplitude of the single-channel currents plotted were measured directly and plotted as a function of the test potential (fig. 3B, open circles). The points were well fit with a straight line with a slope conductance of ~22 pS in 90 mM Ba^{2+}. The amplitude of channel openings were also measured in the absence of the dihydropyridine agonist (solid diamonds), but only over a narrow range of potentials and in a small fraction of the records where there were well-resolved transitions to the open channel level. The amplitude of the single-channel current measured directly was similar to that measured in the presence of dihydropyridine agonist. We observed some variability in the amplitude of single-channel current which could have arisen from the presence of subconductance states (cf Carbone and Lux, 1987b; Plummer, Logothetis & Hess, 1989;

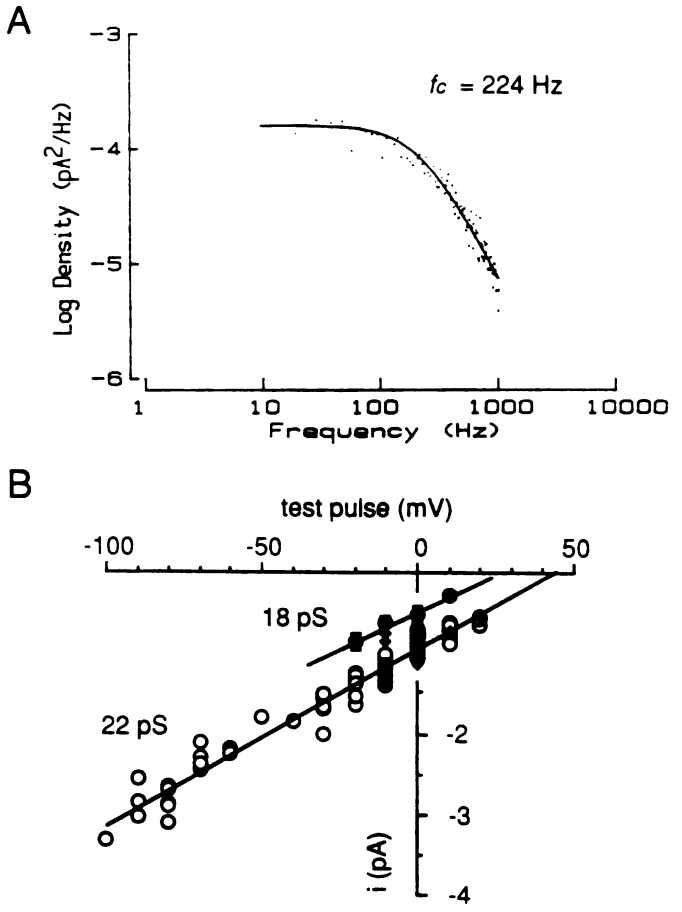

Fig. 3: Estimate of single-channel conductance. **A**, power spectrum of current fluctuations produced by voltage step to -10 mV from a holding potential of -100 mV. Smooth curve drawn to a single Lorentzian of the form,

$$S(f) = \frac{S(0)}{1 + (f/f_c)^2}$$

where the corner frequency f_c = 224 Hz and zero-frequency asymptote S(0) = 1.59×10^{-4} pA^2/Hz. The variance $\sigma^2 = 0.112\ pA^2$ according to Eq. 1. Power spectra of current fluctuations produced by test potentials to -20 and -10 mV were best fit by a single Lorentzian with a corner frequency of 405 ± 100 Hz (mean ± SD, 6 patches) while those produced by test potentials more positive than -10 mV were best fit by a sum of two Lorentzians with an additional corner frequency of 32 ± 14 Hz. The corner frequencies did not appear to change systematically with test potential (cf Fenwick *et al.*, 1982). **B**, amplitudes of unitary current estimated from noise analysis (●, n=4) and from direct measurement of discrete channel openings in the absence (◆, n=9) or presence of +(S)-202-791 (○, n=17) plotted as a function of test potential. The amplitude of unitary current below -50 mV was measured in the presence of agonist immediately following the test pulse at different repolarizaion potentials. Points were fit by linear regression with a conductance of 18 pS (r^2=0.98) for solid circles and 22 pS (r^2=0.94) for open circles.

Lacerda and Brown, 1989). We cannot, however, exclude the possibility that the variability in the size of the single-channel current was due to fluctuations in membrane potential during the recording or from filtering of the rapid gating transitions.

Because the single-channel currents were not well resolved during test pulses more positive than 0 mV, we used noise analysis to estimate the amplitude of the single-channel current (Eqs. 1&2). Fig. 3A shows an example of the power spectrum measured from the single-channel current fluctuations during a test pulse to -10 mV. The points were well fit with a single Lorentzian component (details in figure legend). The solid circles in Fig. 3B show the estimates of the amplitude of the single-channel current obtained from the current noise plotted as a function of test potential. The points were fit by a straight line with a slope conductance of ~18 pS in 90 mM Ba^{2+}. Although the conductance estimated from noise analysis was close to the conductance estimated from measuring individual channel openings, the amplitude of the single-channel current was smaller. Noise analysis, however, can underestimate the amplitude of the single-channel current if a component of the total variance is lost from low-pass filtering (Sigworth, 1980).

Effect of positive prepulses on Ca^{2+} channel activity

In two pulse experiments, a prepulse to potentials near the peak of the current-voltage relation produce maximal suppression of whole-cell Ca^{2+} current evoked by a subsequent test pulse, but more positive prepulses produce less inhibition (Slesinger and Lansman, 1991a). The apparent reduction in the extent of inactivation produced by very positive prepulses could be due to a decrease of the inward Ca^{2+} current as the prepulse was made more positive, which would reduce current-dependent inactivation (Chad and Eckert, 1986), or from potentiation of Ca^{2+} current by the positive prepulses (Hoshi, Rothlein & Smith, 1984; Hoshi and Smith, 1987). The experiment in Fig. 4 was designed to examine whether positive prepulses potentiated the single-channel activity produced by a subsequent test pulse.

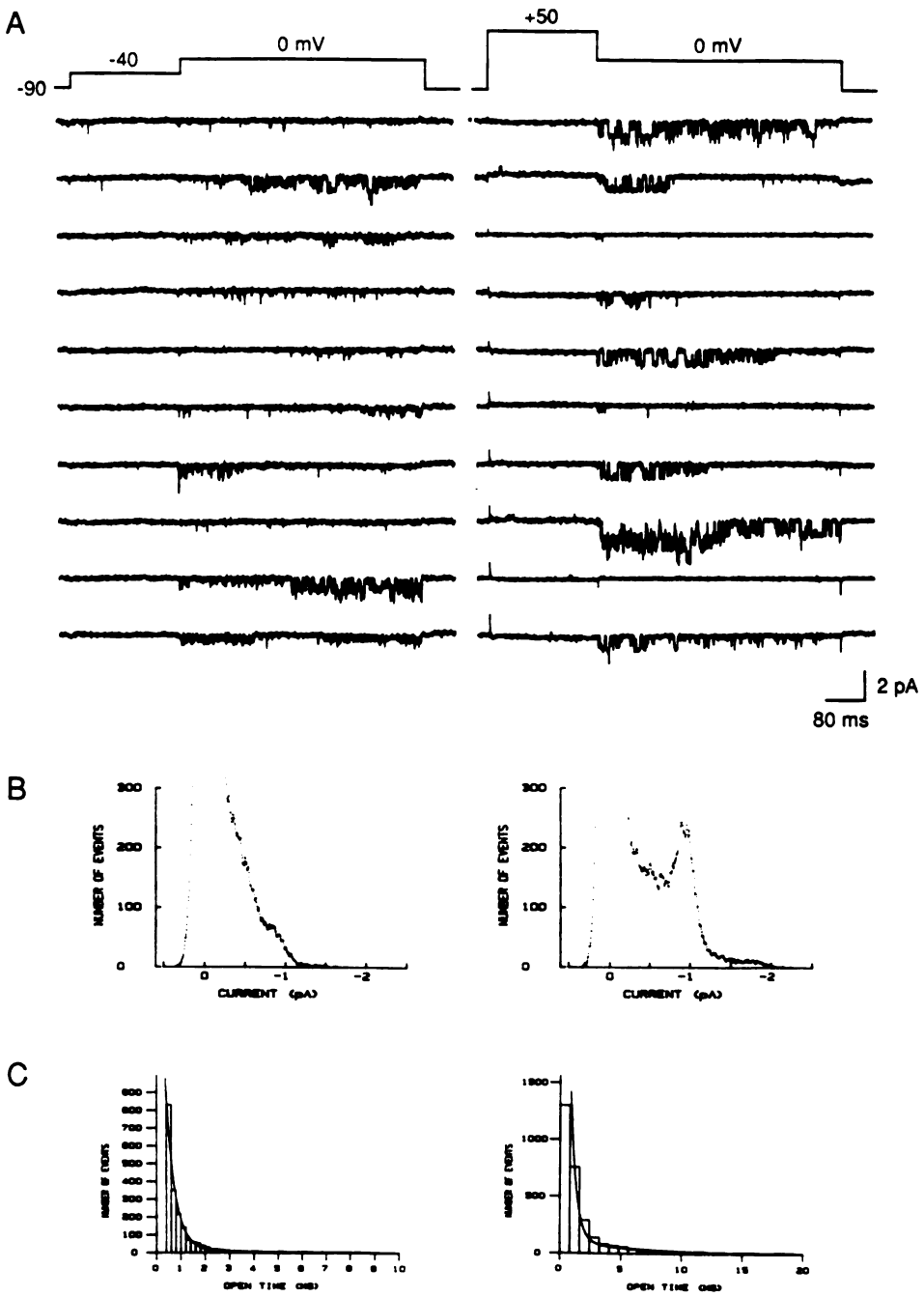

Fig. 4: Effect of positive prepulse on Ca^{2+} channel activity. **A**, consecutive unitary current records obtained from a patch depolarized to 0 mV for 600 ms following a prepulse to either -40 mV or +50 mV for 100 ms. **B**, histogram of unitary current amplitudes measured at 0 mV following a prepulse to -40 mV or +50 mV (current around 0 pA is offscale). **C**, frequency histogram of open channel durations superimposed with double exponential fit (note difference in the time scale). Open times had mean lifetimes of 0.4 & 4 ms (ratio of the exponential components =13.3) when the prepulse = -40 mV, and 0.5 & 5.2 ms (ratio=6.1) when the prepulse = +50 mV. Closed time durations were also measured and had mean lifetimes of 0.8 & 17 ms (ratio=1.6) when the prepulse = -40, and 2.2 & 19 ms (ratio=2.1) when the prepulse =+50 mV (data not shown). The mean lifetimes were corrected for missed events. Currents were sampled at 5 kHz and filtered at 1 kHz.

Fig. 4A shows records of channel activity elicited by a 600 ms test pulse which followed a 100 ms prepulse to either -40 or +50 mV. Following the prepulse to -40 mV, the test pulse to 0 mV produced mostly brief channel openings. By contrast, the prepulse to +50 mV increased the frequency of long openings during the test pulse. The effect of the prepulse on open channel probability was examined by measuring the amplitude of the single-channel current during the test pulse to 0 mV. Fig. 4B shows the histograms of the current amplitude scaled to show the change in the area under the curve near the amplitude of the single-channel current. The prepulse to +50 mV increased the area under the open channel current level when compared with a prepulse to -40 mV, reflecting the higher probability of opening following the more positive prepulse.

The prepulse to +50 mV also produced more long openings during the test pulse to 0 mV. The effect of prepulse potential on the single-channel kinetics was analyzed by measuring the duration of channel opening and closing events. Fig. 4C shows the histograms of channel open times. Both histograms were fit with a double exponential with time constants of ~0.5 and ~5 ms. The number of short events, however, was reduced by half when the test pulse was preceded by a prepulse to +50 mV (see Figure legend for details). The increase in the number of long openings by a positive prepulse was observed in two other patches (see Table 1). Histograms of closed times were best fit by two exponentials, but neither the ratios nor time constants were altered by prepulses (see Table 1). At least part of the increase in the whole-cell Ca^{2+} current by a very positive prepulse is likely to involve an increase in the number of long openings evoked by a the subsequent test pulse.

Effect of cyclic AMP on Ca^{2+} channel activity

Including cyclic AMP in the recording electrode slows washout of the Ca^{2+} current during whole-cell recordings (Slesinger and Lansman, 1991a), indicating that a cyclic AMP-dependent mechanism is involved in maintaining Ca^{2+} channels in a functional state.

TABLE 1: Open and closed channel lifetimes

		τ_f		τ_s	
control	open	0.5 ± 0.1	(10/10)	1.3	(1/10)
	closed	1.8 ± 0.4	(10/10)	17.0 ± 3.9	(10/10)
+(S)-202-791	open	0.5 ± 0.1	(11/11)	5.7 ± 1.3	(11/11)
	closed	1.2 ± 0.3	(11/11)	14.6 ± 2.9	(11/11)
prepulse to:					
-40 mV	open	0.4 ± 0.1	(6/6)	4.1 ± 0.1	(2/6)
	closed	2.5 ± 1.1	(6/6)	19.8 ± 5.5	(6/6)
+50 mV	open	0.4 ± 0.1	(6/6)	4.4 ± 0.9	(3/6)
	closed	2.1 ± 0.3	(6/6)	19.8 ± 3.3	(6/6)

Table 1: Duration of open channel events (ms) were measured in current records elicited by 700 ms test pulses to -10 or 0 mV in the presence or absence of the dihydropyridine agonist +(S)-202-791, and in current records elicited by 600 ms test pulses to -10 or 0 mV preceded by 50-100 ms prepulses to -40 or +50 mV. Distribution of open times was fit by 1 or 2 exponentials. Time constants are mean values (± SEM). Holding potential was -90 mV. Number in parantheses indicates fraction of patches in which the measured vlaues were observed.

Elevating intracellular cyclic AMP would be expected, therefore, to increase channel activity in recordings from cell-attached patches as well as to slow the washout of channel activity that occurs after excising the patch from the surface membrane. To test these predictions, single-channel activity was recorded from granule cells that were preincubated with 8-bromo cyclic AMP (Br-cAMP), a membrane-permeable cyclic AMP analogue, before and after excising the patch from the cell surface.

Fig. 5A shows the single-channel activity produced by voltage steps to 0 mV recorded from the surface of a cell preincubated with 50 μM Br-cAMP. Channel activity recorded from cell-attached patches was generally greater in cells exposed to Br-cAMP, although this was not studied systematically. After excising the patch into the bathing solution, a condition where additional phosphorylation of the channel cannot occur unless both ATP and protein kinase A remain associated with the patch of membrane (Armstrong and Eckert, 1987), Ca^{2+} channel activity decreased. Channel activity could still be observed, however, for over several minutes. Histograms of open times measured at 0 mV before and after excision were well fit by a single exponential with similar time constants (~0.8 ms, data not shown), suggesting there were no major modifications in channel gating kinetics as the number of functional channels decreased after patch excision.

The mean open probability was calculated on a sweep by sweep basis throughout the experiment. Fig. 5B shows that the open probability decreased only slightly following excision. The persistence of channel activity in sweeps following excision of the patch from a cell exposed to Br-cAMP contrasts sharply with the rapid loss of activity after excising a patch from a different cell not exposed to Br-cAMP (Fig. 5C). These results show that a cyclic AMP-dependent mechanism participates in maintaining Ca^{2+} channels in a functional state.

We could observe two distinct patterns of channel gating when channel activity decreased after patch excision to a level where only one channel at a time opened during the voltage step: short bursts that occurred at the beginning of the test pulse and long bursts

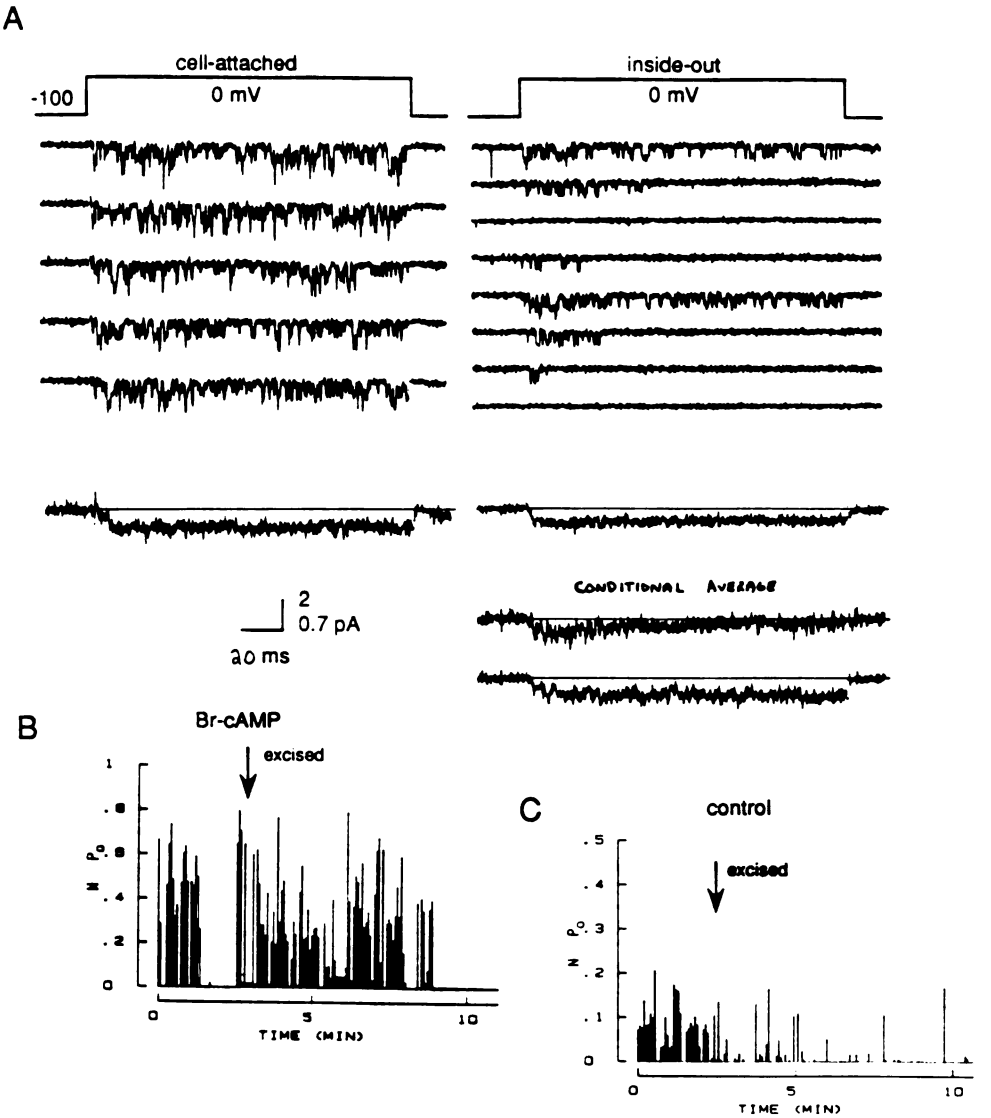

Fig. 5: Effect of intracellular cyclic AMP on washout of Ca^{2+} channel activity. Cell was preincubated in 50 μM 8-bromo cyclic AMP for ~10 minutes and included in the bathing solution during the recording. **A**, representative unitary currents produced in response to voltage steps to 0 mV lasting 160 ms applied to a cell-attached patch (left). Consecutive unitary current records obtained in the same patch ~2.5 minutes after excising the patch from the cell into the bathing solution, forming an inside-out patch (right). Ensemble average of all unitary current records shown below (average of 62 & 80 sweeps, respectively). Conditional average shows the mean current through channels that inactivated in the beginning of the pulse or opened for the duration of the test pulse after excision (average of 13 and 23 sweeps, respectively). **B**, mean open probability calculated on a sweep by sweep basis plotted as a function of time. The blank period around 1-2 minutes was not measured because the holding potential was changed. **C**, mean open probability plotted as a function of time for another cell that was not preincubated with Br-cAMP (note change in ordinate scale). Scale, 2 pA (unitary currents) and 0.7 pA (mean currents). Currents were sampled at 5 kHz and filtered at 2 kHz.

that continued throughout the test pulse. The records on the right (Fig. 5A) are consecutive sweeps showing the short and long bursts. Averaging all of the unitary current responses after patch excision produced a mean current that was only slightly smaller than that obtained before patch excision (compare mean currents on left & right). The mean current obtained after excision, however, decayed little even though some sweeps had activity that occurred only at the beginning of the pulse. Conditional averaging of sweeps in which the channel appeared as either a short burst or a long burst produced decaying and non-decaying mean currents, respectively. Apparently, the non-decaying mean current is made up of inactivating and non-inactivating single-channel activity.

Effect of dihydropyridines on unitary Ca^{2+} channel activity

Dihydropyridine agonist increases whole-cell Ca^{2+} channel current and slows the rate of deactivation, while dihydropyridine antagonist inhibits the current (Slesinger and Lansman, 1991a). We investigated the response of the single-channel activity recorded from cell-attached patches to the dihydropyridine antagonist -(R)-202-791 and agonist +(S)-202-791 (Hof, Rüegg, Hof & Vogel, 1985).

Fig. 6 shows an example of the effect of the antagonist -(R)-202-791 on Ca^{2+} channel activity. Prior to exposing the patch to 1 μM -(R)-202-791, Ca^{2+} channel activity persisted throughout the duration of each of the 700 ms voltage steps to 0 mV (Fig. 6A, left). Exposing the patch to antagonist reduced the overall channel activity produced by a test pulse to the same potential, mainly by increasing the number of sweeps in which the channel failed to open (Fig. 6A, right). In those sweeps with channel activity, the openings frequently appeared as short bursts at the beginning of the voltage step. Averaging the single-channel currents evoked in the presence of antagonist produced a mean current that was smaller and decayed more rapidly than the control mean current (Fig. 6A, bottom). The increase in the number of sweeps in which the channel failed to open and the appearance of short bursts in the beginning of the voltage step suggest that the

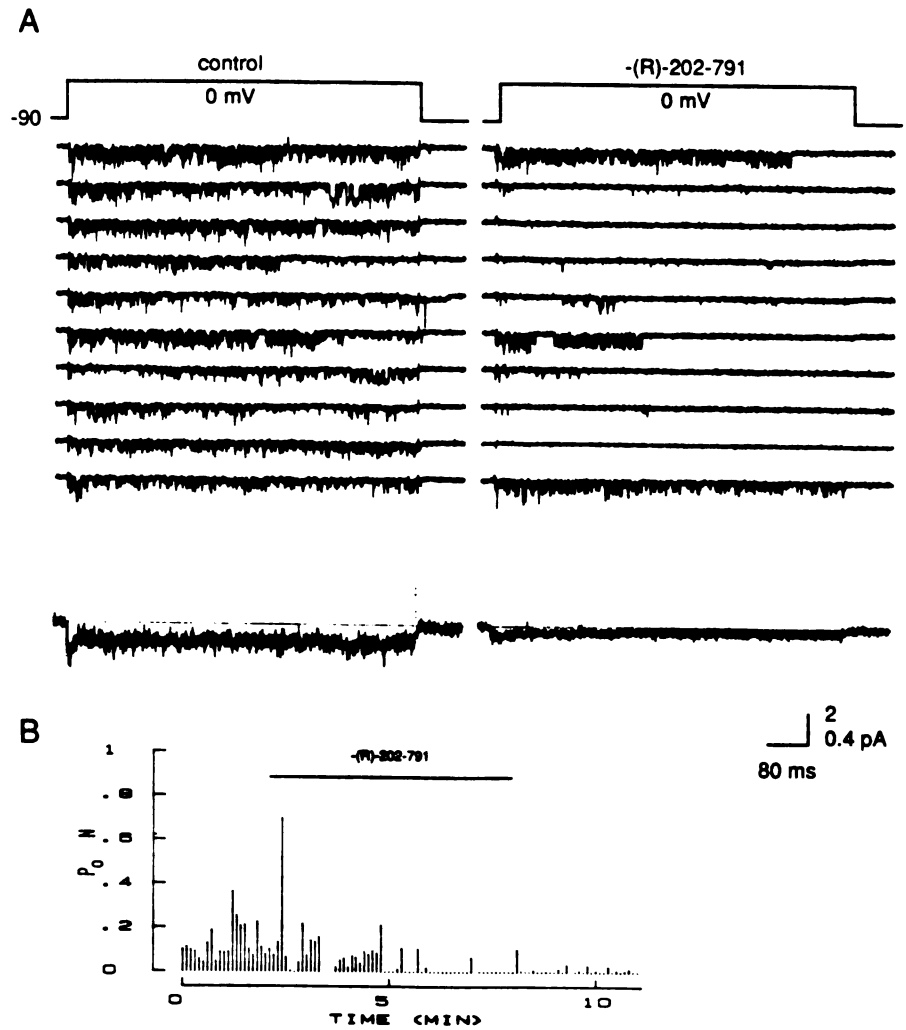

Fig. 6: Effect of the dihydropyridine antagonist -(R)-202-791 on Ca^{2+} channel activity. **A**, unitary current records obtained by consecutive test pulses to 0 mV lasting 700 ms before (left) and after (right) exposing the patch to 1 μM -(R)-202-791. Holding potential was -90 mV. Mean currents shown below (average of 21 & 82 sweeps, respectively). **B**, mean open probability calculated for each sweep plotted as a function of time (bar indicates length of exposure to antagonist). Scale, 2 pA (unitary currents) and 0.4 pA (mean currents). Currents were sampled at 5 kHz and filtered at 1 kHz.

dihydropyridine antagonist binds selectively to the inactivated state (cf Bean, 1984; Gurney, Nerbonne & Lester, 1985; Cohen and McCarthy, 1987).

The mean open probability calculated for each sweep obtained in the absence and then presence of -(R)-202-791 is shown in Fig. 6B. The dihydropyridine antagonist greatly reduced the probability of a channel opening during the 700 ms pulse, with many sweeps containing no channel activity. Channel activity remained low after removing the perfusion pipette containing antagonist from the bath, although brief openings were still detectable, indicating the presence of functional channels. Complete recovery from inhibition over the time course of the recording was not studied because the bathing solution containing antagonist was not exchanged with fresh solution. The same pattern of inhibition was observed in two other patches.

Fig. 7 shows the results of an experiment investigating the effects on Ca^{2+} channel activity of the dihydropyridine agonist +(S)-202-791 . Fig. 7A (left records) shows unitary currents obtained in response to consecutive 700 ms voltage steps from -90 mV to -10 mV applied to the patch. Prior to exposing the cell to 1 μM +(S)-202-791, the test pulse elicited the familiar pattern of gating consisting mostly of brief openings, although there were occasional long openings that appeared toward the end of the pulse (9th record, Fig. 7).

Exposing the cell to dihydropyridine agonist markedly altered the pattern of channel gating (Fig. 7A, middle records), the most striking effect being an increase in the number of long channel openings that occurred during the test pulse. Before exposing the cell to agonist, the histogram of channel open times measured at -10 mV had a single component with a time constant of ~0.6 ms (Fig. 7B). In the presence of drug, the histogram of channel open times had two clearly resolved exponential components with time constants of ~0.5 ms and 16 ms. In contrast to the duration of openings, the duration of the channel closed times were not altered by the drug (cf Hess *et al.*, 1984). Thus, the ~5-fold increase in the amplitude of the mean current in the presence of agonist can be attributed to the

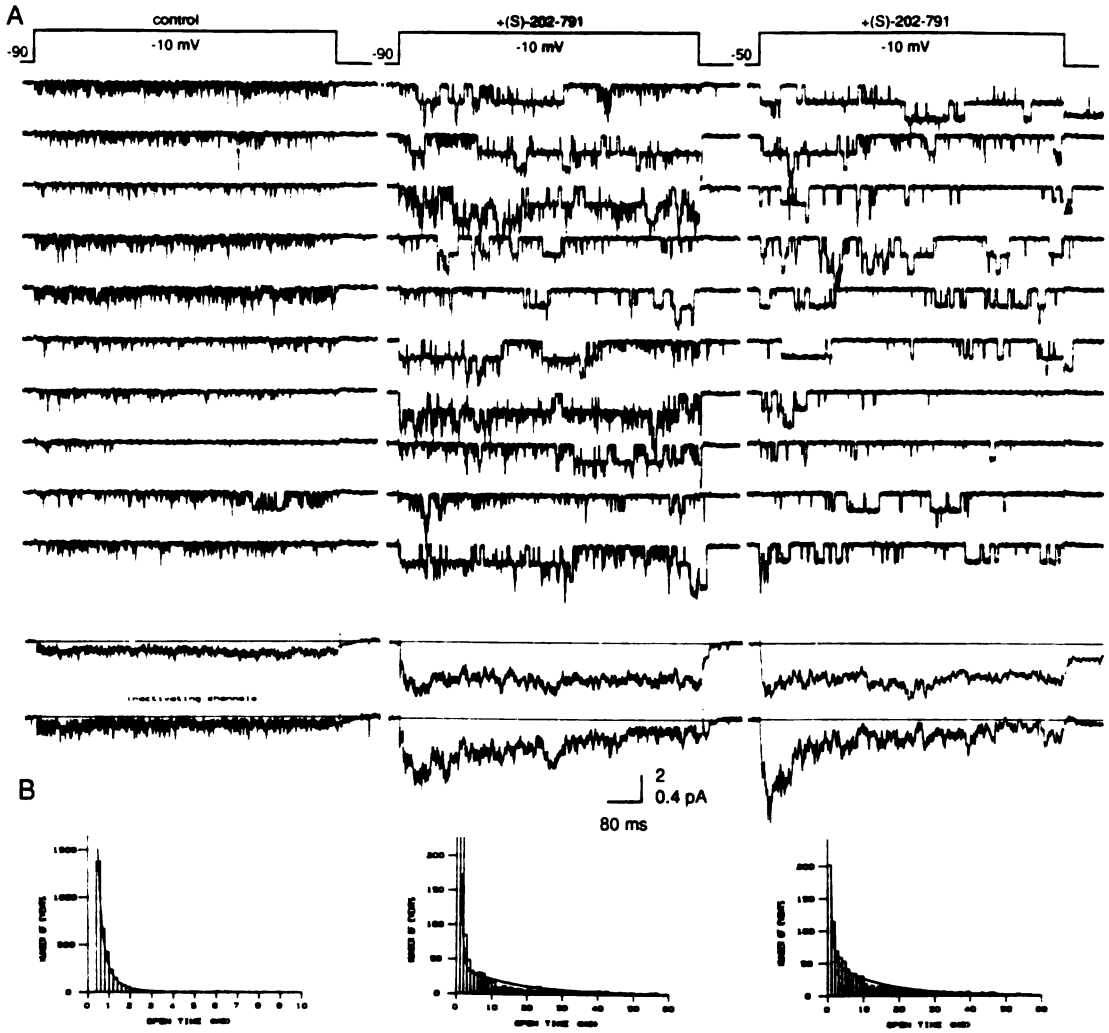

Fig. 7: Effect of the dihydropyridine agonist +(S)-202-791 on Ca^{2+} channel activity. **A**, single-channel current records obtained in response to consecutive 700 ms voltage steps to -10 mV from a holding potential of -90 mV in the absence (left) and presence (middle) of 1 μM +(S)-202-791. Records on right show single-channel currents recorded from the same patch in response to voltage steps to -10 mV from a holding potential of -50 mV. Ensemble averages of single-channel records shown below for all sweeps (average of 30, 43 & 47 sweeps, respectively) or for only those sweeps containing inactivating channels (average of 10, 18 & 16 sweeps, respectively). **B**, histograms of open channel durations measured at -10 mV. Distribution of open times obtained in the absence of agonist was best fit by a double exponential with time constants of 0.2 and 0.6 ms (ratio=3.8). The maximum likelihood method of fitting exponentials sometimes converged on a solution where one of the time constants was faster than the recording bandwidth (< 0.2 ms) and was ignored. Distribution of open times obtained after exposing the patch to agonist was fit by a double exponential with time constants of 0.5 and 16 ms (ratio=1.8) when the holding potential was -90 mV, and 1.0 and 14 ms (ratio=0.21) when the holding potential was -50 mV. Distribution of closed channel durations was fit by a double exponential with time constants of 1.1 and 15 ms (ratio=0.19) for control, 0.6 and 11 ms (ratio=0.16) when the holding potential was -90 mV in the presence of agonist, and 0.7 and 25 ms (ratio=0.16) when the holding potential was -50 mV in the presence of agonist. Mean lifetimes were corrected for missed events (Colquhoun and Sigworth, 1983). Scale, 2 pA (unitary currents) and 0.4 pA (mean currents). Currents were sampled at 5 kHz and filtered at 1 kHz.

increase in the number of sweeps with long channel openings. The dihydropyridine agonist also slowed the rate of channel closing, which can be seen as sweeps in which the channel remained open following termination of the voltage step (Hess *et al.*, 1984).

The long openings in some sweeps also appeared to inactivate shortly after the onset of the test pulse. The sixth and tenth records in Fig. 7A show examples in which the long openings occurred mainly at beginning of the voltage step. The mean current produced by averaging sweeps with long openings that occurred at the beginning of the test pulse produced a decaying mean current (bottom record, Fig. 7A, middle). The average of all sweeps produced a mean current that did not decay (second to bottom record, Fig. 7A, middle), however, indicating that some channels must have opened later in the pulse to produce the non-decaying mean current. The eight record in middle set of records in Fig 7A shows a channel that opened after a delay. The long channel openings recorded in the presence of the agonist apparently produces both inactivating and non-inactivating currents.

Shifting the holding potential to more positive potentials, while keeping the test potential fixed, altered channel gating in such a way that it appeared to influence the short openings rather than the long openings (Fig. 7A, right records). The more positive holding potentials did not change the duration of the channel openings, but reduced the proportion of short to long openings approximately ten-fold (see Figure legend for details). The suppression of the short openings by the positive holding potential did not reduce the amplitude of the mean current, indicating short openings do not contribute much to the overall open probability in the presence of agonist. This contrasts sharply with the ~50% decrease in open channel probability produced by shifting the holding potential to -50 mV in the absence of dihydropyridine agonist (Fig. 2B).

Although the long openings in the presence of agonist are relatively insensitive to changes in holding potential, it is possible that a fraction of sweeps with long openings that inactivate during the voltage step is reduced at the more positive holding potential. The second and seventh records in Fig. 7A (right records), however, show that there are

sweeps with openings that occur primarily at the beginning of the voltage step and, when averaged, produce a decaying mean current. Therefore, a change in the holding potential does not reduce the fraction of inactivating channels with long open times because decaying mean currents with similar amplitudes are produced when the holding potentials was either -90 or -50 mV. The results show that the long openings seen in the presence of dihydropyridine agonist also produce inactivating and non-inactivating single-channel currents, regardless of the holding potential.

Single-channel currents carried by monovalent cations

Monovalent cations carry charge though the Ca^{2+} channel (Hess, Lansman, and Tsien, 1986). Because the whole-cell Ca^{2+} current in granule cells decays with a rate that is independent of the species of divalent cation or the amplitude of the current (Slesinger and Lansman, 1991a), we expected single-channel currents carried by monovalent cations to have kinetics similar to those carried by divalent cations. Accordingly, it should be possible to identify both inactivating and non-inactivating channels even when monovalent ions carry charge through the channel.

Fig. 8 shows single-channel currents recorded in response to a 700 ms voltage step to -50, -30 or -20 mV from a holding potential of -110 mV with 150 mM LiCl in the recording electrode. Single-channel currents activated at more negative test potentials than in the previous experiments. This would be expected if removing divalent cations from the electrode solution produced a large negative surface potential, the effect of which would be to shift activation to more negative voltages (Ohmori and Yoshii, 1977).

Each pair of records in Fig. 8 shows examples of channel activity produced by a voltage step to the indicated potential. Voltage steps to -30 and -20 mV produced Ca^{2+} channel activity that, once again, appeared as short bursts at the beginning of the pulse or as long bursts that lasted throughout the pulse. The presence of short and long bursts is

similar to the behavior observed when divalent cations carry charge through the channel and so it cannot be attributed to the species of charge carrier.

The mean current produced by averaging the single-channel currents produced at each test potential are shown below the single-channel records. The Ca^{2+} channel activity evoked by voltage steps to potentials more positive than -30 mV produced a decaying mean current compared with voltage steps to ~0 mV which were required to produce a decaying mean current when Ba^{2+} was the charge carrier. It is interesting that the the mean current decayed at more negative potentials in the presence of Li^{+} as the charge carrier, since activation also is shifted to more negative potentials. The parallel shift of activation and inactivation suggests they may be coupled processes (Aldrich, Corey & Stevens, 1983).

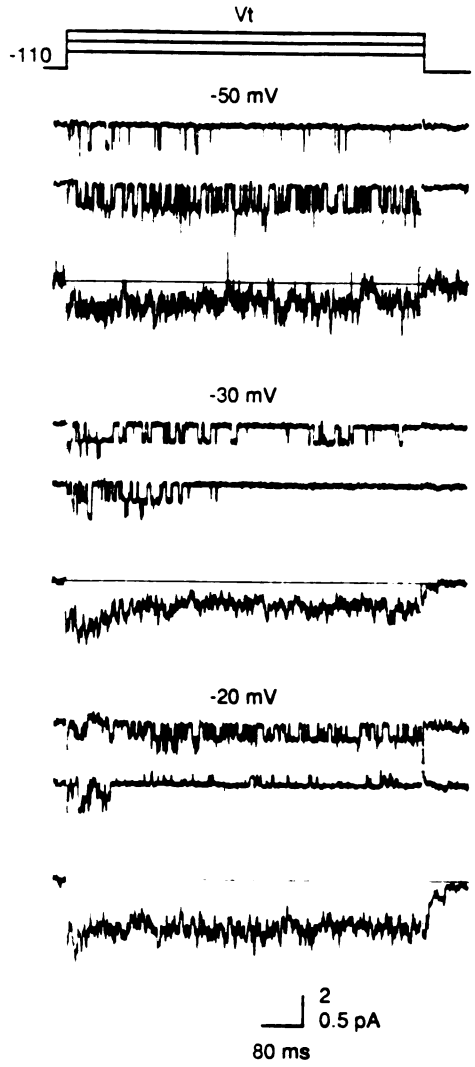

Fig 8: Unitary currents through Ca^{2+} channels recorded with the monovalent cation Li^{+} in the recording pipette. Current responses produced in response to 700 ms voltage steps to -50, -30 and -20 mV from a holding potential of -110 mV. Single sweeps selected to show two types of channel activity: channels that inactivated in the beginning of the test pulse or opened throughout the depolarization. Some sweeps contained channels that carried outward current at positive test potentials (see bottom trace at -20 mV), but not through Ca^{2+} channels. Ensemble average of all single-channel currents shown below (23, 25 and 25 sweeps, respectively). The dihydropyridine agonist +(S)-202-791 (1 μM) was added to the bath to promote long openings, but does not affect the rate of decay of current (Fig. 7, this paper; Slesinger and Lansman, 1991a). The single-channel conductance was ~26 pS in 150 mM Li^{+}. Scale, 2 pA (single-channel currents) and 0.5 pA (mean currents). Currents were sampled at 2 kHz and filtered at 1 kHz.

Discussion

Under favorable conditions when Ca^{2+} channel activity can be reduced so that only one channel at a time is active during a test pulse, a Ca^{2+} channel with a conductance of 22 pS can be seen to produce both inactivating and non-inactivating currents. Inactivating and non-inactivating currents can also be observed in the presence of dihydropyridine agonist and these appear as long openings that occur at the beginning of the test pulse or as long openings that last throughout the duration of the test pulse. Evidently, a single type of dihydropyridine-sensitive Ca^{2+} channel produces decaying and non-decaying currents. We discuss below the extent to which the behavior of the 22 pS channel accounts for the time and voltage dependence of the whole-cell Ca^{2+} current. We also suggest a mechanism by which a single type of Ca^{2+} channel produces a decaying current only when the test pulse is delivered from a negative holding potential.

Does the activity of single Ca^{2+} channels account for the whole-cell Ca^{2+} current?

Our results strongly suggest that the activity of the 22 pS activity Ca^{2+} channel recorded from cell-attached patches can account for the properties of the whole-cell Ca^{2+} current (Slesinger and Lansman, 1991a): (1) averaging many single-channel records evoked by strong depolarizations produces a mean current that decays to a non-zero level along a single exponential time course that is similar to the time course of the whole-cell Ca^{2+} current; (2) the open probability of the single channel increases with depolarization with the same dependence on membrane potential as activation of the whole-cell Ca^{2+} current; (3) the decrease in open probability of the single channel when the holding potential is changed falls within the same range as the inactivation of the whole-cell Ca^{2+} current; (4) the decay of the mean current obtained from single-channel records is reduced after shifting the holding potential to more positive potentials; (5) single Ca^{2+} channels are maintained in a functional state by a cyclic AMP-dependent mechanism; (6) the dihydropyridine agonist increases single-channel open probability and slows deactivation

and dihydropyridine antagonist decreases the single-channel activity. These results indicate that the activity of a dihydropyridine-sensitive Ca^{2+} channel can account for most features of the Ca^{2+} current recorded from granule cells under conditions of whole-cell dialysis (cf Brown, Lux & Wilson, 1984; Carbone and Lux, 1987a,b; Kostyuk, Shuba & Savchenko, 1988; Aosaki and Kasai, 1989; Fenwick *et al.*, 1982; Lux and Brown, 1984; Plummer *et al.*, 1989).

Comparison of Ca^{2+} channels in granule cells with other neuronal Ca^{2+} channels

There is general agreement that many types of excitable cells possess T-type channels that are easily distinguished from the channel activity described here because they have a small single-channel conductance and inactivate rapidly in response to weak depolarizations (reviewed by Bean, 1989; Hess, 1990). Although T-type channels are found in many types of neurones, we rarely saw this type of channel activity in recordings from cerebellar granule cells. We observed a small conductance channel in some patches, but it opened only in response to strong depolarizations and its kinetic behavior suggested that it was a subconductance state of the 22 pS channel (cf. Carbone and Lux, 1987b; Plummer *et al.*, 1989; Lacerda and Brown, 1989). These small conductance channels contributed very little to the channel activity recorded from cell-attached patches on granule cells as they were seen in fewer than ~5% of the patches. It is often difficult, however, to distinguish true subconductance states from poorly resolved channel openings that can result from the filtering of rapid gating transitions by the limited bandwidth of the recording system.

We consider the 22 pS channel in cerebellar granule cells to be an L-type Ca^{2+} channel because dihydropyridine antagonists reduce the current and enhance inactivation, while dihydropyridine agonists increase current (Hess *et al.*, 1984; Nowycky *et al.*, 1985a). Yet, our recordings of both whole-cell and single-channel currents show that the current evoked by a positive voltage step decays during the pulse only when the pulse is delivered from a negative holding potential. The decaying component of current in peripheral neurones,

and dihydropyridine antagonist decreases the single-channel activity. These results indicate that the activity of a dihydropyridine-sensitive Ca^{2+} channel can account for most features of the Ca^{2+} current recorded from granule cells under conditions of whole-cell dialysis (cf Brown, Lux & Wilson, 1984; Carbone and Lux, 1987a,b; Kostyuk, Shuba & Savchenko, 1988; Aosaki and Kasai, 1989; Fenwick *et al.*, 1982; Lux and Brown, 1984; Plummer *et al.*, 1989).

Comparison of Ca^{2+} channels in granule cells with other neuronal Ca^{2+} channels

There is general agreement that many types of excitable cells possess T-type channels that are easily distinguished from the channel activity described here because they have a small single-channel conductance and inactivate rapidly in response to weak depolarizations (reviewed by Bean, 1989; Hess, 1990). Although T-type channels are found in many types of neurones, we rarely saw this type of channel activity in recordings from cerebellar granule cells. We observed a small conductance channel in some patches, but it opened only in response to strong depolarizations and its kinetic behavior suggested that it was a subconductance state of the 22 pS channel (cf. Carbone and Lux, 1987b; Plummer *et al.*, 1989; Lacerda and Brown, 1989). These small conductance channels contributed very little to the channel activity recorded from cell-attached patches on granule cells as they were seen in fewer than ~5% of the patches. It is often difficult, however, to distinguish true subconductance states from poorly resolved channel openings that can result from the filtering of rapid gating transitions by the limited bandwidth of the recording system.

We consider the 22 pS channel in cerebellar granule cells to be an L-type Ca^{2+} channel because dihydropyridine antagonists reduce the current and enhance inactivation, while dihydropyridine agonists increase current (Hess *et al.*, 1984; Nowycky *et al.*, 1985a). Yet, our recordings of both whole-cell and single-channel currents show that the current evoked by a positive voltage step decays during the pulse only when the pulse is delivered from a negative holding potential. The decaying component of current in peripheral neurones,

however, is thought to arise from the activity of N-type channels that are available for opening only from negative holding potentials and that inactivate during a positive test pulse (Nowycky *et al*, 1985b; Fox *et al.*, 1987b; but see Plummer *et al.*, 1989; Aosaki and Kasai, 1989). In our studies of single Ca^{2+} channels in granule cells, we were unable to find a channel that inactivates in a voltage-dependent manner during a positive test pulse and could be distinguished from the 22 pS dihydropyridine-sensitive channel by its single-channel conductance. Our results suggest, instead, that L-type channels carry both the decaying and non-decaying components of the whole-cell Ca^{2+} current in cerebellar granule cells.

Origin of inactivating and non-inactivating single-channel currents

It is unlikely that the decaying component of Ca^{2+} current in granule cells is carried by a distinct type of channel that is available for opening only from negative holding potentials because single-channel currents that inactivate after the onset of the pulse can be seen over a range of holding potentials. This observation also rules out a mechanism in which the holding potential modifies the equilibrium of a single type of channel between two parallel sets of states such that negative holding potentials favors the set of states where open channel inactivation is rapid. We consider below a mechanism which explains inactivating and non-inactivating single-channel currents and the dependence of the decaying component of whole-cell current on the holding potential.

We assume a conventional gating mechanism in which the channel moves sequentially through resting and open states before inactivating. When inactivation from the open state is relatively slow compared to the duration of the voltage step, most channels will open for the duration of the voltage step. Some channels, however, will inactivate shortly after the onset of the voltage step and the rate of open channel inactivation will determine the relative proportion of inactivating and non-inactivating single-channel currents. If the rate of inactivation from the open state does not depend on membrane potential, as suggested by

studies of whole-cell Ca^{2+} currents (Slesinger and Lansman, 1991a), then the relative proportion of inactivating and non-inactivating single-channel currents will also be independent of membrane potential.

Although a simple sequential gating mechanism can account for inactivating and non-inactivating currents, it does not explain why shifting the holding potential to more positive levels abolishes the decaying component of whole-cell Ca^{2+} current. In the experiment shown in Fig. 2, channels become unavailable for opening as the holding potential is shifted in the positive direction. If it is assumed that some of these inactivated channels can return to rest from the inactivated state after the onset of the voltage pulse, these channels will open after a delay. We suggest that the more positive holding potential does not selectively suppress inactivating channels, rather, it increases the fraction of channels that open after a delay because there is a finite rate of return to rest from the inactivated state. When the holding potential is in the range of resting channel inactivation (see Fig. 2C), the current through channels that open rapidly after the onset of the voltage step and inactivate and through those that recover from inactivation during the test pulse and open after a delay will produce a non-decaying mean current. With negative holding potentials, on the other hand, more channels are in the resting state; these open quickly after the onset of the pulse and the fraction that inactivate produces the decaying component of whole-cell current.

A mechanism in which the holding potential modifies the time course of macroscopic current by altering the distribution of the channel among non-conducting states is new for Ca^{2+} channels, but is well known for voltage-gated K^+ channels. K^+ channels open more slowly when the voltage step is preceded by a negative prepulse (Cole and Moore, 1960; White and Bezanilla, 1985; Hoshi and Aldrich, 1988). The negative prepulse simply favors the channel being in the closed state farthest from the open state and so it takes longer to open. The opposite appears to be the case for Ca^{2+} channels in that a negative prepulse favors the removal of inactivation allowing channels to open rapidly after the

pulse. Nonetheless, the underlying gating mechanisms appear to be remarkably similar for these two types of voltage-gated channels.

Chapter 3

INTRODUCTION

Ca^{2+} entry through voltage-gated Ca^{2+} channels in neurons must be sufficient to raise intracellular free Ca^{2+} to the levels that trigger the release of neurotransmitters, activate intracellular enzymes, and regulate repetitive firing by activating ion channels (Tsien and Tsien, 1990). The duration and amplitude of the action potential determines how much Ca^{2+} flows across the cell membrane. If Ca^{2+} channels open during the peak of the action potential, the driving force for ion entry is small and little Ca^{2+} enters the cell. Most Ca^{2+} is likely to enter during action potential repolarization when Ca^{2+} channels are closing (Katz and Miledi, 1967; Llinas et al, 1981; Llinas et al, 1982). Yet, the rate at which Ca^{2+} channels close is fast (Fenwick et al, 1982; Carbone and Lux, 1987; Swandulla and Armstrong, 1988) and may limit Ca^{2+} entry during brief action potentials.

We describe here a previously unrecognized pathway for Ca^{2+} entry through L-type Ca^{2+} channels in mammalian central neurons. Following a strong depolarization, some Ca^{2+} channels are closed immediately after repolarization, but open after a delay of up to many tens of milliseconds (cf Hoshi and Smith, 1987). The delayed opening of Ca^{2+} channels at negative membrane potentials is enhanced by voltages that inactivate channels and inhibited by allowing channels to recover from inactivation, suggesting that some channels recover from inactivation by passing through the open state.

METHODS

See Chapters 1 and 2 for details on methods.

Data Analysis

The probability of a channel reopening after a test pulse, given that the channel was closed after repolarization, was measured by counting the number of sweeps in which the channel reopened and dividing by the total number of sweeps, excluding those sweeps in which the channel was already open. To distinguish channels that reopened from those that were already open after repolarization, a reopening was defined as a single-channel event at the holding potential that occurred after an arbitrary cutoff of 0.4 ms before opening. This cutoff would underestimate the probability of reopening, but was necessary to exclude sampling bias that might mistake a single-channel tail current as a reopening. The sweeps in which there were no openings indicate that either the channel has not reopened by the end of the sweep (< 100 ms) or the channel closed too quickly to be detected.

RESULTS

Figure 1a shows single-channel currents recorded in response to brief depolarizations applied to a cell-attached patch on a cerebellar granule cell. The patch electrode contained Ba^{2+} as the only inward charge carrier. The series of rectangular voltage steps was designed to mimic the brief excursions to positive potentials that would occur during a burst of neuronal action potentials. Ca^{2+} channel activity was undetectable during the brief pulses to +50 mV, presumably because the driving force for ion entry is small and the single-channel currents are within the noise level of the recording system. Large channel openings could be seen to follow some, but not all, of the voltage steps (arrows indicate the time at which the patch potential was returned to -90 mV). The channel opening shown in the top record is re-plotted on an expanded time scale below and shows that the channel was closed immediately after the membrane potential was returned to -90 mV and then opened after a delay of ~1 ms (figure 1a, bottom record). These delayed openings are distinguished from single-channel tail currents where the channel is already open after repolarization. We refer to these delayed channel openings as reopenings as the experiments described below show they can be explained by the return of channels from an inactivated state.

To identify the type of channel that opened after repolarization, we examined the response of the single-channel activity to the selective dihydropyridine agonist and antagonist, +(S)-202-791 and -(R)-202-791 (Hof et al, 1985). Dihydropyridines regulate the activity of the class of L-type Ca^{2+} channels which have a relatively large single-channel conductance and slow inactivation (Tsien et al, 1988). Figure 2a shows the effect of dihydropyridine agonist on channel opening after the test pulse at negative potentials. The top two records show the single-channel activity that is produced after repolarizing to -70 mV from a test potential of +50 mV in the absence (figure 2a i) and presence (figure 2a ii) of agonist. Exposing the patch to 1 μM of the dihydropyridine agonist +(S)-202-791

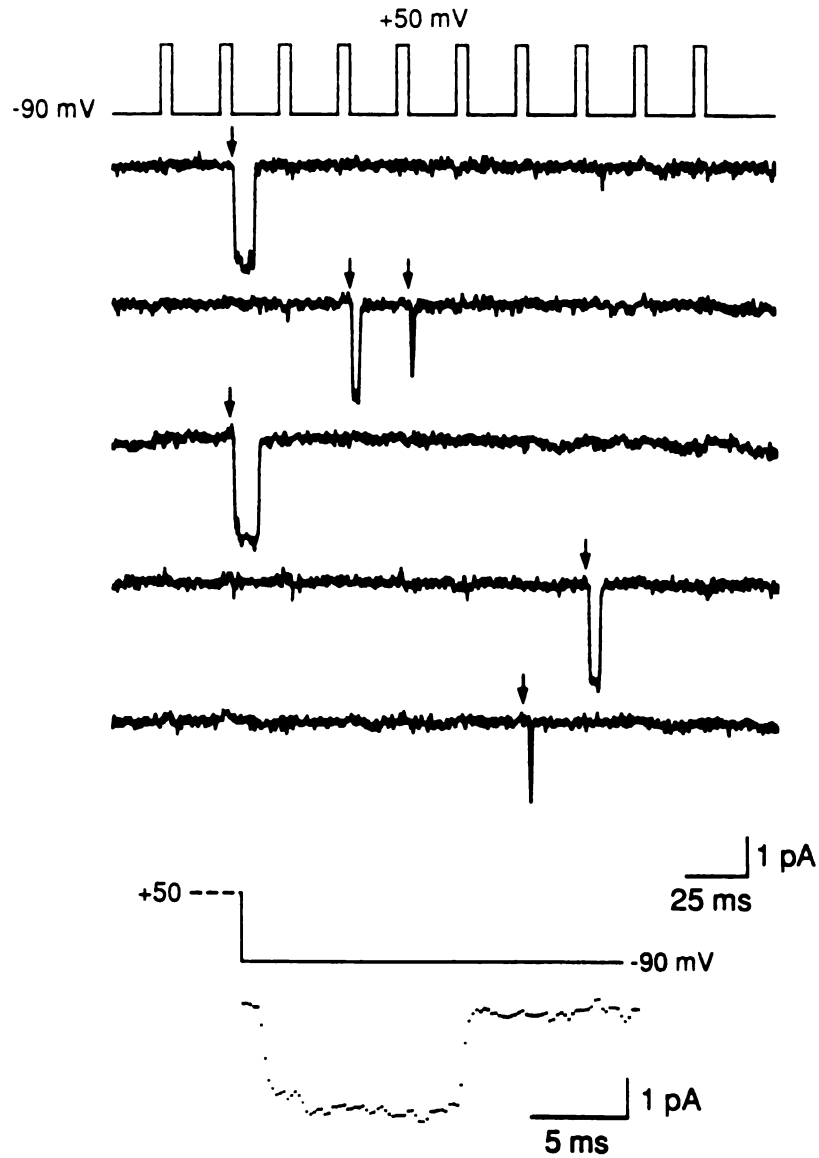

Figure 1. Single-channel currents evoked by brief depolarizations applied to a cell-attached patch on a cerebellar granule cell. The voltage protocol consisted of ten voltage steps to +50 mV, each voltage pulse lasting 5 ms. The leak-subtracted current responses are shown below the voltage protocol and the arrows mark the time at which the patch potential was repolarized to -90 mV. Downward deflection of the current record indicates the opening of a Ca^{2+} channel at the holding potential of -90 mV. Bottom record, the opening in the first record re-plotted on an expanded time scale to illustrate that the channel was closed immediately following repolarization and then opened after a delay. Channel openings recorded at -90 mV following 150 repetitive 10 ms pulses to +50 mV were tested for statistical independence by a runs analysis, taking each voltage step as an independent trial (Horn, 1984). Channel reopenings were not clustered, but occurred randomly (random test variable $Z = \sim 0 \pm 1$, mean ± SD).

increased the duration of the openings after the voltage step as well as the number of openings. The mean current was also larger and decayed more slowly, consistent with the known effects of dihydropyridine agonists on L-type Ca^{2+} channels (Hess et al, 1984). When the single-channel amplitude of the delayed openings were measured at different repolarization potentials (in the absence of any drug, solid symbols) and compared with the amplitude of L-type Ca^{2+} channels currents measured in the presence of dihydropyridine agonist (figure 2c, Δ), the single-channel conductances were indistinguishable.

Figure 2b shows the effect of the dihydropyridine antagonist -(R)-202-791 on the single-channel activity during and after a voltage step. Single-channel activity was recorded during test pulses to 0 mV (figure 2bi) as well as following test pulses to +50 mV (figure 2bii) to compare the effect of the antagonist on channels that opened during the voltage step with those that opened after repolarization at negative potentials. Figure 2bi shows the mean current through channels that opened in response to test pulses to 0 mV. Exposing the patch to 1 μM -(R)-202-791 reduced the amplitude of the mean current during the pulse. As shown in figure 2b ii, the antagonist also reduced the mean current obtained by averaging the current through the channels that opened after the voltage step (details in figure legend). In three other recordings from granule cells, -(R)-202-791 reduced the current during the voltage step to 68± 22% (mean ± SEM) of control and reduced the delayed openings following repolarization to 27± 2% of control. Inhibition of the current after the voltage step was always greater than the inhibition of the mean current measured during the voltage step, suggesting that the effects of the antagonist may be greater at +50 mV than at 0 mV. Nifedipine, another dihydropyridine antagonist, neither inhibited the channel activity during a voltage step to 0 mV (103 ± 6%, mean ± SEM, n=4) nor the openings after repolarizing the membrane (144 ± 22%), perhaps reflecting a mixed agonist and antagonist action.

The Ca^{2+} current in cerebellar granule cells is sensitive to both dihydropyridines as well as ω-conotoxin, but neither drug selectively inhibits a distinct kinetic component of

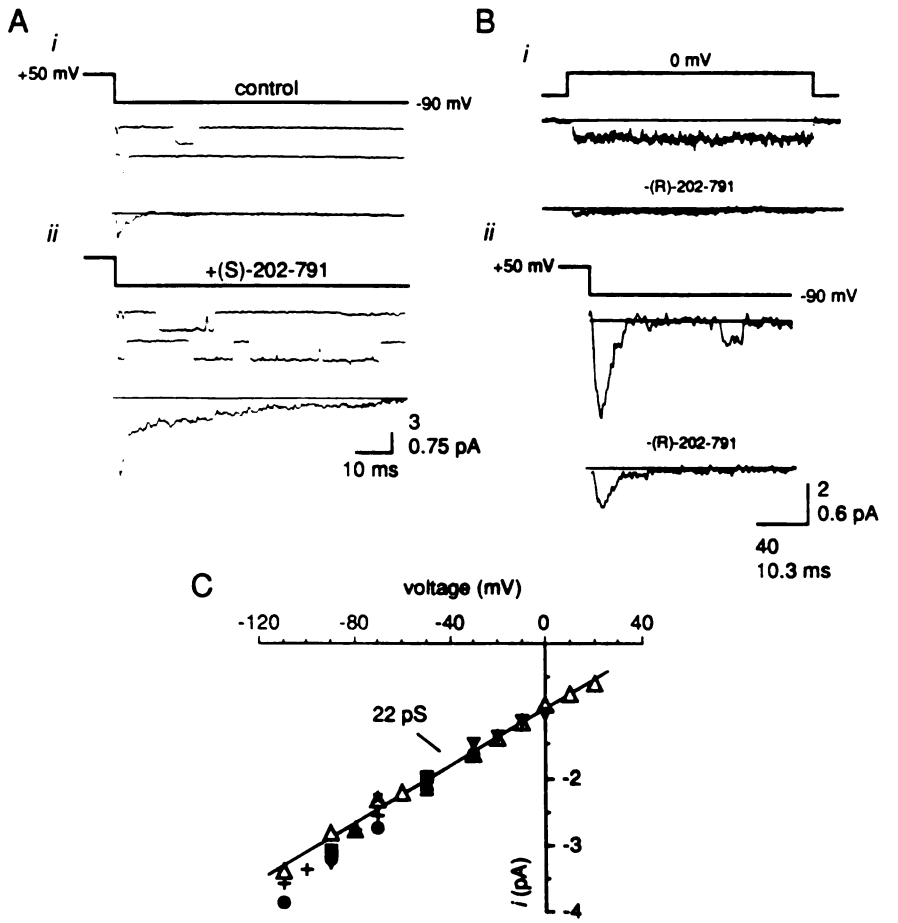

Figure 2: The channel openings at negative membrane potentials are modified by dihydropyridine Ca^{2+} channel agonist and antagonist. **(A)** The response to dihydropyridine agonist. Top two current records show channel openings before (i) and after (ii) exposing the patch to the dihydropyridine agonist +(S)-202-791 (1 μM). Channel events were recorded at the holding potential of -90 mV following a test potential to +50 mV that lasted for 150 ms. The mean current is shown below each pair of records and are the averages of 46 (control) and 49 (drug) individual sweeps. **(B)** The response to dihydropyridine antagonist. (i) Mean currents obtained by averaging single-channel activity recorded during a test pulse to 0 mV in the absence and presence of the dihydropyridine antagonist -(R)-202-791 (1 μM). The mean currents are the averages of 12 and 18 sweeps in the absence and presence of drug, respectively. (ii) The mean current shown on an expanded time scale of the current through channels that opened at -90 mV following test pulses to +50 mV that lasted 200 ms. The mean currents are the averages of 10 and 38 individual sweeps in the absence and presence of drug, respectively. Sweeps in which the channel was already open after repolarization were excluded. **(C)** The amplitude of the single-channel current measured after repolarization from +50 mV to different membrane potentials plotted as a function of repolarization potential (4 cells, solid symbols). The single-channel i-V relation for the 22 pS L-type Ca^{2+} channel measured in the presence of 1 μM +(S)-202-791 is shown for comparison (Δ, Slesinger and Lansman, 1991b).

high-threshold current (Slesinger and Lansman, 1991a,b and unpublished observations). Although cerebellar granule cells possess multiple pharmacological components of Ca^{2+} current, the kinetic behavior of a single type of channel is sufficient to explain the time and voltage dependence of the whole-cell current (Slesinger and Lansman 1991b). The channels that open after a delay at negative membrane have both short and long open times, are modified by dihydropyridines, show fast block of the open channel in the presence of multivalent cations, and wash-out after patch excision (Slesinger and Lansman, submitted for publication and unpublished observations). These properties are most consistent with the behavior of L-type Ca^{2+} channels (Bean, 1989; Hess, 1990).

Ca^{2+} channels were more likely to reopen after a long voltage step lasting hundreds of milliseconds rather than after brief voltage step. Figure 3a shows the single-channel activity recorded after brief (20 ms, left) and long voltage steps (120 ms, right). There were more sweeps in which the channel reopened after the longer voltage step and the average of the single-channel currents increased nearly three-fold (figure 3a, bottom records). The average single-channel current also had a distinct rising phase as expected if channels were closed immediately following repolarization and then opened. The probability of reopening was measured as the number of sweeps in which the channel reopened after a test pulse divided by the total number of sweeps, excluding those sweeps in which the channel was already open at the end of the voltage step. Because the number of channels in the patch varied in different experiments and could not be determined with certainty, the probability of reopening is expressed as a fraction of the probability measured at 200 ms. The probability of reopening increased as the duration of the test pulse increased, reaching a maximum with test pulses longer than ~150 ms (figure 3b, ●). The probability of reopening increased along an exponential time course with a time constant of ~48 ms (smooth curve).

The whole-cell Ca^{2+} channel current evoked by a test pulse to +50 mV also decays along an exponential time course as channels inactivate (figure 3b, inset; Slesinger and

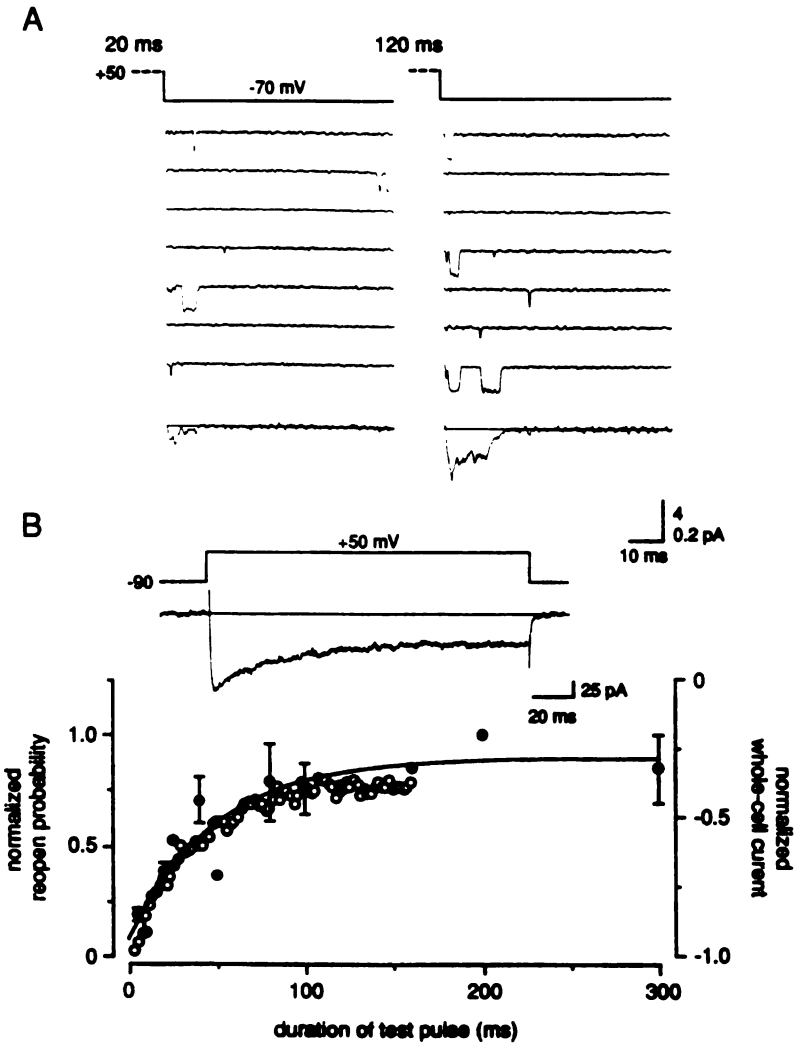

Figure 3: The probability of a Ca^{2+} channel reopening at negative potentials increases as channels inactivate during a voltage step. (**A**) Single-channel currents recorded at -70 mV following consecutive test pulses to +50 mV that lasted either 20 ms (left) or 120 ms (right). The mean currents are shown below (28 and 31 sweeps, respectively, lower scale bar). (**B**) The mean probability of reopening normalized to the probability at 200 ms plotted as a function of test pulse duration (● ± SEM, n=7). Points have been fit by a single exponential plus a constant (time constant = 48 ms, amplitude = 0.81, constant = 0.11, smooth curve) with use of a least-squares algorithm. (**inset**) The whole-cell Ca^{2+} channel current elicited by a 160 ms voltage step to +50 mV recorded from another granule cell. The whole-cell current was normalized to peak current obtained by back-extrapolation to the beginning of the pulse and superimposed on single-channel data (right axis, —o—). The time constant for the decay of whole-cell Ca^{2+} channel current from a number of recordings was 53 ± 6 ms (± SEM, n=17). The time course of the decay of whole-cell Ca^{2+} channel current is independent of either the concentration of external Ba^{2+} or amplitude of current (Slesinger and Lansman, 1991a).

Lansman, 1991a). If the Ca^{2+} channels that reopen do so from an inactivated state, then the probability of reopening would increase with a time course that follows the rate at which channels enter the inactivated pool. Figure 3b (—o—) shows the whole-cell current normalized to its peak amplitude and superimposed on the change in the probability of reopening. The decay of whole-cell Ca^{2+} channel current follows closely the the probability of reopening for single Ca^{2+} channels, suggesting that channels reopen only after they inactivate during the test pulse.

If channels reopen after inactivating, then voltage steps to potentials that produce little inactivation during the voltage step would produce few, if any, reopenings after repolarization. Figure 4 shows the results of an experiment in which we measured the probability of reopening following test pulses that varied in amplitude. Figure 4a shows the single-channel activity produced during a 200 ms test pulses and, on an expanded time scale, following repolarization at the holding potential of -90 mV. Ca^{2+} channels opened in response to the test potential to -10 mV, but did not reopen after the pulse (figure 4a i). By contrast, channels also opened during each test pulse to +20 mV but reopened following many of the test pulses (figure 4a ii). Note that the mean current does not decay during the test pulse to -10 mV, but rises to a peak and decays during the test pulse to +20 mV (compare lower traces in figure 4a i,ii) and the probability that a channel reopened after the pulse increased from 0 to 0.26. Channels are not likely to reopen from closed states in activation pathway, since voltage steps that open channels during the pulse, but are not sufficiently strong to inactivate channels, fail to produce reopenings after the pulse.

Figure 4b shows the probability of reopening following voltage steps of increasing amplitude measured in a number of different experiments. The probability of reopening is small after voltage steps to -10 or 0 mV and increases steeply to a maximum with more positive test potentials (solid circles). The points were well described by a Boltzmann relation with a half-activation potential ($V_{1/2}$) of +14 mV and a slope k= 5.6 mV. Evidently, Ca^{2+} channels reopen after voltage steps that are ~20 mV more positive than

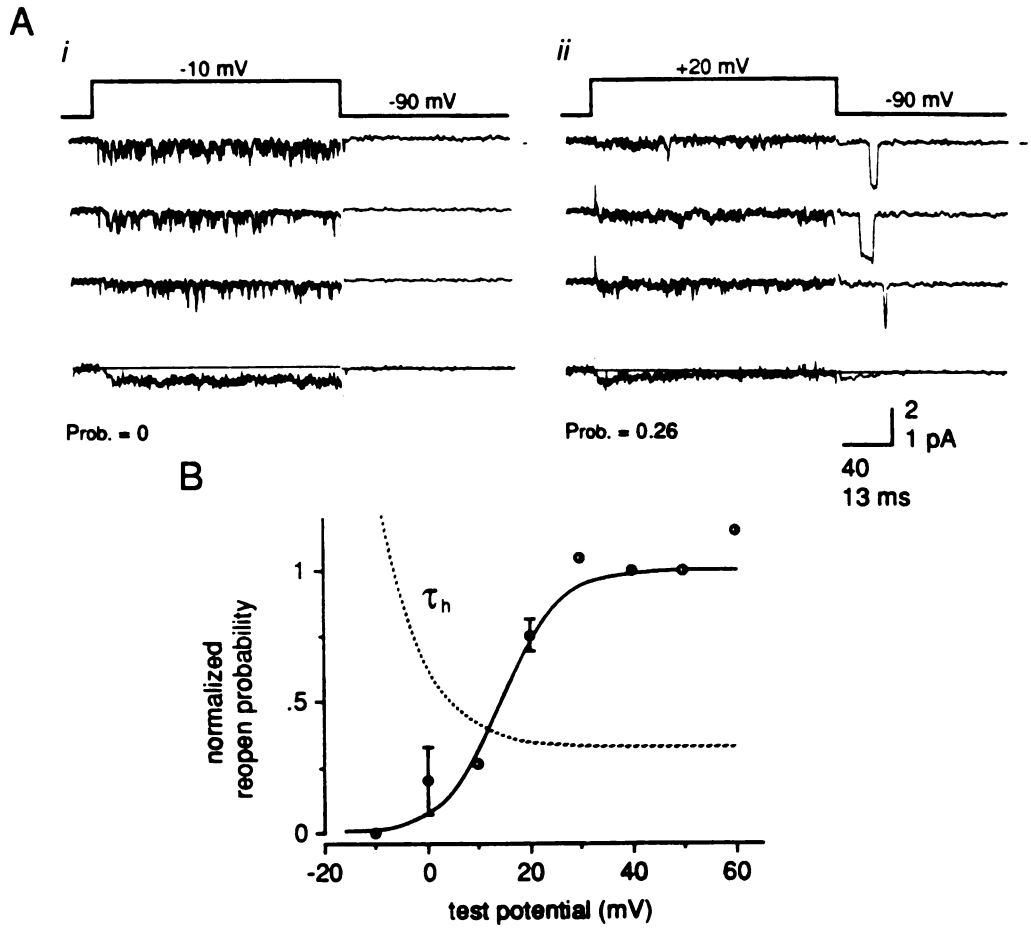

Figure 4: Effect of voltage of the test pulse on the reopenings after the pulse. (**A**) Single- channel activity produced in response to a 200 ms voltage step to (i) -10 mV or (ii) +20 mV. The currents after repolarization to the holding potential of -90 mV are shown on an expanded time scale. The probability of reopening for this recording (see Methods for details) and the mean currents shown below each set of current records (averages of 17 and 37 sweeps). (**B**) Probability of reopening after a voltage step normalized to that at +40 mV plotted as a function of the test potential (mean ± SEM, n= 4, half-filled circles are single points). Smooth curve shows the fit to a Boltzmann relation of the form

$$\frac{P}{P_{40}} = \frac{1}{1+e^{\frac{-(V-V_{1/2})}{k}}}$$

with a half-activation potential ($V_{1/2}$) of +14 mV and a slope k= 5.6 mV. Dashed line shows the relative change in the time constant (τ_h) which describes the rate of decay of the whole-cell Ca^{2+} channel current at different test potentials (Slesinger and Lansman, 1991a). We estimate that the change in surface potential by increasing external Ba^{2+} from 20 to 90 mM to be no more than +10 mV.

those which open channels from rest. The dashed curve shows the normalized time constant of the decay of whole-cell Ca^{2+} current during voltage steps to various potentials (Slesinger and Lansman, 1991a). With voltage steps more positive than +20 mV, the rate of decay of the whole-cell current becomes insensitive to membrane potentials and the probability of reopening reaches a maximum, consistent with the interpretation that entry into an inactivated state determines whether a channel subsequently reopens at negative potentials.

If channels reopen from an inactivated state, the probability of reopening should fall as channels recover from inactivation at negative membrane potentials. Figure 5 shows an experiment designed to test this prediction. A strong prepulse was applied to the patch to inactivate channels and, after a variable recovery interval, the probability of reopening was measured after a brief test pulse (see figure legend). The normalized probability of reopening decreased along an exponential time course as the interval between prepulse and the test pulse increased (figure 5b, solid circles). Figure 5b (·--o--) shows the time course of the recovery of the whole-cell Ca^{2+} channel current following a strong prepulse. As the duration of the recovery interval increased, the normalized current increased with a rate that was similar to the decrease in the probability of reopening (figure 5b, smooth curve). Evidently, fewer channels are available to reopen as they recover from inactivation and a component of the fast recovery process must include channels that pass through the open state before returning to rest. The slow component of recovery, however, must involve electrically silent closed states, because we do not see a large inward whole-cell current during the long recovery interval (cf Bezanilla and Armstrong, 1977).

Although voltage dependent inactivation reduces the number of channels that are available for conducting ions during the pulse, it increases the probability that a channel reopens after a pulse. This leads to the expectation that Ca^{2+} influx after a voltage step may be enhanced as inactivation develops. The single-channel recordings suggest that the time course of the tail current measured after a long voltage step represents the current that flows

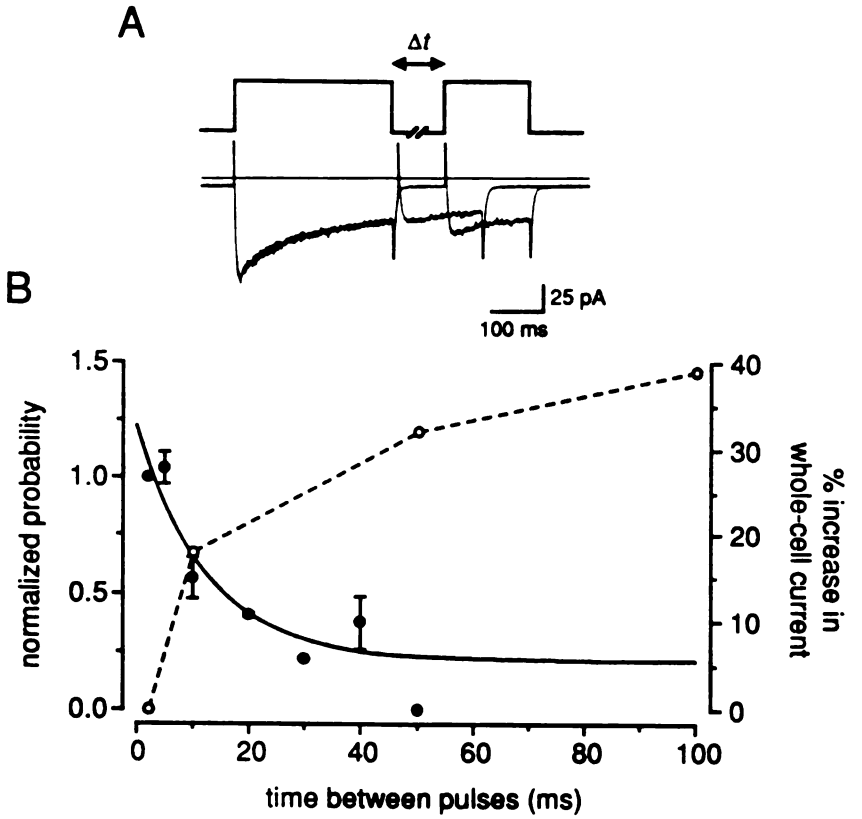

Figure 5: The probability of reopening decreases as channels recover from inactivation. (A) Whole-cell Ca^{2+} channel currents elicited by a two-pulse voltage-clamp protocol with an interpulse interval of either 10 or 100 ms (Δt) at -90 mV. The prepulse and test potentials were +30 mV, each lasting 300 and 160 ms, respectively. Current records are not leak-subtracted (line indicates zero current level). (B) Peak whole-cell Ca^{2+} channel current elicited by the test pulse normalized to peak current during the prepulse plotted as a function of the duration of the recovery interval between pulses (right axis, ·--o--). The recovery of the whole-cell current from inactivation was fit by a double exponential with fast and slow time constants of 9 ms (amplitude=0.13) and 672 ms (amplitude=0.52), respectively (the slow component is not shown and the points have been scaled to show the fast component of recovery). To measure the reduction in the probability of reopening during recovery, the patch potential was stepped to +50 mV for 200 ms to inactivate channels and then a test pulse to +50 mV was applied after a recovery interval at -90 mV that lasted 2-30 ms. The probability of reopening following the second pulse normalized to that measured after the recovery interval of 2 ms is plotted as a function of the interpulse interval (● ± SEM, n=4). The smooth curve shows the fit to a single exponential with a time constant of 12 ms (amplitude=1.0) plus a constant= 0.21. The probability asymptotes near 0.2 because the test pulse in the absence of the prepulse produces reopenings (see fig. 3). The holding potential was -90 mV.

through channels that are open and then rapidly close as well as current that flows through channels that reopen as they pass through the open state before returning to rest. We tested the idea that as inactivation of whole-cell Ca^{2+} channel current develops during a voltage step, the amount of Ca^{2+} that enters the cell after the voltage step increases.

Figure 6a shows an example of the whole-cell Ca^{2+} tail currents produced after the membrane potential was quickly shifted to -90 mV after a test pulse lasting either 5, 50 or 140 ms (the arrow marks the beginning of the repolarization, the current during the test pulse is not shown). The time course of the tail current is slower after the longest test pulse, which is better seen in the inset of figure 6a in which the tail currents following the 5 and 140 ms voltage steps are scaled so that the peak amplitudes are the same. To estimate the amount of Ca^{2+} that enters the whole-cell through channels that reopened, we measured the total charge carried by the tail current at a time when ~90% of the channels that were open at the end of the test pulse would have closed directly from the open state after repolarization (Slesinger and Lansman 1991a).

Figure 6b (▲) shows the total charge flowing into the cell after repolarization increases with the duration of the preceding voltage step along a single exponential time course that is indistinguishable from the rate of decay of the whole-cell current during the pulse (figure 6b, ○). If channels simply closed after repolarization, the amount of charge that flows during the tail should decrease to the same extent as the current during the pulse, since the number of available channels decreases. The charge that flowed during the tail, however, increased by ~40% even though the current during the pulse decreased by roughly the same amount. In four other recordings, the current decreased by 31± 5% (mean ± SD) by the end of a 160 ms voltage step, while the charge increased by 40± 43%.

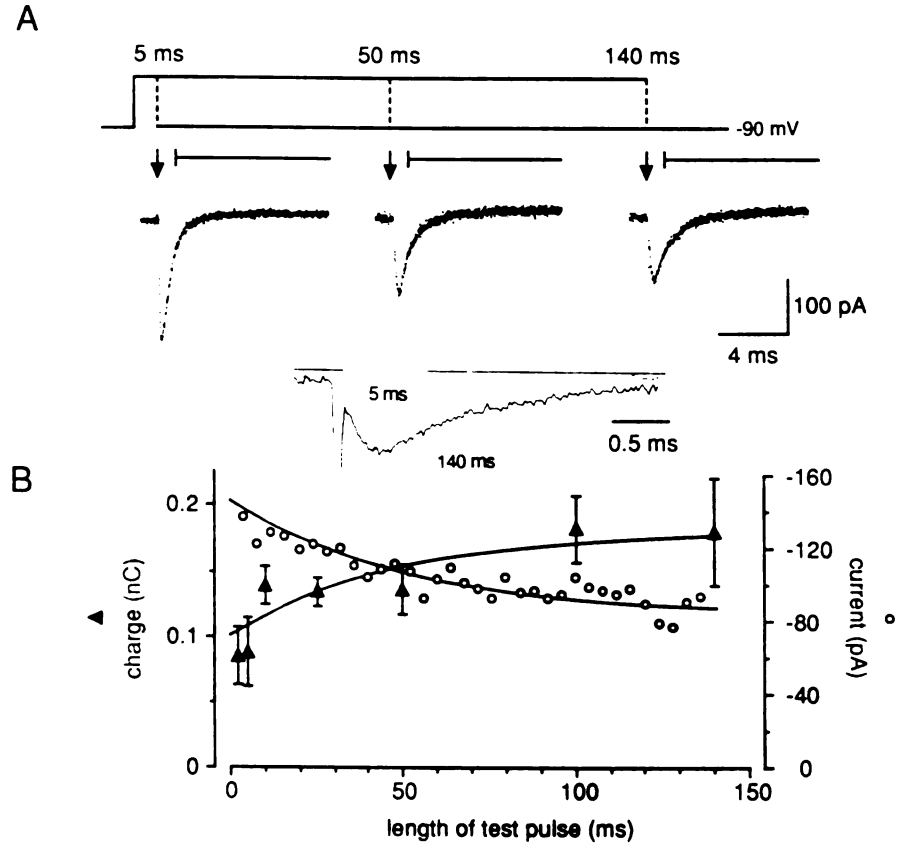

Figure 6: The effect of the test pulse duration on the amount of Ca^{2+} that flows into the whole cell after repolarizing the membrane potential to -90 mV. (A) Ca^{2+} channel tail currents measured after rapidly repolarizing the membrane to -90 mV from a test pulse to +60 mV that lasted 5, 50 or 140 ms (arrow marks beginning of repolarization to -90 mV, see Slesinger and Lansman, 1991a). (**Inset**) Ca^{2+} channel tail currents measured after voltage steps that lasted either 5 (dots) or 140 ms (line) scaled so that the peak amplitudes are the same. (B) The whole-cell Ca^{2+} channel current during a test pulse to +20 mV (O) and the amount of charge carried by Ca^{2+} during the tail (▲ ± SD) plotted as a function of the duration of the test pulse. The current during the test pulse was measured at +20 mV because the amplitude of the current during a voltage step to +60 mV was too small to measure accurately. This would produce a negligible error in the corresponding time constant because the decay of current is voltage-independent at test potentials more positive than +10 mV, Slesinger and Lansman, 1991a). The current during the test pulse (shown inverted) was fit with a single exponential with a time constant of ~ 52 ms plus a constant (smooth curve). The smooth curve through the ▲'s shows the single exponential fit with a time constant of ~47 ms plus a constant. The amount of Ca^{2+} that enters during the tail was measured by integrating the tail current 1 ms after repolarizing to -90 mV (solid bars indicate the time over which the amount of change flowing was measured). We estimate that ~90% of the channels have closed by 1 ms following repolarization (Slesinger and Lansman, 1991a), leaving channels that reopen. Small deviations in the zero current level that could produce an error in the measured charge were minimized by setting the last 5 ms of the 20 ms tail current to zero.

DISCUSSION

The main finding of this paper is that L-type Ca^{2+} channels recover from voltage dependent inactivation by passing through the open state. This component of recovery produces large single-channel events at negative membrane potentials that occur after a delay of one to many tens of milliseconds after the initial depolarization, providing a pathway for Ca^{2+} entry at membrane potentials where there is a large driving force for ion entry.

The results are consistent with a "ball and chain" model for inactivation in which membrane depolarization drives an inactivation particle into the open channel (Armstrong and Bezanilla, 1977; Hoshi et al., 1990). If it is assumed that the inactivation particle holds the channel open, then channels will reopen as the inactivation gate leaves the channel at negative potentials. The extent to which the inactivation gate stabilizes the open state will determine the relative proportion of channels that return to rest through the open state and the proportion that return to rest through electrically silent closed states that are generally considered to be the primary pathway for recovery of inactivated channels (Armstrong and Bezanilla, 1977). We estimate from measurements of the probability of reopening that roughly 10-20% of the channels recover through the open state. Because this estimate is obtained by normalizing the measured probability for reopening by number of channels in a patch, which cannot be determined precisely, it represents an upper limit.

Implications for Ca^{2+} channel gating

Studies of single Ca^{2+} channels have led to different views about the mechanism of channel gating. In contrast to conventional stochastic gating schemes in which channels move between distinct closed, open, and inactivated states, Ca^{2+} channel gating transitions have often been described in terms of gating modes in which the channel switches between sets of states, each governed by its own set of rate constants. A switch between gating

modes was proposed to explain the appearance of long duration openings of L-type Ca^{2+} channels in response to dihydropyridine agonists, β-adrenergic stimulation, or strong depolarizations (Hess et al, 1984; Yue et al, 1990; Pietrobon and Hess, 1990). Modal gating schemes, however, fail to account for the finding that the L-type Ca^{2+} channels described here can be closed immediately following repolarization and then enter a long duration open state after a delay ranging from roughly a millisecond to tens of milliseconds. Modal gating predicts that strong depolarizations would drive channels into the long duration open state without an appreciable delay after repolarization. The rate constants for the transition between modes measured recently by Pietrobon and Hess (1990), moreover, predict that transitions from the short to long open state mode at negative potentials would be extremely rare, although we find that both types of transitions occur with roughly equal probabilities after repolarization (Slesinger and Lansman, submitted for publication). On the other hand, the measured rate for the transition between gating modes is similar to the rate of inactivation of whole-cell L-type Ca^{2+} current in cardiac myocytes. The experimental results support a more conventional gating scheme in which the channel moves among kinetically distinct open and inactivated states at positive test potentials and the inactivated state is the primary pathway to a second open state, as originally proposed by Chandler and Meves (1970) for axonal Na^{+} channels.

Reopening of Ca^{2+} channels is not unique to Ca^{2+} channels in cerebellar granule cells (hippocampal neurons: figure 11, Fisher et al, 1990) and would occur whenever there is a component of recovery from voltage-dependent inactivation that occurs through the open state. A similar conclusion was reached for the behavior of rapidly inactivating *Shaker* K^{+} channels by Demo and Yellen (1991) who found that brief depolarizations produced single-channel tail currents from channels that were open during the pulse, while long voltage pulses produced openings that occurred with a delay after repolarization even though the channels had inactivated during the voltage pulse. We speculate that inactivation serves a

double purpose: to terminate channel opening as it does in Na^+ channels and to provide a mechanism for delaying opening beyond the initial stimulus. Between these extremes, opening and reopening may be finely balanced to be optimally suited for the signaling requirements of specific types of neurons in the central nervous system.

Chapter 4

INTRODUCTION

Ca^{2+} influx is an important signalling pathway for triggering the release of neurotransmitters, controlling neuronal excitability and neurite outgrowth (for review, see Bean, 1989; Augustine et al., 1987; Tsien and Tsien, 1990). Recordings of single Ca^{2+} channels have shown a previously unrecognized component of Ca^{2+} entry through L-type Ca^{2+} channels that are closed immediately after repolarization and then open after a delay (Slesinger and Lansman, 1991c). The delayed openings at negative membrane potentials are enhanced as channels enter the inactivated pool and suppressed as channels recover from inactivation, suggesting that some channels return to rest by passing through the open state (Slesinger and Lansman, 1991c). Delayed openings are expected for a model of Ca^{2+} channel gating in which an inactivation "gate" occludes the open channel and prevents the activation gate from quickly closing after repolarization. In this paper, we analyzed the kinetics of channels opening from rest during the normal activation process and during recovery from inactivation to understand the conformational transitions underlying these two distinct channel opening processes. The results are discussed in terms of a general model for Ca^{2+} channel gating which describes the coupling of channel opening to inactivation and predicts the time course of Ca^{2+} entry following test pulses. The model is compared with other models of Ca^{2+} channel gating which explain the actions of dihydropyridines or mechanism of prepulse potentiation. Some of these data have been reported in abstract form (Slesinger and Lansman, 1991d).

METHODS

See Chapters 1 and 2 for details on methods.

Data Analysis

To distinguish single-channel tail currents from channels that are open at the beginning of repolarization from channels that are closed and then open after a delay, a delayed opening was defined as a channel that was closed for a minimum of 400 μs before opening. The distribution of waiting times measured for delayed openings and simulations of single-channel recordings suggested that the number of events that occur during the first 400 μs after repolarization is small (<5%).

The waiting time was measured as the time taken before a channel opens for the first time in idealized current records using a half-threshold criterion (Colquhoun and Sigworth, 1983). Waiting time measurements are shown either as a histogram of the number of events for a given duration or as an integrated form which shows the probability of a channel opening before the time *t*. Each waiting time distribution was fitted to either Eq. 1 or 2 as judged by least-squares minimization routine,

$$P(t) = 1-(-R_2\exp(-tR_1)+R_1\exp(-tR_2))/(R_1-R_2) \quad \text{Eq. 1}$$

$$P(t) = 1-(A_1\exp(t/\tau_1)+A_2\exp(t/\tau_2)) \quad \text{Eq. 2}$$

where $1/R_1$, $1/R_2$, τ_1 and τ_2 are the relative time constants. Eq. 1 describes the probability of opening as a function of time for a sequential scheme with two closed states and one open state, given that the channel opens from the first closed state (Patlak and Horn, 1982). The interpretation of Eq. 2 is discussed in Results. Although there were two channels in the patch during a typical recording as judged by the number of superimposed single-channel events, we did not correct the distribution of waiting times for the number of channels. The time constants for the waiting times would be slower than indicated, but if it is assumed that the number of channels is constant during a recording, then the voltage dependence of the time constants from different experiments should be comparable.

Open channel durations were measured from idealized current records by a half-threshold detection method (Colquhoun and Sigworth, 1983). Histograms of open channel durations were fitted with a power density function as a sum of exponential components by use of a maximum-likelihood fitting routine. The power density functions were corrected for missed events by setting a cutoff at 400 μs which was subtracted from the maximum-likelihood estimate of the time constants (see Colquhoun and Sigworth, 1983).

Simulation of single-channel and whole-cell Ca^{2+} channel activity

Whole-cell currents currents that would flow in response to positive voltage steps from a negative holding potential were simulated by numerical integration of scheme 3 (Appendix). We assumed that channels are in the resting state farthest from the open state (C_1) at t=0 and then redistribute among the closed, open and inactivated states according to the rate constants given in Table 1. The probability of channels being either open or inactivated changes as a function of time and was used to simulate the tail current that would flow after repolarizing the membrane (see Appendix for details). Single channel activity was simulated by calculating the waiting time and probability of moving to an adjacent state using scheme 3, given that the channel starts from an inactivated state (a general procedure described by DeFelice and Clay, 1983). The calculations for each state were repeated until a single epoch equivalent to 160 ms was completed.

RESULTS

Figure 1 shows that Ca^{2+} channels open after a delay at negative membrane potentials following a strong depolarization. Each current record shows the single-channel activity that was recorded at -70 mV following a 200 ms test pulse to +50 mV. The recording electrode contained 90 mM Ba^{2+} as the charge carrier. In some sweeps, the channel was closed immediately after the membrane potential was returned to -70 mV, but then opened after a delay that ranged from ~1 to 64 ms (time indicated to the right of each sweep). In two sweeps, no channel activity was detected following repolarization, indicating that the channel failed to open by the end of the sweep (~100 ms) or that the channel closed quickly. These delayed openings arise from the activity of L-type Ca^{2+} channels because they are sensitive to dihydropyridine agonist and antagonist, and have a conductance that is indistinguishable from L-type Ca^{2+} channels (Tsien et al., 1988; Slesinger and Lansman, 1991c).

The average of all channel activity produced at -70 mV following the pulse to +50 mV is shown at the bottom of figure 1. The mean current decays slowly to zero, falling to half its peak amplitude by ~7 ms. The decay of current is slower than the Ca^{2+} tail current measured after short test pulses in granule cells (Slesinger and Lansman, 1991a) and in other preparations (Swandulla and Armstrong, 1987; Carbone and Lux, 1987a; Fenwick et al., 1982). However, most of the channels open at the time of repolarization would close too quickly to be detected with a 200 μs sampling interval. The time course of the single-channel tail current is therefore determined primarily by the delay before a channel opens and the duration of the opening.

Analysis of waiting times for channels opening from resting and inactivated states

Previous experiments showed that opening of Ca^{2+} channels after a delay at negative potentials was enhanced as more channels enter the inactivated pool and suppressed as

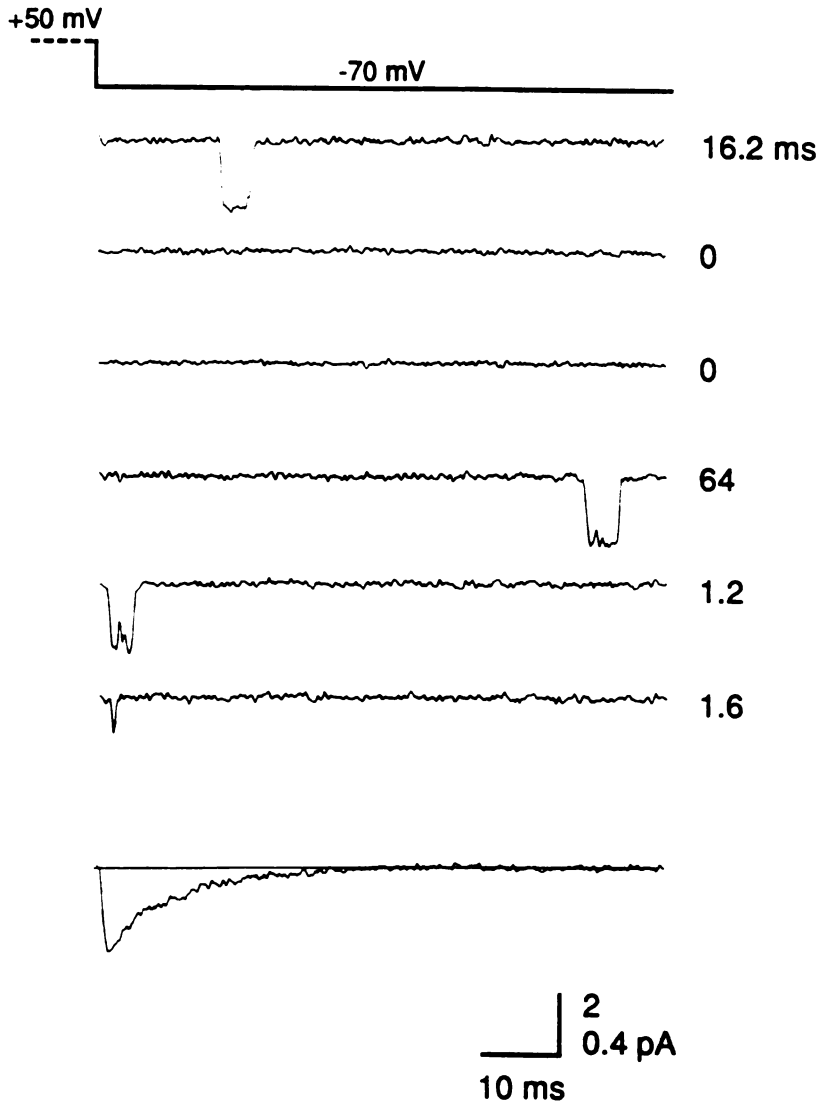

Figure 1: L-type Ca^{2+} channels open after a delay at negative membrane potentials following large depolarizations. Records show single-channel activity recorded at -70 mV following test potentials to +50 mV that lasted 200 ms. These delayed openings appear because some inactivated channels return to rest by passing through the open state (Slesinger and Lansman, 1991c). The time taken before the channel opened indicated to the right of each sweep. Sweeps in which no reopenings were detected indicated as 0 ms. Average of all channel activity that occurred after the pulse shown at bottom (244 sweeps). Capacity transients were removed by subtracting an average of sweeps without openings from the current record (see Methods). Single-channel activity was recorded from cell-attached patches on the soma of cerebellar granule cells with 90 mM Ba^{2+} in the pipet. An isotonic K^+ solution was used to zero the cell's resting potential (see Methods).

channels recovered from inactivation (Slesinger and Lansman, 1991c). The results can be described by a simple linear scheme,

$$C \underset{\beta}{\overset{\alpha}{\rightleftharpoons}} O \underset{k\text{-}1}{\overset{k1}{\rightleftharpoons}} I$$

Scheme 1

Membrane depolarization drives channels from the resting state (C) to the open state (O) from which they can inactivate. After repolarization, inactivated channels return to rest by passing through the open state. For simplicity, we assume that there is no other pathway for returning to rest and consider this pathway later. The delay before the channel opens during recovery from inactivation is determined by the rate constant for leaving the inactivated state (k_{-1}). Scheme 1 suggests that the rate constant governing the transition from the resting to open state should differ from that for inactivated to open state.

This simple scheme was tested by measuring the delay before channels opened for the first time at different membrane potentials. The arrow in Figure 2a (inset) marks the waiting time (Δt) before the channel opened in response to a test pulse to -10 mV. The histogram below shows the frequency of observing the waiting times shown on the horizontal axis measured in a series of consecutive depolarizations. The distribution of waiting times reaches a maximum at a time later than zero and then decays, indicating that the channel passes through multiple closed states before opening (Patlak and Horn, 1982). The smooth curved shows the fit by a power density function for a channel which must move sequentially through two closed states before reaching the open state (Eq. 1). Thus, Scheme 1 must be modified to include an additional closed state in the activation pathway.

$$C_1 \rightleftharpoons C_2 \rightleftharpoons O \rightleftharpoons I_2$$

Scheme 1a

The delay before a channel opened from the inactivated state, on the other hand, behaved quite differently. The arrow in figure 2b (inset) marks the waiting time for a channel to open (Δt) after repolarizing the membrane potential to -70 mV from a positive

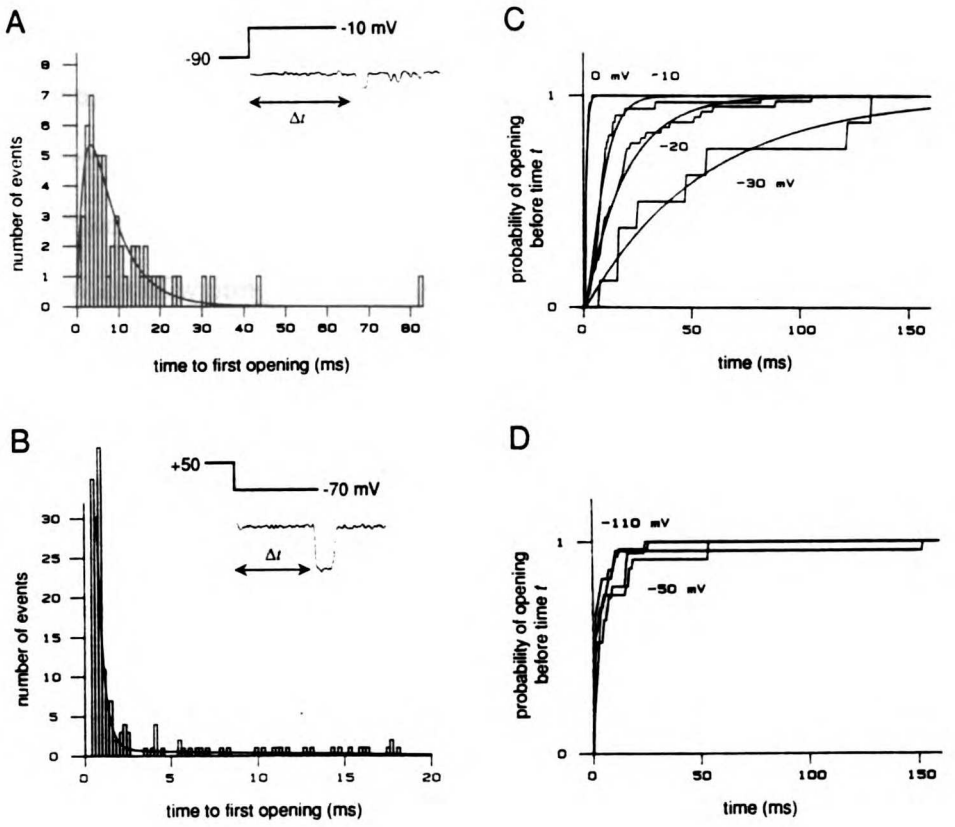

Figure 2: Comparison of the waiting times for Ca^{2+} channels that open from resting and inactivated states. (**A**) The histogram plots the frequency of waiting times measured from the onset of the test pulse (-10 mV) to the time when the channel first opened (arrow, Δt). The smooth curve shows the fit to Eq. 1 (time derivative) with time constants of 6.6 and 1.8 ms. Holding potential was -100 mV. (**B**) Distribution of waiting times for openings that occurred after repolarization. Time measured from the beginning of repolarization to when the channel reopened (arrow, Δt). Smooth curve shows the best fit to Eq. 2 with time constants of 0.4 and 12 ms (ratio = 7.3). (**C**) Time course of waiting times for channels opening from rest in response to different test potentials. The histogram plots the probability of an opening occurring before the time *t* indicated on the horizontal axis. Each curve has been normalized and fit by Eq.1 with time constants of τ_1= 0.3 and τ_2= 56 ms at -30 mV, τ_1= 1.2 and τ_2= 18 ms at -20 mV, τ_1= 4.4 and τ_2= 4.4 ms at -10 mV and τ_1= 0.6 and τ_2= 0.8 ms at 0 mV. (**D**) Time course of waiting times for channels opening from inactivated states at repolarization potentials ranging from -110 to -50 mV.

test pulse. The histogram of waiting times shows that the channel frequently reopened within milliseconds after repolarization, but occasionally reopened after tens of milliseconds (fig. 2b). Note that the distribution of waiting times lacked the initial rising phase that was observed in the histogram for channels opening from rest, although a very rapid rising phase could have been missed because of the dead time (see Methods). The frequency of openings that occurred after a delay of 1 ms or longer was best fit as the sum of two exponentials with fast and slow components (Eq. 2), rather than the single component observed for opening from rest. The smooth curve shows a double exponential fit with fast and slow time constants of 0.4 and 12 ms.

The distribution of waiting times for delayed opening can be explained if the channel moves between at least two inactivated states before opening. During recovery from inactivation the channel can either enter the open state directly, producing a short delay, or enter another inactivated state before returning to the open state after a longer delay (scheme 2, dashed arrow), unlike the activation process in which the channel always opens from the closed state farthest from the open state. Alternatively, the channel returns to the open state from two inactivated states, but with different rates (scheme 2, solid arrow).

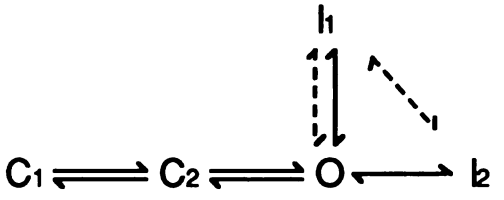

Scheme 2

Although the distribution of waiting times for channels opening from rest and those returning to the open state after inactivating differed, it was possible that some of the delayed openings involved closed states in the activation pathway. Because activation is strongly voltage-dependent, we investigated whether channels opening from inactivated states showed the same or different dependence on membrane potential. Figure 2c shows the waiting times for channels opening at different test potentials. The data are shown in a form which shows the probability that the channel opened before the time *t* indicated on the

abscissa. Each curve is normalized to its maximum value so that the relative time courses can be compared. Ca^{2+} channels open slowly in response to a weak depolarization (-30 mV), but open briskly at more positive test potentials. The smooth lines show the best fit using the equation for two sequential closed and one open state (Eq. 1). The slow time constant increased nearly 100-fold for a 30 mV change in the amplitude of the test potential. Figure 2d shows the waiting times for channels that opened after a delay at four different repolarization potentials. Apparently, the time taken for channels to move from the inactivated to open state changes little with membrane potential over a 60 mV range.

Figure 3 shows the fast and slow time constants for delayed openings plotted as a function of repolarization potential for different patches. The slow time constant increased slightly with more positive membrane potentials, whereas the fast time constant changed little over the range of potentials studied. These results confirm that the rate constants governing the transitions from inactivated to open states are much less sensitive to voltage than those governing transitions from resting to open states. Furthermore, depolarization slows the time it takes for channels to open from inactivated states, the opposite of a channel opening from rest.

These results show that the pathway for channel opening from rest can be distinguished from the pathway for opening from the inactivated state (scheme 2). If the transition from the last closed to the open state in the activation pathway is voltage-insensitive, as has been proposed for other voltage-gated ion channels (Bezanilla and Armstrong, 1977; Zagotta and Aldrich, 1990; Chen and Hess, 1990), the fast component to the delayed openings might arise from a transition between the last closed state preceding the open state. We consider this transition to contribute minimally to the delayed openings primarily because delayed openings are not detected following voltage pulses that are sufficient to open channels from rest, but not sufficiently strong to cause channels to enter the inactivated pool (Slesinger and Lansman, 1991c). If channels open from the closed

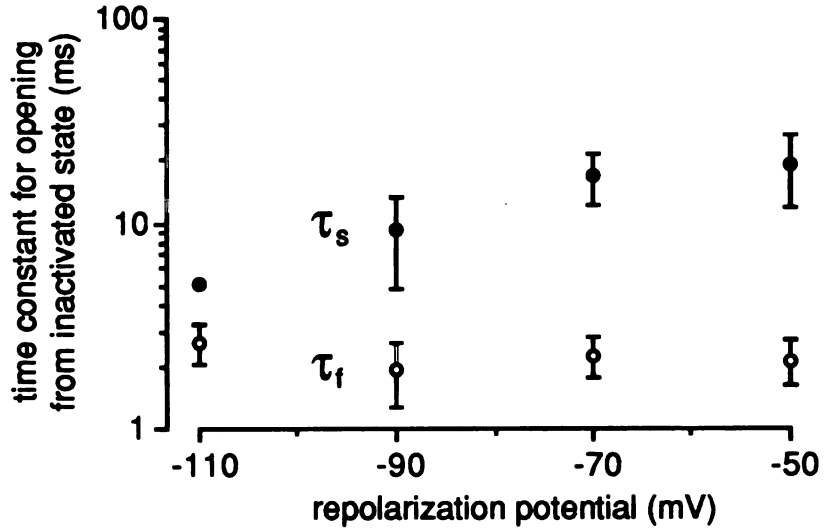

Figure 3: Effect of membrane potential on the rate of opening from inactivated states. Plot shows the fast and slow time constants obtained by fitting a sum of two exponentials to waiting time histograms for opening like the one shown in Figure 3d (Eq. 2). Values are mean ± SEM (n=6).

state preceding the open state, we would expect delayed openings to occur over the same range of potentials that open channels from rest.

Another test of whether channels open from the inactivated state, rather than a closed state in the activation pathway, is to compare the waiting times for channels opening at a fixed test potential in the range of activation, but in the absence and presence of a conditioning prepulse. If strong depolarizing prepulses simply redistributed the channel among closed states along the activation pathway, but not inactivated states, we would expect channels to open more quickly after a conditioning prepulse to +50 mV. Figure 4a shows the channel activity that is produced at -20 mV after a prepulse to +50 mV. The channel opened and closed for the duration of the test pulse, producing both short and long duration openings (cf Slesinger and Lansman, 1991b). Figure 4b shows the time course of opening at -20 mV after a prepulse to +50 mV and in the absence of a prepulse recorded from a different patch. Channels open more slowly at -20 mV following a prepulse to +50 mV than in the absence of a prepulse, suggesting that channels open from closed states not in the activation pathway.

Ca^{2+} channels enter two distinct open states following repolarization

The duration of many of the single-channel events shown in figure 1 is much longer than the mean open time of 0.5 ms measured for Ca^{2+} channel activity produced during voltage steps to moderate potentials (Slesinger and Lansman, 1991b), but is similar to the long duration openings produced by large depolarizations (Hoshi and Smith, 1987; Pietrobon and Hess, 1990; Slesinger and Lansman, 1991b). We measured the duration of all openings that occurred after a delay at -70 mV following test pulses to +50 mV. The histogram in Figure 5a shows the distribution of open channel durations superimposed with the maximum likelihood fit with two exponentials having time constants of 0.5 and 4.5 ms (smooth curve). The number of the short and long-duration events are roughly equal, indicating that channels enter either open state with roughly equal probability.

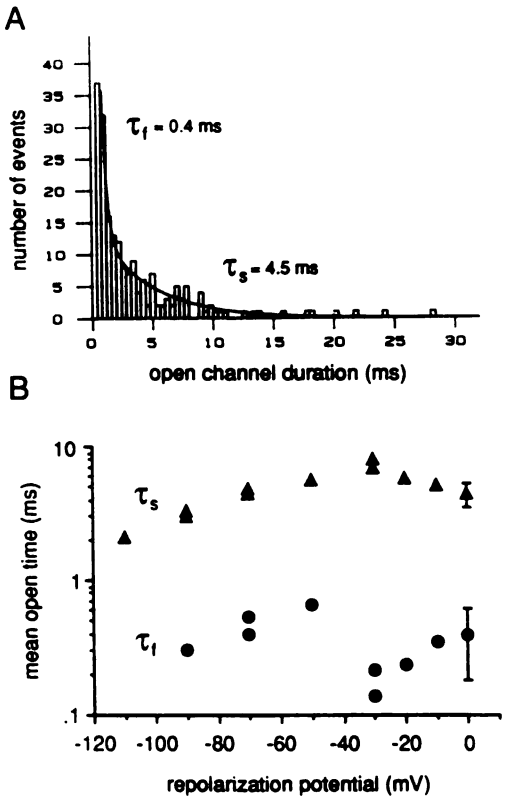

Figure 4: Comparison of waiting times for channels opening in response to a test potential delivered before or after a prepulse. **(A)** Consecutive current records showing single-channel activity produced at -20 mV following test potentials to +50 mV (250 ms). Holding potential was -90 mV. **(B)** Time course of waiting times for channels openings at -20 mV with and without a prepulse (two different recordings). Smooth curve shows double exponential fit having time constants of 1.4 and 63 ms (ratio of fast to slow exponential was 1.09) for the recording in A.

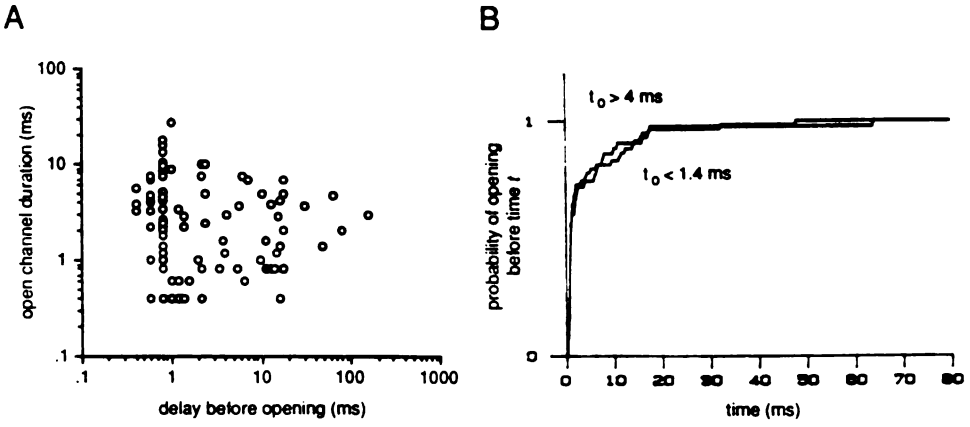

Figure 5: Ca^{2+} channels enter two distinct open states following positive test potentials. (A) Histogram of open channel durations measured at -70 mV following test pulses to +50 mV that lasted 200 ms. Distribution of open times fitted by a sum of two exponentials (smooth curve) with the indicated time constant (ratio of the fast to slow exponential components is 1.36). Same patch recording as in figure 1. (B) The fast (circles) and slow (triangles) time constant obtained from exponential fits to histograms of open channel durations plotted as a function of repolarization potential. Test potential was either +40 or +50 mV. The data points at 0 mV (mean ± SEM) measured previously (Slesinger and Lansman, 1991b).

Because channels enter two distinct open states after repolarization, we examined whether the pathway from the inactivated states to the long-lived open state was kinetically distinct from that to the short-lived open state. Figure 6a shows the duration of the opening plotted as a function of the delay before the channel opens (same patch as in figure 1 & 2a). Both short- and long-duration openings occurred over a wide range of delays. Figure 6b shows the results of a conditional measurement of waiting times. The waiting times for openings that lasted for less than 1.4 ms and those that lasted for longer that 4 ms were divided into two groups, the latter group containing nearly all long duration openings (see figure legend for details). The histogram in figure 6c shows the that the distribution of waiting times for brief openings is indistinguishable from that for long openings. Thus, the rates governing the transition from inactivated to long-lived open state are similar to those for entering the short-lived open state, suggesting that the pathways from inactivated to open states are similar.

Effect of permeant ion on delayed openings

Inactivation of Na^+ and K^+ currents occurs through a mechanism in which an inactivation gate occludes the open channel (Armstrong and Bezanilla, 1977; Hoshi et al., 1990). Elevating external K^+ speeds the recovery from inactivation produced by quarternary ammonium blockers, suggesting that the permeant cation forces the exit of the inactivation gate (Armstrong, 1971). If the time taken before Ca^{2+} channels open at negative potentials depends on the stability of the inactivated state, then lowering the concentration of external cations should change the time course with which channels open from inactivated states. In figure 7, we examined the effect of concentration and species of permeant cation on channels that open from inactivated states.

Figure 7a shows the Ca^{2+} channel openings that occur after repolarizing the membrane to -90 mV with 10 mM Ba^{2+} in the recording electrode. The single-channel conductance is reduced to ~13 pS in 10 mM Ba^{2+} (vs 22 pS in 90 mM Ba^{2+}, Slesinger and Lansman,

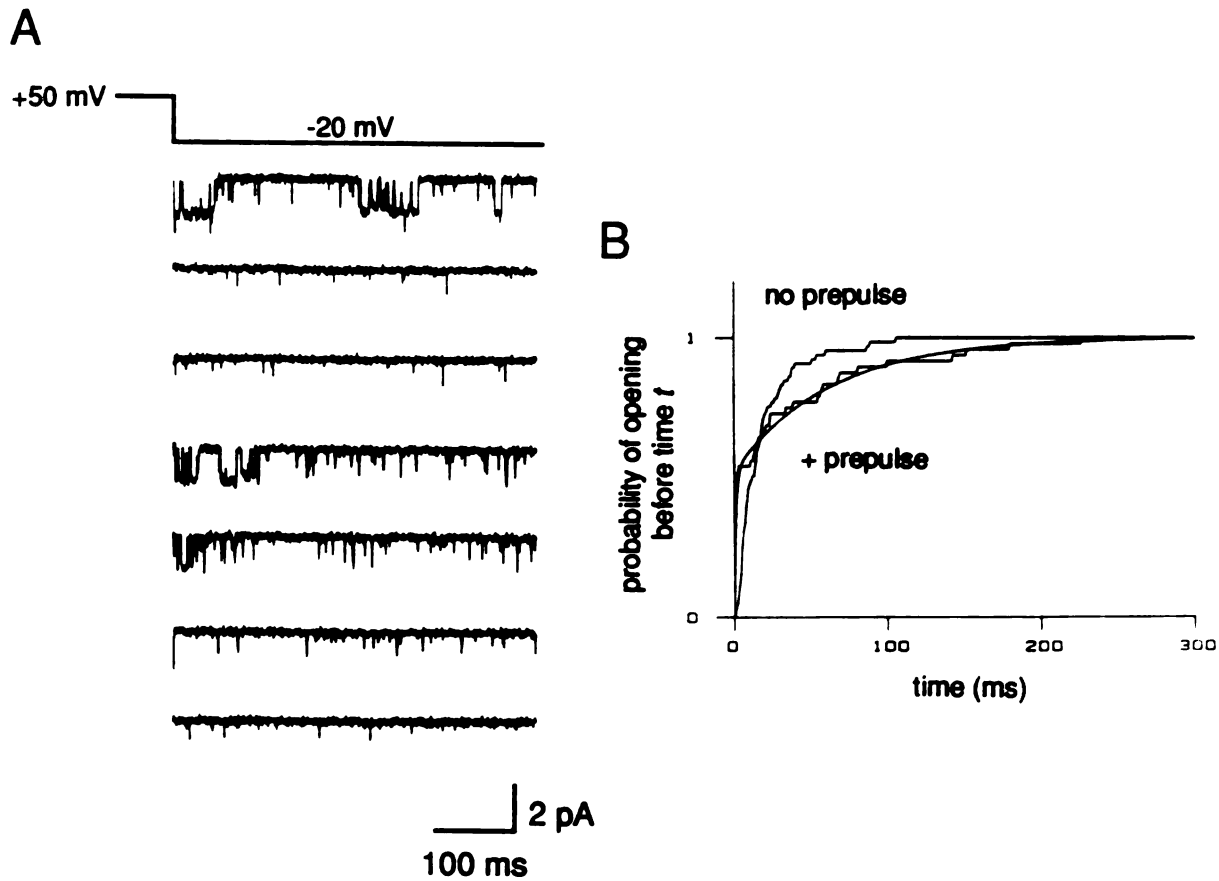

Figure 6: Comparison of the delay before opening and the duration of the opening. **(A)** The time taken before the channel opened plotted as a function of the open channel duration at -70 mV. Same patch recording as in figure 1. **(B)** Histogram of waiting times for delayed openings were divided into two groups based on the open channel duration, those open for less than 1.4 ms or longer than 4 ms. Time courses were normalized and fitted by a sum of two exponentials with similar fast and slow time constants (1.2 and 12 ms for t_o <1.4 ms, 1.3 and 10.4 ms for t_o> 4 ms) and similar ratios ($r_{1.4}$ = 2.13, r_4 = 1.91). Based on the open time histogram shown in figure 5a, channels that open for 4 ms or longer have a greater than 99% chance of being in the long-lived open state.

1991c). Figure 7b compares the waiting time to the first opening measured with 10 mM or 90 mM Ba^{2+} in the recording electrode. The frequency of openings that occur after a long delay is reduced in 10 mM Ba^{2+} (cf Demo and Yellen, 1991). In three patches, the relative proportion of short to long latency openings at -90 mV was high (30, 5 and >100), compared to 1.65 ± 0.42 in 90 mM Ba^{2+} (n=5). The overall probability of opening after a delay in 10 mM Ba^{2+} ($0.46 \pm .03$, n=3), however, was not different from that in 90 mM Ba^{2+} (0.56 ± 0.10, n=7).

We next investigated the effect of replacing Ba^{2+} with Ca^{2+}, which binds more tightly to the channel and has a lower ion transfer rate (Tsien et al., 1987), on the process of opening from inactivated states. Figure 7c shows the Ca^{2+} channels that open after a delay at -90 mV with 90 mM Ca^{2+} in the recording electrode. The amplitude of the single-channel current recorded with 90 mM Ca^{2+} is smaller than that recorded with 90 mM Ba^{2+} (Figure 7c), as expected for an L-type Ca^{2+} channel (Tsien et al., 1987). Figure 7d shows that the time course of opening with 90 mM Ca^{2+} is indistinguishable from that obtained with 90 mM Ba^{2+}. The results show that the concentration, and not species, of permeant cation affects the rate of opening from inactivated states, consistent with the idea that increasing the concentration of the permeant cation destabilizes the inactivated state.

A model for gating of L-type Ca^{2+} channels

The Ca^{2+} channels that recover from inactivation by passing through the open state produce a component of current that is delayed with respect to the time of excitation and that depends on the extent of inactivation during the depolarization (Slesinger and Lansman, 1991c). The analysis of waiting times and open times described in this paper provides direct information on the transition rates between resting and open, and inactivated and open states. We have used this kinetic information to develop a model of Ca^{2+} channel gating which takes into account transitions from inactivated states into short- and long-lived

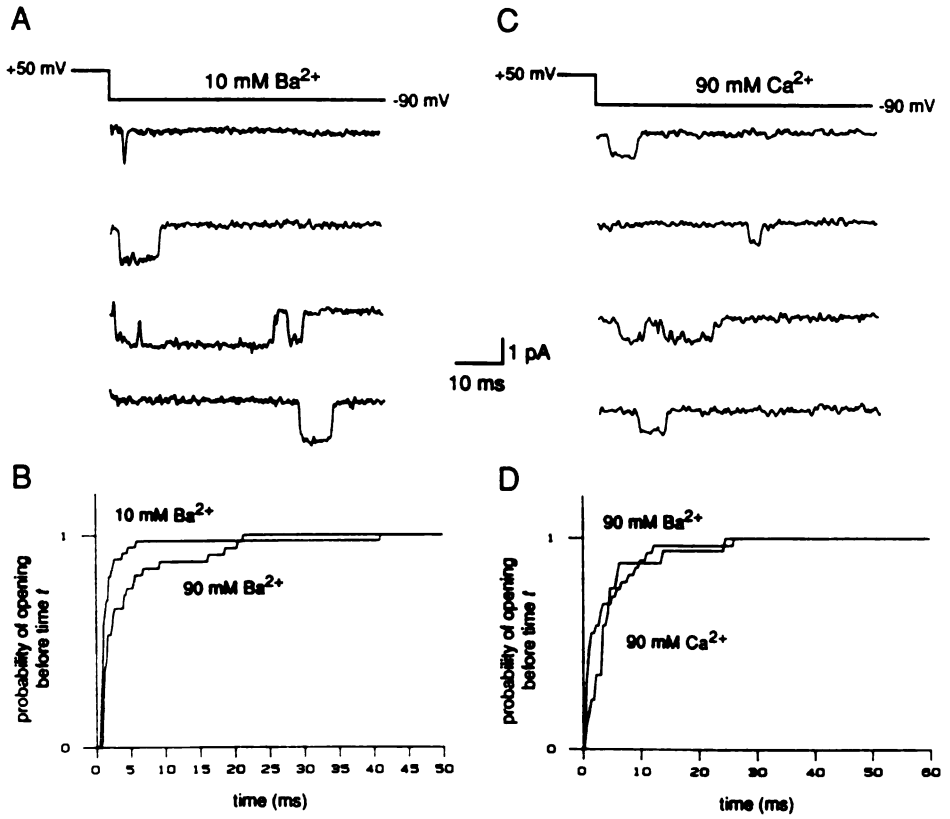

Figure 7: Effect of the concentration and species of permeant cation on Ca^{2+} channels opening from inactivated states. **(A)** Single-channel activity recorded at -90 mV following test potentials of +50 mV with 10 mM Ba^{2+} in the recording electrode. Single-channel conductance was ~13 pS. Holding potential was -90 mV. **(B)** Histogram of the waiting times for channels opening after a delay at -90 mV with either 10 or 90 mM Ba^{2+}. Data from two different patch recordings. **(C)**. Single-channel activity recorded at -90 mV with 90 mM Ca^{2+} in the recording electrode. For the recordings with Ca^{2+}, patches were held at +50 mV to suppress K^+ channel activity and then repolarized to -90 mV for ~200 ms. **(D)** Comparison of waiting times for opening after a delay at -90 mV with 90 mM Ba^{2+} or Ca^{2+} in the recording electrode. Data from two different patch recordings.

open states and shows the change in the time course of Ca^{2+} entry as channels enter the inactivated pool.

The general features of the model are: (i) membrane depolarization drives channels from rest through a number of closed states to the open states in which the final transition to the open state is insensitive to voltage; (ii) strong depolarizations to positive potentials redistribute channels among the open and inactivated states, with channels occasionally entering the long-lived open state from the inactivated state; (iii) channels recover from inactivation after repolarization by passing through either of two distinct open states or by returning directly to rest.

Figure 9 shows the simulations of whole-cell and single-channel data using scheme 3 and the rate constants in table 1 in the Appendix. Figure 9a illustrates the whole-cell current that would be produced at a positive test potential. The large decaying curve shows time course of current from channels entering primarily the short-lived open state and, less frequently at moderate potentials, the long-lived open state (small curve). The current decays with a time constant of ~40 ms, consistent with the rate of decay of whole-cell Ca^{2+} current measured at positive test potentials (Slesinger and Lansman, 1991a). Superimposed on the current traces is a curve showing the probability of entering the inactivated state (CI) as a function of time. During the depolarization, channels accumulate in the inactivated pool, reducing the number of channels available to open. The time course of entering the inactivated state matches the curve derived from measuring the probability of delayed openings following test pulses that varied in length (Slesinger and Lansman, 1991c).

The time course of the tail current results from current flowing through channels that are open at the beginning of repolarization as well as through channels that open from inactivated states after a delay. Previous results show that the time course of the tail current slows with longer duration test pulses as more channels enter the inactivated state (Slesinger and Lansman, 1991c). Figure 9b shows the whole-cell tail current after a 10 or

150 ms test pulse (the time axis begins after repolarization). After a short test pulse, the tail current decays rapidly to zero current along a roughly exponential time course. The amplitude of the tail current after the long test pulse is smaller, but decays much more slowly ~ 1 ms after repolarization than that after the short pulse. This slow component to the tail current is carried by channels that pass through both short- and long-lived open states during recovery from inactivation. The single-channel activity produced after the long pulse is shown in figure 9c. The traces show examples of channels that were closed at the beginning of repolarization, but then opened after a delay. Both long and short openings appear in the simulated current records. The average current through channels that open after a delay, shown below, is qualitatively similar to the mean current in figure 1. In addition, the time course of opening from inactivated states has fast and slow components (figure 9d) comparable to those in figure 3b.

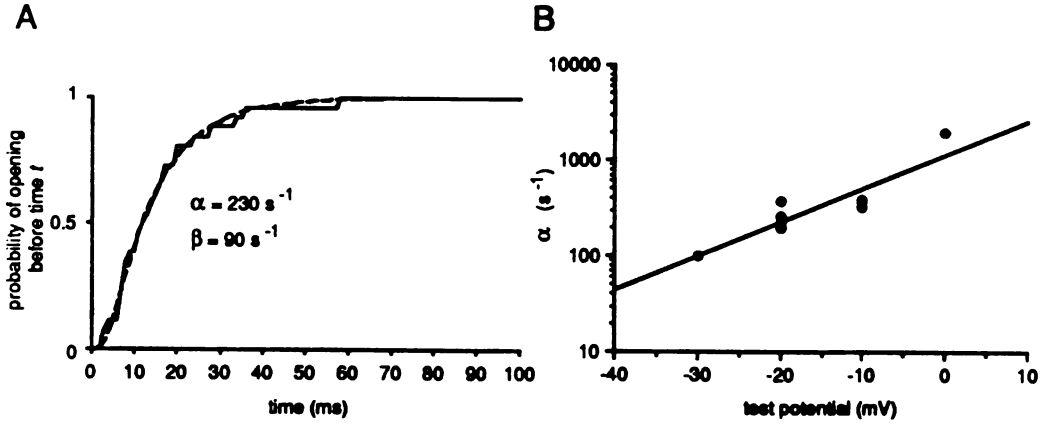

Figure 8: Estimate of the voltage-dependent rate constants for Ca^{2+} channels opening from rest. (A) Waiting time histogram for a channel opening in response to a test potential of -10 mV from a negative holding potential shown with the best fit to scheme 3 (dashed line) as judged by eye (see Appendix). (B) The forward rate constant (α) plotted as a function of test potential for two recordings. Straight line show the best fit to an equation describing the voltage-dependence of α, $\alpha = \alpha_0 \exp(V*k)$, where α_0 is the rate constant at 0 mV (1175 s^{-1}) and k (0.083 mV) = Fzq/RT (F, R and T have their usual meaning, q is the electronic charge movement and z=1).

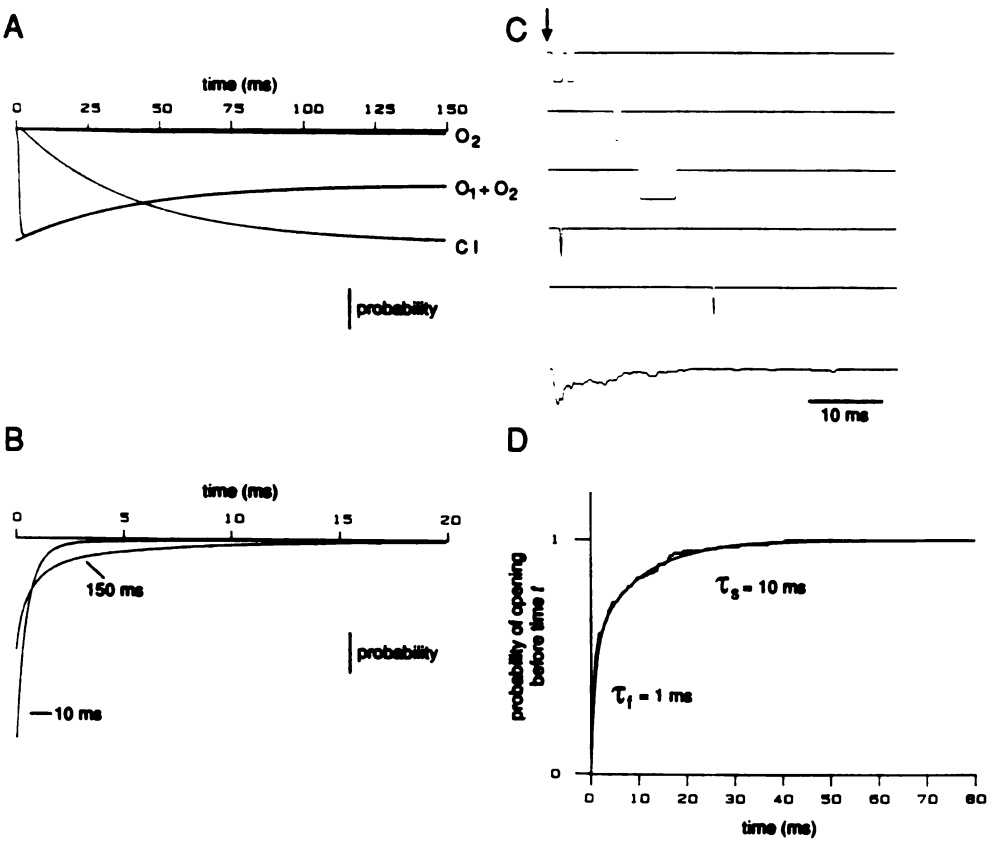

Figure 9: Simulations of whole-cell and single-channel currents using scheme 3. (**A**) Simulated whole-cell current that would occur in response to a positive test potential. Solution to scheme 3 using the rate constants in Table 1 for a positive potential (see Appendix). Curves show the probability of entering O_1+O_2, CI, and O_2 as a function of time (shown inverted). The line through the probability curve for O_1+O_2 shows a single exponential fit with a time constant of ~40 ms. Sampling rate was ~7 kHz. (**B**) Simulated tail currents that would occur by rapidly repolarizing the membrane potential to rest. Probability curves show the solution to scheme 3 using the probability of being open or inactivated from (A) as starting values for the numerical solution to Scheme 3 using the rate constants in Table 1 for a negative membrane potential. The starting probabilities for O_1, O_2 and CI states were 0.44, 0, and 0.08 at 10 ms, and 0.23, 0.02, and 0.49 at 150 ms. The probability of entering the remaining inactivated states during the 160 ms test pulse was negligible. Sampling rate was 50 kHz. (**C**) Simulated single-channel activity produced at a negative membrane potential following the 150 ms pulse. Arrow marks the beginning of repolarization. Average of all channel activity shown below (200 sweeps). Sampling rate was 5 kHz. (**D**) Analysis of the waiting time for first opening in the records shown in C. Smooth curve shows the best fit to distribution of waiting times using Eq. 2 having fast and slow time constants of 1.0 and 10.2 ms (ratio = 1.2).

DISCUSSION

The analysis of waiting times before a channel opens, which provides a direct measure of the transitions between resting and open, and inactivated and open states, showed that: 1) the rates governing the transition from rest to open are strongly voltage-dependent, whereas the rates for opening from inactivated states change little with voltage; 2) depolarization slows the rate of opening from inactivated states, but speeds the rate of opening from rest; 3) channels take longer to open at positive test potentials that are preceded by a strong, inactivating prepulse; and 4) channels returning from inactivation enter a long-lived open state more frequently than during activation.

The opening of Ca^{2+} channels at negative membrane potentials will produce a component of Ca^{2+} entry that is delayed, as channels return from inactivation, and large due to the long duration of the openings and the large driving force for ion entry. Our results suggest that changes in the stability of the inactivated states affect both the time before channels open from the inactivated state and the proportion of inactivated channels that close directly without opening after repolarization.

Implications for mechanism of inactivation

Armstrong and Bezanilla (1977) proposed that Na^{+} channels inactivate by a mechanism in which a "ball" attached to the end of a "chain" swings into the channel pore, blocking the flow of current. The ball and chain model, shown schematically below, can be used to explain the delayed opening of Ca^{2+} channels at negative membrane potentials. Membrane depolarization drives channels from rest to the open state (top right), whereupon the inactivation gate enters the open channel (bottom right). After repolarization, inactivated channels either pass through the open state or return to rest through electrically silent states. The delay before opening represents the time it takes for the inactivation gate to leave the channel.

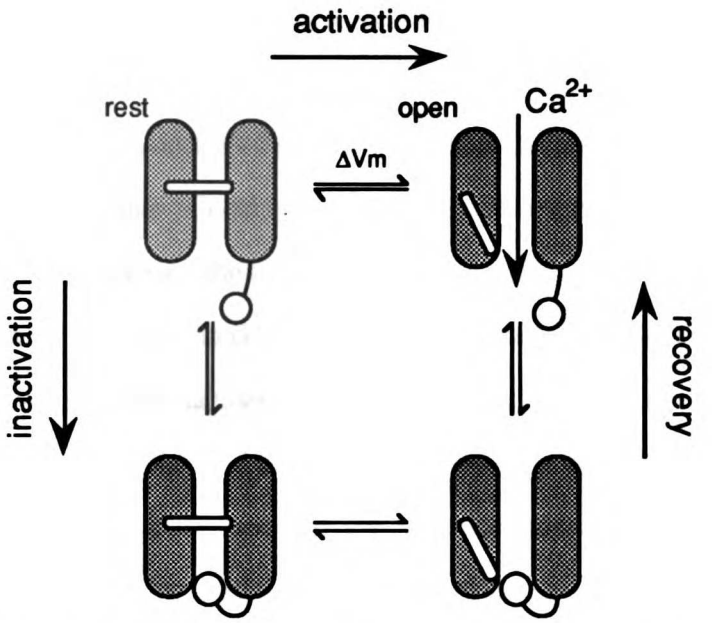

It has been proposed that the inactivation of Na^+ channel is coupled to activation in such a way that the inactivation gate locks the channel in an open but inactivated conformation that is energetically stable (Armstrong and Bezanilla, 1977; Armstrong and Gilly, 1979; Stimers et al., 1985). Our results support the idea that Ca^{2+} channels accumulate in an open but inactivated state, from which they return to rest either directly or after the inactivation gate exits the channel. Unlike Ca^{2+} channels that recover from inactivation, few, if any, Na^+ channels recover from inactivation by passing through the open state because an inward current associated with recovery was not detected, suggesting that most inactivated Na^+ channels close directly (Bezanilla and Armstrong, 1977).

Both hyperpolarization and raising the concentration of the external permeant cation speed the recovery from inactivation presumably by forcing out the inactivation gate (cf Armstrong, 1971; Demos and Yellen, 1991). We found that hyperpolarization and raising the concentration of the external permeant cation enhanced the rate of opening from inactivated states. The effect of raising external Ba^{2+} was complex, however, because the frequency of openings that occurred after a long delay increased even through the probability of opening after repolarization did not change. Because the rate of inactivation

is independent of the concentration of permeant cation (Slesinger and Lansman, 1991a), the probability of opening is not affected by the permeant cation. The increase in the delay before opening with high Ba^{2+}, on the other hand, suggests the permeant cation interacts directly with the inactivation gate. Consistent with the idea that a cytoplasmic inactivation gate occludes the channel, exposing the intracellular surface of L-type Ca^{2+} channels to a protease slows the rate of inactivation (Hescheler and Trautwein, 1988). We conclude that mechanism of voltage-dependent inactivation of Ca^{2+} channels is quite similar to the "ball and chain" model proposed for Na^+ and K^+ channels. It will be of interest to determine whether Ca^{2+} channels recover from current-dependent inactivation, a form of inactivation which depends on elevations in intracellular Ca^{2+} and activation of second messengers (Eckert and Chad, 1984), by passing through the open state.

Comparison to other models of channel gating

Using the waiting times before a channel opens as a guide for the transition among closed, open, and inactivated states, we developed a kinetic model (scheme 3) for Ca^{2+} channel gating which shows that Ca^{2+} channels accumulate in the inactivated pool during membrane depolarization and then recover from inactivation following repolarization by passing through either of two open states or closing directly. The model is similar to the simple sequential scheme originally proposed for squid axon Na^+ channels by Chandler and Meves (1970) in which strong depolarizations drive channels through an inactivated state into a second open state. The model of Ca^{2+} channel gating, however, includes additional inactivated states so that time course of channels opening from inactivated states has fast and slow components. Other models of Na^+ channel gating (Armstrong and Bezanilla, 1977; Armstrong and Gilly, 1979; Horn and Vandenberg, 1984) do not explain the fast and slow components to the delay before channels open from inactivated states as well as the existence of two open states described here for Ca^{2+} channels.

Several models have been proposed to explain the appearance of long duration Ca^{2+} channel openings that occur in response to positive test potentials, dihydropyridine agonists, or β-adrenergic stimulation (Hess et al, 1984; Nowycky et al., 1985a; Hoshi and Smith, 1987; Lacerda and Brown, 1989; Yue et al, 1990; Pietrobon and Hess, 1990). Hess et al.(1984) proposed a gating scheme in which Ca^{2+} channels switch between different sets of states or modes, each of which produces either short or long openings. Modal gating as originally described, however, does not explain the observation that Ca^{2+} channels are closed immediately after repolarization and then open after a delay into either short or long-lived state nor can it explain the effect of permeant ion on the delayed openings. Lacerda and Brown (1989) suggested a modulated-receptor in which dihydropyridines bind to Ca^{2+} channels in the closed state conformation causing the changes in open time and conductance.

Our data support a modulated-receptor model, but one in which dihydropyridines bind to the inactivated states of the channel. Stabilization of the inactivated state by dihydropyridine antagonist has been suggested previously (Bean, 1984; Gurney et al, 1985; Cohen and McCarthy, 1987). Dihydropyridine agonist may also selectively stabilize the inactivated state, but in a manner that allows equilibration into the long-duration open state. Thus the model can explain the mixed agonist and antagonist actions of dihydropyridines by state-dependent binding to the inactivated channel (Brown et al., 1986; Docherty and Brown, 1986; Kamp et al., 1989), such as the potentiation of the tail current at negative potentials that is produced by dihydropyridine agonist even though the current at positive potentials is suppressed (Regan et al., 1991; Slesinger and Lansman 1991a). The model also provides an alternative explanation for prepulse potentiation of Ca^{2+} current (Hoshi et al., 1987; Elmsie et al., 1990; Artalejo et al., 1990). Rather than causing a shift between parallel willing and reluctant pathways, or recruiting "silent" Ca^{2+} channels, strong depolarizations simply drive channels into an inactivated state that has access to the long-duration open state.

Appendix

The results showed that the kinetics of channels opening from rest differed from channels opening from inactivated states. Using the analysis of waiting times as a guide for the transitions between closed and open, and inactivated and open states, we developed a kinetic model of Ca^{2+} channel gating similar to scheme 2 except that we assumed that the Ca^{2+} channel has five closed states preceding the open state, where the first four transitions are governed by voltage-dependent rates that are integral multiples of each other and the last transition is voltage-insensitive (cf Bezanilla and Armstrong, 1977; Zagotta and Aldrich, 1990). Although good fits were obtained with as few as two closed states (see figure 3), we used four voltage-dependent closed states to represent the gating of four S4 domains in the channel protein (Morey et al., 1991). In addition, it was necessary to include a minimum of four inactivated and two open states to satisfy the following criteria: the current decays at positive potentials along an exponential time course with a time constant of ~40 ms, the rates governing the transitions in and out of the open states are insensitive to membrane potential, there are two open states each accessed by the same closed and inactivated states, and the time course for channels opening after a delay contains fast and slow components. The general strategy was to measure the voltage-dependent rate constants for channels opening from rest by fitting the waiting time histogram using scheme 3, vary the transition rates among inactivated states so that the current would decay at positive test potentials, and finally, use the probability of being in the inactivated and open states as a function of time to simulate whole-cell tail currents that would occur following repolarization.

Although the scheme 3 contains 9 pairs of rate constants, many rates are constrained by the available whole-cell and single-channel data. First, the mean open time sets an upper limit for the rate constants leaving the short-lived (O_1: 1/0.5 ms^{-1}) or long-lived open state (O_2: 1/4 ms^{-1}) and is insensitive to membrane potential. Because inactivation is slow

relative to channel closure, the mean open time is dominated by the closing rate. Second, the short closed time which we assume is voltage insensitive (cf Zagotta and Aldrich, 1990; Chen and Hess, 1990) determines the rate into the short-lived open state (1/0.5 ms^{-1}, see Slesinger and Lansman, 1991b). Third, the rate constants governing the transitions among inactivated states must produce a current that decays with a time constant of 40-60 ms to a non-zero level by the end of a 150 ms test pulse. Fourth, the pathway from inactivated to open states must have rate constants which account for the fast and slow components for delayed openings at negative potentials.

At membrane potentials near the foot of the activation curve, both the forward and backward rate constants (α and β) contribute to the time course of the distribution of waiting times for first opening. We assumed that channels are in the resting state farthest from the open state and varied α and β to obtain the best fit to the waiting time histogram as judged by eye. Figure 8a shows that adequate fits to the waiting times for channel opening measured at -20 were obtained with scheme 3 (smooth curve). Figure 8b plots the forward rate constant (α) as a function of test potential to show the voltage dependence of opening. The straight line drawn is the best fit to Eq. 3,

$$\alpha = \alpha_0 \exp(V*k) \qquad \text{Eq. 3}$$

where α_0 is the rate constant at 0 mV and $k = Fzq/RT$ (F,R and T have their usual meaning, z=1 and q, the electronic charge movement in the forward direction, equals ~2 e^- charges). The forward rate constant shows a steep dependence on membrane potential, changing e-fold for every +12 mV. The backward rate (β), on the other hand, changed little with voltage presumably because the backward rate constant increases exponentially with potentials that are more negative than the range of potentials studied (data not shown).

After channels have reached the open state during membrane depolarization, some channels accumulate in the inactivated pool and become unavailable for opening. We assumed that the rate constant governing the transition from the inactivated to open state is voltage-insensitive and must therefore be no slower than the fast component for opening

from inactivated states. This rate of return from the inactivated to open state would be too fast to simulate a decaying current at positive potentials, so it was necessary to include another inactivated state (CI) governed by voltage-dependent transitions from which channels returned to the open state slowly. We varied the rate constants for channels entering and leaving the CI state so that the current decayed with a time constant of ~40 ms. The rate constant for returning from the inactivated states to the long-lived open state is slower than that for returning to the short-lived open state because long openings are rarely observed by the end of a 150 ms test pulse (Slesinger and Lansman, 1991b). The simulated current is shown in figure 9a.

To simulate the tail current at negative potentials, the forward rate constant (α) was estimated by extrapolating the curve in figure 8b to -90 mV, the backward rate (β) was assumed to be five times faster than the voltage-insensitive rate from the last closed state to the open state (k_1) (because the voltage dependence of β was not known we used a value that allowed the channels to open from the closed state <2% of the time), and the rate constants for leaving the inactivated state (CI) were varied to produce fast and slow components to the waiting time histogram (figure 9d). It was necessary to add an additional inactivated state (CI_2) to produce the slow component to channel opening. The rate constant for inactivated channels closing without opening was set so that greater than 50% of the inactivated channels close directly. The contribution of slow inactivation which decays with a time constant of seconds was not studied in these experiments and was excluded from the model (see Slesinger and Lansman, 1991a).

(Scheme 3)

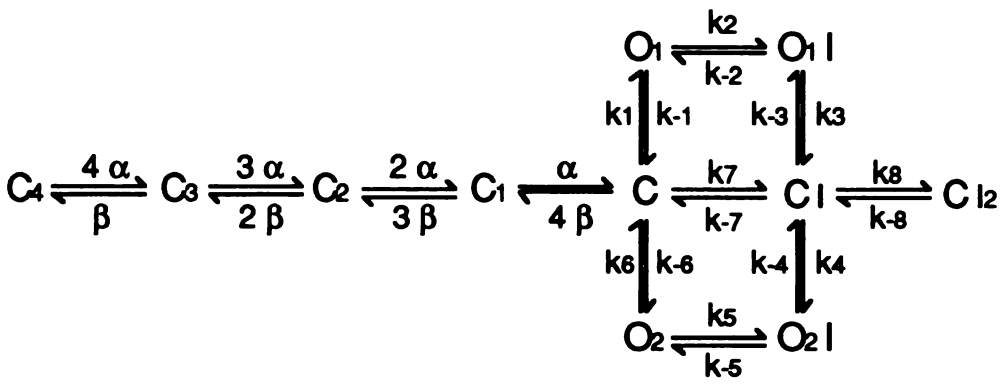

Table 1: rate constants for Scheme 3

	+	-		+	-		+	-
α	2000	0.7	k_3	2000	*	k_6	200	*
β	0	10,000	k_{-3}	8	700	k_{-6}	1	*
k_1	2000	*	k_4	6	700	k_7	1	*
k_{-1}	2000	*	k_{-4}	2000	*	k_{-7}	2	1200
k_2	50	*	k_5	50	*	k_8	2	900
k_{-2}	1000	*	k_{-5}	1000	*	k_{-8}	150	*

Rate constants at positive$^{(+)}$ and negative$^{(-)}$ membrane potentials. Asterisk indicates voltage-independent rate constants. All rates are in s^{-1}.

CONCLUSIONS

Mechanism of inactivation of Ca^{2+} channels

Strong depolarizations from a negative holding potential elicit an inward Ca^{2+} current that decays with fast and slow rates that vary with voltage. The results showed that the rate of inactivation from the open state is insensitive to voltage, while inactivation from the closed state is strongly voltage-dependent (cf Zagotta and Aldrich, 1990; Chen and Hess, 1990; Armstrong and Gilly, 1979), consistent with the gating model in which inactivation is coupled to the activation process.

Like the Ca^{2+} current in peripheral neurons, a test pulse delivered from a depolarized holding potential produces a non-decaying current while a pulse to the same potential but from a hyperpolarized holding potential produces a decaying current. Yet, single-channel recordings showed a single type of Ca^{2+} channel that accounts for both decaying and non-decaying currents. The loss of the decaying current at depolarized holding potential can be explained if some inactivated channels open after a delay in response to a voltage step. The sum of the current through channels that inactivate during the voltage step and the current through channels that open after a delay would produce a non-decaying current. In support of this explanation, some channels opened after a long delay following strong depolarizations delivered from more positive holding potentials.

The finding that inactivated channels return to rest at negative potentials by passing through open state provided new information on the mechanism of Ca^{2+} channel inactivation. Both hyperpolarization and raising the concentration of permeant cation (external) affected the process of channel reopening in a manner suggesting that the mechanism of inactivation is similar to the "ball and chain" model proposed for Na^+ and K^+ channels (Armstrong, 1971; Armstrong and Bezanilla , 1977). The recent cloning of a brain Ca^{2+} channel (Mori et al., 1991) showed that the basic architecture of the neuronal Ca^{2+} channel is similar to that of Na^+ and K^+ channels, suggesting that cytoplasmic

structures such as the amino terminus may be involved in inactivation. Future experiments should investigate the interaction between the inactivation gate and the activation gate as viewed through channels that recover from inactivation. Do mutations that alter the stability of the inactivated state affect the proportion of channels that return to rest by passing through the open state? Do changes in the rate of inactivation affect how often channels enter the long-lived open state?

A new role for channel inactivation?

The possibility that inactivation enhances rather than reduces Ca^{2+} entry provides a new interpretation for the role of channel inactivation in neuronal signaling and may be a previously unrecognized mechanism for regulating Ca^{2+} entry. While a single action potential may be too brief to produce significant inactivation, Ca^{2+} channels may accumulate in the inactivated pool after a long train of action potentials (Schroeder et al, 1990). The amplitude and frequency of a train of neuronal action potentials would regulate Ca^{2+} influx through channels that reopen by the time and voltage dependence of the inactivation process. Ca^{2+} channel reopening may play a role in the frequency dependent release of neurohormones (Ip and Zigmond, 1984) and certain forms of synaptic plasticity which depend on the frequency of stimulation (Zucker, 1989). Neurotransmitters which alter the time course of channel inactivation (Tsien et al, 1988) may modify Ca^{2+} entry by activating a component of Ca^{2+} influx through channels that reopen. Inappropriate reopening of Ca^{2+} channels following action potentials, however, may produce afterdepolarizations involved in hyperexcitability which may also lead to ischemic injury (Wong and Prince, 1981; Meyer, 1989).

REFERENCES

Aldrich, R.W. and Stevens, C.F. (1983) Inactivation of open and closed sodium channels determined separately. *Cold Spring Harbor Symposia on Quantitative Biology* **48**:147-153.

Aldrich, R.W., Corey, D.P. and Stevens, C.F. (1983) A reinterpretation of mammalian sodium channel gating based on single channel recordings. *Nature* **306**: 436-441.

Altman, J. (1972) Postnatal development of the cerebellar cortex in the rat. I. The external germinal layer and the transitional molecular layer. *Journal of Comparative Neurology* **145**: 353-398.

Aosaki, T and Kasai, H. (1989) Characterization of two kinds of high-voltage-activated Ca-channel currents in chick sensory neurons. *Pflügers Archiv* **414**:150-156.

Armstrong, C.M. (1971) Interaction of tetraethylammonium ion derivatives with the potassium channels of giant axons. *J. Gen. Physiol.* **58**:413-437

Armstrong, C.M. and Bezanilla, F. (1977) Inactivation of the sodium channel. II. Gating current experiments. *J. Gen. Physiol.* **70**:567-590

Armstrong, C.M. and Gilly, W.F. (1979) Fast and slow steps in the activation of sodium channels. *Journal of General Physiology* **74**:691-711.

Armstrong, C.M., Bezanilla, F. and Rojas, E. (1973) Destruction of sodium conductance inactivation in squid axon perfused with pronase. J. *Gen. Physiol.* **62**:375-391.

Armstrong, D. and Eckert, R. (1987) Voltage-activated calcium channels that must be phosphorylated to respond to membrane depolarization. *Proceedings of the National Academy of Sciences* **84**: 2518-2522.

Artalejo, C.R., Ariano, M.A., Perlman, R.L. and Fox, A.P. (1990) Activation of facilitation calcium channels in chromaffin cells by D_1 dopamine receptors through a cAMP/protein kinase A-dependent mechansims. *Nature* **348**:239-242.

Augustine, G.J., Charlton, M.P. and Smith S.J. (1987) Calcium action in synaptic transmitter release. *Ann. Rev. Neurosci.* **10**: 633.

Bean, B.P. (1984) Nitrendipine block of cardiac channels: high affinity binding to the inactivated state. *Proceedings of the National Academy of Sciences* **81**: 6388-6392.

Bean, B.P. (1989) Classes of calcium channels in vertebrate cells. *Ann. Rev. Physiol.* **51**:367-384.

Bezanilla, F. and Armstrong, C.M. (1977) Inactivation of the sodium channel. I. Sodium current experiments. *J. Gen. Physiol.* **70**:549-566.

Bley, K.R., Lipscombe, D. and Tsien, R.W. (1990) Neurotransmitter modulation of N-type Ca channels by shifts between modes of gating. *Soc. Neurosci.* **16**:261.3

Brown, A.M., Kunze, D.L. and Yatani, A. (1986) Dual effects of dihydropyridines on whole cell and unitary calcium currents in single ventricular cells of guinea pigs. *Journal of Physiology* **379**:495-514.

Brown,, A.M., Lux, H.D. and Wilson, D.L. (1984) Activation and inactivation of single calcium channels in snail neurons. *Journal of General Physiology* **83**: 751-769.

Burgoyne, R.D. and Cambray-Deakin, M.A. (1988) The cellular neurobiology of neuronal development: the cerebellar granule cell. *Brain Research Reviews* **13**: 77-101.

Byerly, L. and Yazejian, B. (1986) Intracellular factors for the maintenance of calcium currents in perfused neurones from the snail, *Lymnaea stagnalis*. *Journal of Physiology* **370**: 631-650.

Carbone, E. and Lux, H.D. (1987a) Kinetics and selectivity of a low-threshold voltage-activated calcium current in chick and rat sensory neurones. *J. Physiol.* **386**:547-570.

Carbone, E. and Lux, H.D. (1987b) Single low-voltage-activated calcium channels in chick and rat sensory neurones. *Journal of Physiology* **386**:571-601.

Carboni, E. and Wojcik, W.J. (1988) Dihydropyridine binding sites regulate calcium influx through specific voltage-sensitive calcium channels in cerebellar granule cells. *Journal of Neurochemistry* **50**: 1279-1286.

Chad, J.E. and Eckert, R. (1986) An enzymatic mechanism for calcium current inactivation in dialysed Helix neurones. *Journal of Physiology* **378**: 31-51.

Chandler, W.K. and Meves, H. (1970) Evidence for two types of sodium conductance in axons perfused with sodium fluoride solution. *J. Physiol.* **211**:653-678.

Chen, C. and Hess, P. (1990) Mechanism of gating of T-type calium channels. *J. Gen. Physiol.* **96**:603-630.

Cohen, C.J. and McCarthy, R.T. (1987) Nimodipine block of calcium channels in rat anterior pituitary cells. *Journal of Physiology* **387**: 195-225.

Cole, K.S. and Moore, W.J. (1960) Potassium ion current in the squid giant axon; dynamic characteristics. *Biophysical Journal* **1**: 1-14.

Colquhoun, D. and Sigworth, F.J. (1983) Fitting and statistical analysis of single-channel records. In: Single Channel Recording, Eds. Sakmann, B. and Neher, E. p. 191-263.

Connor, J.A., Tseng, H-Y. and Hockberger, P.E. (1987) Depolarization- and transmitter-induced changes in intracellular Ca^{2+} of rat cerebellar granule cells in explant cultures. *Journal of Neuroscience* **7(5)**: 1384-1400.

Cota, G. and Armstrong, C.M. (1989) Sodium channel gating in clonal pituitary cells: The inactivation step is not voltage dependent. *J. Gen. Physiol.* **94**:213-232.

Cull-Candy, S.G., Howe, J.R. and Ogden, D.C. (1988) Noise and single channels activated by excitatory amino acids in rat cerebellar granule neurones. *Journal of Physiology* **400**: 189-222.

Cull-Candy, S.G., Marshall, C.G. and Ogden, D. (1989) Voltage-activated membrane currents in rat cerebellar granule neurones. *Journal of Physiology* **414**:179-199.

DeFelice, L.J. and Clay, J.R. (1983) Membrane current and membrane potential from single-channel kinetics. In: Single Channel Recording, Eds. Sakmann, B. and Neher, E. p. 323-342.

Demo, S.D. and Yellen, G. (1991) Recovery from fast inactivation in *Shaker* K^+ channels is speeded by external K^+ and often occurs through the open state. *Biophys. J.* **59**:4a.

Docherty, R.J. (1988) Gadolinium selectively blocks a component of calcium current in rodent neuroblastoma x glioma hybrid (NG108-15) cells. *Journal of Physiology* **398**: 33-47.

Docherty, R.J. and Brown, D.A. (1986) Interaction of 1,4-dihydropyridines with somatic Ca currents in hippocampal CA_1 neurones of the guinea pig in vitro. *Neuroscience Letters* **70**: 110-115.

Eckert, R. and Chad, J.E. (1984) Inactivaiton of Ca channels. *Prog. Biophys. molec. Biol.* **44**:215-267.

Elmslie, K.S., Zhou, W. and Jones, S.W. (1990) LHRH and GTP-γ-S modify caclium current activation in bullfrog sympathetic neurons. *Neuron* **5**:75-80.

Fedulova, S.A., Kostyuk, P.G. and Veselovsky, N.S. (1981) Calcium channels in the somatic membrane of the rat dorsal root ganglion neurons, effect of cAMP. *Brain Research* **214**:210-214.

Fedulova, S.A., Kostyuk, P.G. and Veselovsky, N.S. (1985) Two types of calcium channels in the somatic membrane of new-born dorsal root ganglion neurones. *Journal of Physiology* **359**: 431-446.

Fenwick, E.M., Marty, F.A. and Neher, E. (1982) Sodium and calcium channels in bovine chromaffin cells. *J. Physiol.* **331**:599-635.

Fisher, R.E., Gray, R. and Johnston, D. (1990) Properties and distribution of single voltage-gated calcium channels in adult hippocampal neurons *J. Neurophysiol.* **64(1)**:91-104.

Fox, A.P., Nowycky, M.C. and Tsien, R.W. (1987a) Kinetic and pharmacological properties distinguishing three types of calcium currents in chick sensory neurones. *Journal of Physiology* **394**: 149-172.

Fox, A.P., Nowycky, M.C. and Tsien, R.W. (1987b) Single-channel recordings of three types of calcium channels in chick sensory neurones. *Journal of Physiology* **394**: 173-200.

Gurney, A.M., Nerbonne, J.M. and Lester, H.A. (1985) Photoinduced removal of nifedipine reveals mechanisms of calcium antagonist action on single heart cells. *Journal of General Physiology* **86**: 353-378.

Hagiwara, S. and Byerly, L. (1981) Calcium channel. *Annual Review of Neuroscience* **4**: 69-125.

Hagiwara, S. and Ohmori, H. (1982) Studies of calcium channel in rat clonal pituitary cells with patch electrode voltage clamp. *Journal of Physiology* **50**: 583-601.

Hamill, O.P., Marty, A., Neher, E., Sakmann, B. and Sigworth, F.J. (1981) Improved patch clamp techniques for high-resolution current recording from cells and cell-free membrane patches. *Pflügers Archiv* **391**:85-100.

Hatten, M.E. and Sidman, R.L. (1978) Cell reassociation behavior and lectin-induced agglutination of embryonic mouse cells from different brain regions. *Experimental Cell Research* **113**: 111-125.

Hescheler, J. and Trautwein, W. (1988) Modifation of L-type calcium current by intracellularly applied trypsin in guinea-pig ventricular myocytes. *J. Physiol.* **404**:259-274.

Hess, P. (1990) Calcium channels in vertebrate cells. *Annual Review of Neuroscience* **13**:337-356.

Hess, P., Lansman, J.B. and Tsien, R.W. (1984) Different modes of calcium channel gating behaviour favoured by dihydropyridine agonists and antagonists. *Nature* **311**:538-544.

Hess, P., Lansman, J.B. and Tsien, R.W. (1986) Calcium channel selectivity for divalent and monovalent cations. Voltage and concentration dependence of single channel current in ventricular heart cells. *Journal of General Physiology* **88**: 293-319.

Hirano, T., Kubo, Y. and Wu, M.M. (1986) Cerebellar granule cells in culture: monosynaptic connections with Purkinje cells and ionic currents. *Proceedings of the National Academy of Sciences* **83**: 4957-4961.

Hirning, L.D., Fox, A.P., McCleskey, E.W., Olivera, B.M., Thayer, S.A., Miller, R.J. and Tsien, R.W. (1988) Dominant role of N-type Ca^{2+} channels in evoked release of norepinephrine in sympathetic neurons. *Science* **1**: 57-61.

Hockberger, P.E., Tsen, H-Y. and Connor, J.A. (1987) Immunocytochemical and electrophysiological differentiation of rat cerebellar granule cells in explant cultures. *Journal of Neuroscience* **7(5)**: 1370-1383.

Hodgkin, A.L. and Huxley, A.F. (1952a) The dual effect of membrane potential on sodium conductance in the giant axon of *Loligo*. *J. Physiol.* **116**:497-506.

Hodgkin, A.L. and Huxley, A.F. (1952b) A quantitative description of membrane current and its application to conduction and excitation in nerve. *J. Physiol.* **117**:500-544.

Hof, R.P., Rüegg, U.T., Hof, A. and Vogel, A. (1985) Stereoselectivity at the calcium channel: opposite action of the enantiomers of a 1,4-dihydropyridine. *Journal of Cardiovascular Pharmacology* **7**: 689-693.

Horn, R. (1984) Gating of channels in nerve and muscle: A stochastic approach. In: *Ion Channels: Molecular and Physiological Aspects* **21**:53-97, Ed., F. Bronner, New York: Academic Press

Horn, R. and Vandenberg, C.A. (1984) Statistical properties of single sodium channels. *J. Gen. Physiol.* **84**:505-534.

Hoshi, T. and Aldrich, R.W. (1988) Gating kinetics of four classes of voltage-dependent K^+ chanels in pheochromocytoma cells. *Journal of General Physiology* **91**: 107-131.

Hoshi, T. and Smith, S.J. (1987) Large depolarization induces long openings of voltage dependent calcium channels in adrenal chromaffin cells. *J. Neurosci.* **7(2)**:571-580.

Hoshi, T., Rothlein, J. and Smith, S.J. (1984) Facilitation of Ca^{2+}-channel currents in bovine adrenal chromaffin cells. *Proc. Natl. Acad. Sci.* **81**:5871-5875.

Hoshi, T., Zagotta, W. and Aldrich, R.W. (1990) Biophysical and molecular mechanisms of *Shaker* potassium channel inactivation. *Science* **250**:533-538.

Huck, S. and Lux, H.D. (1987) Patch-clamp study of ion channels activated by GABA and glycine in cultured cerebellar neurons of the mouse. *Neuroscience Letters* **79**: 103-107.

Imredy, J.P. and Yue, D.T. (1991) Voltage dependence of closure from short and long-lasting openings of L-type Ca channels. *Biophys. J.* **59**:274a

Ip, N.Y. and Zigmond, R.E. (1984) Patterned presynaptic nerve activity can determine the type of neurotransmitter regulating a postsynaptic event. *Nature* **311**:472-474.

Jones, S.W. and Marks, T.N. (1989) Calcium currents in bullfrog sympathetic neurons. *Journal of General Physiology* **94**:169-182.

Kalman, D. and Armstrong, D.L. (1988) Protein phosphorylation and the inactivation of dihydropyridine-sensitive calcium channels in mammalian pituitary tumor cells. In The Calcium Channnel: Structure, Function and Implications. p1-14.

Kamp, T.J., Sanguinetti, M.C. and Miller, R.J. (1989) Voltage- and use-dependent modulation of cardiac calcium channels by the dihydropyridine (+)-202-791. *Circulation Research* **64**:338-351.

Kasai, H. and Aosaki, T. (1988) Divalent cation dependent inactivation of the high-voltage-activated Ca-channel current in chick sensory neurons. *Pflugers Arch.* **411**:695-697.

Katz, B. and Miledi, R. (1967) A study of synaptic transmission in the absence of nerve impulses. *J. Physiol.* **192**:407-436.

Kingsbury, A. and Balázs, R. (1987) Effect of calcium agonists and antagonists on cerebellar granule cells. *European Journal of Pharmacology* **140**: 275-283.

Kostyuk, P.G., Shuba, Ta. M. and Savchenko, A.N. (1988) Three types of calcium channel in the membrane of mouse sensory neurons. *Pflügers Archiv* **411**: 661-669.

Lacerda, A.E. and Brown, A.M. (1989) Nonmodal gating of cardiac calcium channels as revealed by dihydropyridines. *J. Gen. Physiol.* **93**:1243-1273.

Lansman, J.B. (1990) Blockade of current through single calcium channels by trivalent lanthanide cations: Effect of ionic radius on the rates of ion entry and exit. *Journal of General Physiology* **95**:679-696.

Lansman, J.B. and Slesinger, P.A. (1991) Inactivating and non-inactivating dihydropyridine-sensitive calcium channels in cerebellar neurons. *Biophysical Journal* **59**:537a.

Lansman, J.B., Hess, P. and Tsien, R.W. (1986) Blockade of current through single calcium channels by Cd^{2+}, Mg^{2+}, and Ca^{2+}. Voltage and concentration dependence of calcium entry into the pore. *Journal of General Physiology* **88**: 321-347.

Llinás, R., Steinberg, I.Z. and Walton, K.(1981) Presynaptic calcium current in squid giant synapse. *Biophys. J.* **33**:289-322.

Llinás, R., Sugimori, M. and Simon, S.M. (1982) Transmission by presynaptic spike-like depolarization in the squid giant synapse. *Proc. Natl. Acad. Sci. USA* **79**:2415-2419.

Lux, H.D. and Brown, A.M. (1984) Patch and whole cell calcium currents recorded simultaneously in snail neurons. *Journal of General Physiology* **83**:727-750.

Markwardt, F. and Nilius, B. (1988) Modulation of calcium currents in guinea-pig single ventricular heart cells by the dihydropyridine Bay K 8644. *Journal of Physiology* **399**: 559-575.

Matteson, D.R. and Armstrong, C.M. (1986) Properties of two types of calcium channels in clonal pituitary cells. *Journal of General Physiology* **87**: 161-182.

Messer, A. (1977) The maintenance and identification of mouse cerebellar granule cells in monolayer culture. *Brain Research* **130**: 1-12.

Meyer, F.B. (1989) Calcium, neuronal hyperexcitability and ischemic injury. *Brain Res. Reviews* **15**:227-243.

Miller, R.J. (1987) Multiple calcium channels and neuronal function. *Science* **235**:46-52.

Moorman, J.R., Kirsch, G.E., Brown, A.M. and Joho, R.H. (1990) Changes in sodium channel gating produced by point mutations in a cytoplasmic linker. *Science* **250**:688-691.

Mori, Y. et al. (1991) Primary structure and functional expression from complementary DNA of a brain calcium channel. *Nature* **350**:398-402.

Narahashi, T., Tsumoo, A and Yoshi, M. (1987) Characterization of two types of calcium channels in mouse neuroblastoma cells. *Journal of Physiology* **383**: 231-249.

Nowycky, M.C., Fox, A.P. and Tsien, R.W. (1985a) Long-opening mode of gating of neuronal calcium channels and its promotion by the dihydropyridine calcium agonist Bay K 8644. *Proc. Natl. Acad. Sci USA* **82**:2178-2182.

Nowycky, M.C., Fox, A.P. and Tsien, R.W. (1985b) Three types of neuronal calcium channel with different calcium agonist sensitivity. *Nature* **316**: 440-443.

Ohmori, H. and Yoshii, M. (1977) Surface potential reflected in both gating and permeation mechanisms of sodium and calcium channels of the tunicate egg cell membrane. *Journal of Physiology*, **267**:429-463.

Patlak, J. and Horn, R. (1982) Effect of *N*-bromacetamide on single sodium channel currents in excised membrane patches. *J. Gen. Physiol.* **79**:333-351.

Pietrobon, D. and Hess, P. (1990) Novel mechanism of voltage dependent gating in L-type calcium channels. *Nature* **346**:651-655.

Plummer, M.R., Logothetis, D.E. and Hess, P. (1989) Elementary properties and pharmacological sensitivities of calcium channels in mammalian peripheral neurons. *Neuron* **2**:1453-1463.

Ramón Y Cajal, S. (1904) La textura del sistema nervioso del hombre y los vertebrados. Moya, Madrid.

Regan, L.J., Say, D.W.Y. and Bean, B.P. (1991) Ca^{2+} channels in rat central and peripheral neurons: high-threshold current resistant to dihydropyridine blockers and ω-conotoxin. *Neuron* **6**:269-280.

Schroeder, J.E., Fischbach, P.S., Mamo, M. and McCleskey, E.W. (1990) Two components of high-threshold Ca^{2+} current inactivate by different methods. *Neuron* **5**:445-452.

Sigworth, F.J. (1980) The variance of sodium current fluctuations at the node of ranvier. *Journal of Physiology* **307**:97-129.

Slesinger, P.A. and Lansman, J.B. (1989) Dihydropyridine-sensitive Ca channels in dissociated granule cells cultured from mouse cerebellum. *Biophysical Journal* **55**: 302a.

Slesinger, P.A. and Lansman, J.B. (1990) Just one type of Ca^{2+} channel underlies the macroscopic Ca^{2+} channel current in cerebellar granule cells. *Biophysical Journal* **57**: 524a.

Slesinger, P.A. and Lansman, J.B. (1991a) Inactivation of calcium currents in granule cells cultured from mouse cerebellum. *J. Physiol.* **435**:101-121.

Slesinger, P.A. and Lansman, J.B. (1991b) Inactivating and non-inactivating dihydropyridine-sensitive Ca^{2+} channels in cerebellar granule cells. *J. Physiol.* **439**:301-323

Slesinger, P.A. and Lansman, J.B. (1991c) Reopening of Ca^{2+} channels in mouse cerebellar neurons at resting membrane potentials during recovery from inactivation. *Neuron.* (in press)

Slesinger, P.A. and Lansman, J.B. (1991d) Reopening of calcium channels at negative membrane potentials depends on channel inactivation. *Biophys. J.* **537a.**

Somogyi, P., Halasy, K., Somogyi, J., Storm-Mathisen, J. and Ottersen, O.P. (1986) Quantification of immunogold labelling reveals enrichment of glutamate in mossy and parallel fibre terminals in cat cerebellum. *Neuroscience* **19**:1045-1050.

Stimers, J.R., Bezanilla, F. and Taylor, R.E. (1985) Sodium channel activation in the squid axon. *Journal of General Physiology* **85**:65-82

Swandulla, D. and Armstrong, C.M. (1988) Fast deactivating calcium channels in chick sensory neurons. *J. Gen. Physiol.* **92**:197-218.

Tsien, R.W. and Tsien, R.Y. (1990) Calcium channels, stores, and oscillations. *Ann. Rev. Cell. Biol.* **6**:1-55.

Tsien, R.W., Hess, P., McCleskey, E.W. and Rosenberg, R.L. (1987) Calcium channels: mechanisms of selectivity, permeation, and block. *Ann. Rev. Biophys. Chem.* **16**:265-290.

Tsien, R.W., Lipscombe, D., Madison, D.V., Bley, K.R. and Fox, A.P. (1988) Multiple types of neuronal channels and their selective modulation. *Trends in Neurosciences* **11**: 431-437.

VanDongen, A.M., Frech, G.C., Drewe, J.A., Joho, R.H. and Brown, A.M. (1990) Alternation and restoration of K^+ channel function by deletions at the N- and C-termini. *Neuron* **5**:433-443.

Vassilev, P.M., Scheuer, T. and Caterall, W.A. (1988) Identification of an intracellular peptide segment involved in sodium channel inactivation. *Science* **241**:1658-1661

Wanke, E., Ferroni, A., Malgaroli, A., Ambrosini, A., Pozzan, T. and Meldolesi, J. (1987) Activation of a muscarinic receptor selectively inhibits a rapidly inactivated Ca^{2+} current in rat sympathetic neurons. *Proceedings of the National Academy of Sciences* **84**: 4313-4317.

White, M.M. and Bezanilla, F. (1985) Activation of squid axon K channels: ionic and gating studies. *Journal of General Physiology* **85**: 539-554.

Wong, R.K.S. and Prince, D.A. (1981) Afterpotential generation in hippocampal pyramidal cells. *J. Neurophysiol.* **45(1)**:86-97.

Yaari, Y., Hamon, B. and Lux, H.D. (1987) Development of two types of calcium channels in cultured mammalian hippocampal neurons. *Science* **235**: 680-682.

Yue, D.T., Herzig, S., and Marban, E. (1990) β-Adrenergic stimulation of calcium channels occurs by potentiation of high activity gating modes. *Proc. Natl. Acad. Sci. USA* **87**:753-757.

Zagotta, W.N. and Aldrich, R.W. (1990) Voltage dependent gating of *Shaker* A-type potassium channels in *Drosophila* muscle. *J. Gen. Physiol.* **59**:29-60.

Zagotta, W.N., Hoshi, T. and Aldrich, R.W. (1990) Restoration of inactivation in mutants of shaker potassium channels by a peptide derived from ShB. *Science* **250**:568-571.

Zhu, X-Z and Chuang, D-M. (1987) Modulation of calcium uptake and D-aspartate release by $GABA_B$ receptors in cultured cerebellar granule cells. *European Journal of Pharmacology*.**141**: 401-408.

Zucker, R.S. (1989) Short term synaptic plasticity. *Ann. Rev. Neurosci.* **12**:13-31.